

THE ROLE OF B-RAF IN EMBRYONIC DEVELOPMENT OF MOUSE FOREBRAIN

Dissertation

For completion of the Doctorate degree in Natural Sciences at the
Bayerische Julius-Maximilians-Universität Würzburg



Chaomei Xiang

from Hubei, China

Würzburg 2006

The hereby submitted thesis was completed from April 2002 until January 2006 at the Institut für Medizinische Strahlenkunde und Zellforschung, Bayerische Julius-Maximilians Universität, Würzburg under the supervision of **Prof. Dr. U. R. Rapp** (Faculty of Medicine), **PD Dr. R. Götz** (Faculty of Medicine), **Prof. Dr. E. Buchner** (Faculty of Biology) and **Prof. Dr. U. Scheer** (Faculty of Biology).

Submitted on:

Members of the thesis committee:

Chairman: Prof. Dr. M. Müller

Examiner: PD Dr. R. Götz

Examiner: Prof. Dr. E. Buchner

Date of oral exam:

Certificate issued on:

ACKNOWLEDGMENTS

First of all, I would like to thank Prof. Dr. Ulf Rapp for inviting me to the MSZ and for his strong scientific guidance during my studies, as well as for providing an international atmosphere at the institute. I would also like to thank Prof. Erich Buchner and Prof. Ulrich Scheer for accepting me to the faculty of biology, and for their support during my doctorate study. Also thanks to Prof. Michael Sendtner and Prof. Heiner Westphal for the fruitful collaboration.

My research work, supported by Deutsche Forschungsgemeinschaft, SFB 581 TP B5 and GK1048, was undertaken in the group “AG Mouse Genetics”, under the direction of PD Dr. Rudolf Götz. Many special thanks to Rudolf for fully training me in his group and for the excellent supervision I received. I am deeply grateful to Dr. Guadalupe Camarero for the excellent and impressive theoretic and technical mentorship in mouse neurobiology, to Hilde Troll for her perfect expertise in blastocyst injection.

In the mouse club, Agnes, Simone, Verena, Fatih, Christian, Christiaan, Mattias, Maureen, Doris, Nikolai, Tamara, and Antje, I would like to thank for the many social and scientific events we have shared. I would not forget to thank those ex-members: Oleg, Lev, Roland, Daniel, Svetlana and Alla for the past in common.

I am very grateful to Reinhold, Renate, Barbara and Ludmilla for their support in DNA sequencing, protein analysis, cell culture and molecular cloning. Thanks a lot to AG Biochem (especially Ulrike), Eugene Group, Joe Group as well as Prof. Müller’s group and Prof. Raab’s group for some kind assistance.

Thanks a lot to Ms. Krämmer for supporting us with clean supplies and for excellent hygiene and to our animal caretakers: Galina, Jaklin, Markus, and Viktor for keeping our mice healthy and happy.

I’m very grateful to Rosemarie Röder, Ewald Lipp and Regine Blättler for their patience in helping me in so many things concerning paper work. Special thanks to Ralf Schreck, Silvia Pfränger and Gunther Titsch.

It is difficult to express in a few sentences the gratitude for my family, for their love and support.

The greatest acknowledgement I reserve for my wife Jing and our daughter Enya, supporting me every time either mentally or in reality, to whom I dedicate this dissertation.

TABLE OF CONTENTS

ZUSAMMENFASSUNG	1
SUMMARY	2
1. INTRODUCTION	3
1.1. The <i>RAF</i> family as proto-oncogenes	3
1.2. Signalling of <i>RAF</i> kinases	4
<i>Structure of <i>RAF</i> proteins</i>	4
<i>Activation of <i>RAF</i>s by small <i>GTPases</i></i>	5
<i>Modification of <i>RAF</i>s by phosphorylation</i>	7
<i>Interaction of <i>B-RAF</i> and <i>C-RAF</i></i>	10
<i>Regulation of <i>RAF</i>s by scaffold proteins</i>	11
<i>MEK-ERK activation by <i>RAF</i> kinases</i>	12
<i>Other cellular targets of <i>RAF</i>s</i>	13
1.3. Biological importance of <i>RAF</i>s	15
<i>Expression and localization of individual <i>RAF</i>s</i>	15
<i>Physiological roles of <i>RAF</i> isotypes</i>	16
<i>Cellular function of individual <i>RAF</i>s</i>	19
1.4. Experimental design and aim of the project	20
<i>Potential role of <i>B-RAF</i> in forebrain development</i>	20
<i>Rescued <i>B-RAF</i> null mice to be analyzed</i>	21
<i>Conditional <i>B-RAF</i> KOs to be generated</i>	23
2. RESULTS	24
<i>Part I. Analysis of <i>B-RAF</i> null mice</i>	
2.1. Developmental expression of <i>B-RAF</i> kinase in embryonic forebrain	24
2.2. Unimpaired self-renewal NSCs in <i>B-RAF</i> deficient forebrains at E10.5	26
2.3. Affected neocortical development in <i>B-RAF</i>^{KIN/KIN} mice	27
2.4. Reduced proliferation of late progenitor cells in <i>B-RAF</i>^{KIN/KIN} cortex	33
2.5. Impaired migration of late-born cortical neurons in <i>B-RAF</i>^{KIN/KIN}	35
2.6. Attenuated activation of ERK in <i>B-RAF</i>^{KIN/KIN} telencephalon	35
2.7. Abnormalities of actin cytoskeleton in <i>B-RAF</i>^{KIN/KIN} cortical neurons	38
2.8. p35 expression in <i>B-RAF</i>^{KIN/KIN} cortical neurons	38

<i>Part II. Generation of conditional KOs</i>	
2.9. Constructing of targeting vectors for conditional KOs	41
2.10. Production of targeted ES clones	44
2.11. Test of Cre/loxP system and tet-switch in targeted clones	46
2.12. Chimera formation and mating for germline transmission	49
2.13. Preparation for a tetracycline-regulated B-RAF transgenic line	52
3. DISCUSSION	54
3.1. <i>B-RAF</i> ^{KIN/KIN} animals as rescued B-RAF null mice	54
3.2. NSCs in forebrain during midgestation stage	56
3.3. Cortical defect in neocortex development	56
3.4. Progenitor proliferation associated with ERK activation	58
3.5. Affected neuronal migration probably due to cell autonomous defect	58
3.6. Role of B-RAF in FGF2 and TrkB signalling during cortex development	60
3.7. Generation of conditional KO by gene targeting	62
3.8. Preparation of tet-regulated B-RAF transgenic line as an alternative way.....	65
4. MATERIALS AND METHODS	67
4.1. Materials	67
4.1.1. Instruments.....	67
4.1.2. Chemical reagents and general materials.....	68
4.1.3. Cell culture and embryo manipulation materials.....	69
4.1.4. Antibodies used for Western blot and immunochemistry.....	70
4.1.5. Enzymes.....	70
4.1.6. Kits.....	71
4.1.7. Plasmid DNA.....	71
4.1.8. Oligonucleotides.....	72
4.1.9. Cell lines, mouse lines and bacterial strains.....	73
4.2. Solutions and buffers	73
4.2.1. Bacterial medium and DNA isolation buffers.....	73
4.2.2. DNA buffers.....	74
4.2.3. Protein analysis buffers.....	75
4.2.4. Histological buffers.....	76
4.3. Methods	76
4.3.1. Bacterial manipulation.....	76

4.3.1.1. Preparation of competent cells (CaCl ₂ method).....	76
4.3.1.2. Transformation of competent bacteria.....	77
4.3.2. DNA methods.....	77
4.3.2.1. Electrophoresis of DNA on agarose gel.....	77
4.3.2.2. Isolation of plasmid DNA from agarose (QIAEX II agarose gel extraction protocol).....	77
4.3.2.3. Purification of plasmid DNA (QIAquick PCR purification kit).....	77
4.3.2.4. Ligation of DNA fragments.....	78
4.3.2.5. Cohesive-end ligation.....	78
4.3.2.6. Mini-preparation of plasmid DNA.....	78
4.3.2.7. Maxi-preparation of plasmid DNA.....	78
4.3.2.8. Measurement of DNA concentration.....	79
4.3.2.9. DNA Sequencing (Sanger Dideoxy Method).....	79
4.3.2.10. Isolation of genomic DNA from cell and tissue.....	80
4.3.2.11. Southern blot.....	80
4.3.3. RNA methods.....	81
4.3.3.1. Isolation of RNA from cells and tissues.....	81
4.3.3.2. RT-PCR.....	81
4.3.4. Protein methodologies.....	81
4.3.4.1. Measurement of Protein concentration (Bio-Rad protein assay).....	81
4.3.4.2. Sodium dodecyl sulfate polyacrylamide gel electrophoresis (SDS PAGE).....	81
4.3.4.3. Immunoblotting.....	82
4.3.4.4. Immunoblot stripping.....	83
4.3.4.5. Luciferase reporter gene assay.....	83
4.3.5. Cell culture techniques.....	83
4.3.5.1. <i>in vitro</i> neurosphere assay for neural stem cells.....	83
4.3.5.2. Primary cortical cell culture.....	84
4.3.5.3. ES cell maintenance.....	84
4.3.5.4. Targeting of ES cell by vectors.....	85
4.3.5.5. Identification of positive clones.....	85
4.3.5.6. Transduction and induction of targeted ES cells.....	85
4.3.5.7. Blastocyst injection of targeted ES cells.....	86
4.3.5.8. Transient transfection of NIH3T3 CMV-tTA.....	86
4.3.6. Histological methods.....	86

4.3.6.1. Embedding in paraffin.....	86
4.3.6.2. Hematoxylin/eosin staining.....	87
4.3.6.3. Immunohistochemistry.....	87
4.3.6.4. BrdU labelling	87
4.3.7. Statistical analysis.....	88
REFERENCES	89
APPENDIX	101
CURRICULUM VITAE	104

Zusammenfassung

Die Familie der RAF-Kinasen umfasst drei Mitglieder, A-RAF, B-RAF und C-RAF. Nur für die B-RAF-Isoform wurde eine wichtige Funktion für die Entwicklung des Zentralen Nervensystems (ZNS) gefunden. Das Fehlen von B-RAF führt bei neu generierten embryonalen Neuronen zum Zelltod, weil sie *in vitro* nicht auf Überlebensfaktoren reagieren können. Bei einer zweiten Zelllinie, die durch die Abwesenheit von B-RAF beeinträchtigt ist, handelt es sich um endotheliale Zellen. Ihr Zelltod führt zu inneren Blutungen und zu Letalität von *B-RAF*^{-/-}-Mäusen zwischen Tag 10.5 (E10.5) und 12.5 (E12.5) der Embryonalentwicklung. Dies verhinderte bisher weitere Untersuchungen der neuralen B-RAF-Funktion bei späteren Stadien.

Im Gegensatz zu *B-RAF*^{-/-}-Mäusen überleben *B-RAF*^{KIN/KIN}-Mäuse die Mitte der Embryonalentwicklung, da ihre Endothelzellen vor Apoptose geschützt sind. Diese Tiere besitzen kein B-RAF, stattdessen wird im *B-RAF-Locus* ein chimäres Protein exprimiert, das den N-Terminus von B-RAF sowie alle Domänen von A-RAF umfasst. Der Schutz vor abnormaler neuraler Apoptose im Vorderhirn macht diese Tiere zu einem potentiellen Modell zur Untersuchung der Proliferations- und Differenzierungsfunktion von B-RAF, die die Kinase neben der Überlebensfunktion in der ZNS-Entwicklung ausübt.

Die detaillierte Untersuchung der *B-RAF*^{KIN/KIN}-Tiere konzentrierte sich auf die Entwicklung der Hirnrinde. Augenscheinlich waren kortikale Defekte im *B-RAF*^{KIN/KIN} Vorderhirn: Der Verlust von B-RAF führte zu einer starken Reduzierung von Brn-2 exprimierenden pyramidalen Projektions-Neuronen begleitet von einer Störung der Dendritenbildung mit weniger und dünneren Dendriten in diesen oberen Schichten. Weitere Untersuchungen mit BrdU-Markierungsexperimenten zeigten in der ventrikulären Schicht reduzierte Zellproliferation für E14.5-E16.5 der Mutantenembryonen und ein Migrationsdefizit der spätgebildeten kortikalen Neuronen. Während der Proliferationsdefekt der Hirnrinden-Vorläuferzellen mit einer reduzierten ERK-Aktivierung einherging, bleibt der Mechanismus der gestörten neuralen Migration zu erklären. Unsere Hypothese ist, dass die subzelluläre Lokalisation von Phospho-ERK in den wandernden Hirnrinden-Neuronen der *B-RAF*^{KIN/KIN}-Mäuse verändert sein könnte.

Zur Bestätigung der *in vivo*-Funktion von B-RAF und weiteren Studien zu ihrer unbekannt Rolle in der embryonalen Neurogenese sowie anderen Morphogenesen wäre die konditionale *B-RAF* Inaktivierung erforderlich. Durch die Deletion des genetischen Materials bzw. die Inaktivierung der Genfunktion in ausgewählten Zellen zu einem bestimmten Zeitpunkt ließen sich die Embryo-Letalität sowie unerwünschte pleiotrope Nebeneffekte vermeiden und akkumulierende, kompensierende Entwicklungsveränderungen von Beginn an ausschließen. Um die Cre Rekombinase-Methode einsetzen zu können, wurden *floxed B-RAF* embryonale Stammzell (ES)-Zelllinien generiert. Außerdem wurde ein auf dem Tetrazyklin Operator basierendes Schaltallel in den *B-RAF* Genort von embryonalen Stammzellen integriert, so dass die B-RAF Expression konditional und reversibel durch die Zugabe von Doxyzyklin angeschaltet werden konnte. Bisher wurden hochgradige chimäre Mäuse nach Blastozysten-Injektion geboren. Die Keimbahnübertragung dieser chimären Mäusen wird momentan untersucht.

Wenn beide konditionale Mauslinien bereit sind, könnte die Entwicklung ihres Zentralnervensystems untersucht werden, um die Rolle von B-RAF in der Entwicklung des Nervensystems herauszufinden.

SUMMARY

The RAF family of protein kinases consists of three members, A-RAF, B-RAF and C-RAF. Unlike the other isoforms, B-RAF has been found to have an important function for normal development of the central nervous system (CNS), because newly generated embryonic neurons lacking B-RAF cannot respond to survival factors and undergo cell death *in vitro*. A second cell lineage affected by the absence of B-RAF are endothelial cells and their death leads to internal bleedings and lethality of *B-RAF*^{-/-} mice between embryonic day 10.5 (E10.5) and E12.5 precluding an opportunity to further analyze neural B-RAF function at a later stage.

In contrast to *B-RAF*^{-/-} mice, *B-RAF*^{KIN/KIN} mice, which are B-RAF deficient but express a chimeric protein consisting of the unique N terminus of B-RAF and all the domains of A-RAF in the *B-RAF* gene locus, survive after midgestation because their endothelial cells are protected from apoptosis. More importantly, overall prevention of abnormal neural apoptosis in the forebrain allows us to study proliferation- or differentiation-oriented function of B-RAF other than its survival effects in CNS development.

The detailed investigation of *B-RAF*^{KIN/KIN} animals was concentrated on cortical development. There were apparent cortical defects in *B-RAF*^{KIN/KIN} forebrain: Loss of B-RAF led to severe reduction of Brn-2 expressing pyramidal projection neurons accompanied by a disruption of dendrite formation in the upper layers. In further analysis, BrdU labelling experiments showed that from E14.5 to E16.5 cell proliferation in the ventricular zone of the mutant mice was reduced and that the late-born cortical neurons failed to migrate properly. While the proliferation defect of cortical progenitors was associated with reduced ERK activation, the mechanism causing impaired neuronal migration remains to be determined. Our hypothesis is that the subcellular localization of phospho-ERK may be altered in migrating cortical neurons in *B-RAF*^{KIN/KIN} mice.

To confirm *in vivo* function of B-RAF and further study unknown roles in embryonic neurogenesis as well as other morphogenesis, conditional *B-RAF* knockouts would be the ideal models, which can efficiently avoid embryonic lethality, prevent unwanted pleiotropic side effects and exclude accumulative compensatory developmental changes from the earliest developmental stage on, through the deletion of genetic material/gene function in selected cells at a specific time. The use of site-specific recombinases such as Cre and the successful development of the reversible tetracycline-based switch have provided powerful venues for creating conditional loss-of-function mouse models. Generation of *tetracycline-regulated B-RAF* and *floxed B-RAF* mouse embryonic stem (ES) cell lines was performed. Up to now, high-grade chimeric mice were obtained after blastocyst injection of the modified ES cell clones. The germline transmission from these chimeric mice is currently under investigation.

When either of conditional mouse lines is ready, detailed examination in their CNS development would be done to reveal how B-RAF plays a real role for normal development of the nervous system.

1. INTRODUCTION

1.1. The *RAF* family as proto-oncogenes

The founding member of the *RAF* family was discovered as the oncogene of mouse sarcoma virus 3611 (Rapp et al., 1983). In vertebrate species, three *RAF* genes (*A-RAF*, *B-RAF* and *C-RAF*) have been identified (Hagemann and Rapp, 1999; Chong et al., 2003).

RAFs are protein serine/threonine kinases active at the head part of a conserved signalling module that transduces signals from the cell surface to the nucleus (Fig. 1.1). Binding of extracellular ligands such as growth factors, cytokines and hormones to their cell-surface receptors, receptor tyrosine protein kinases (RTK) or G protein coupled receptors (GPCR), activates the RAS family of small G proteins. As the upstream regulators of all RAF proteins, RAS then initiates activation of RAF (Robbins et al., 1994). This leads to activation of the dual-specificity protein kinases MEK1 and MEK2 and subsequently the MAPK/ERK proteins ERK1 and ERK2.

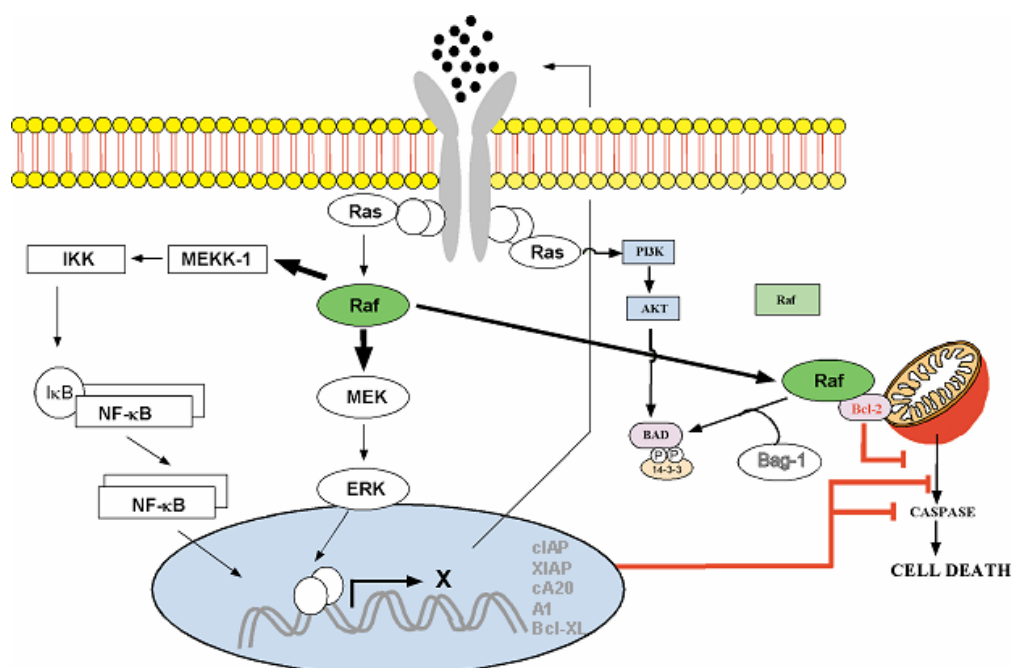


Fig. 1.1 The main pathways of RAF signalling, including ERK-dependent and -independent pathways.

Depending on the cellular context, this classic pathway mediates diverse biological functions such as cell proliferation, survival, differentiation and motility predominantly through the regulation of transcription, metabolism and cytoskeletal rearrangements. The RAF-mediated RAS/ERK pathway has been tightly associated with human cancers, because oncogenic mutations in *ras* occur in about 15% of cancers (Davies et al., 2002) and ERK is hyperactivated in about 30% of cancers (Allen et al., 2003). Consistent with this finding, *B-RAF* has been recently found to mutate at a high frequency in human cancers, particularly melanoma (30–60%), thyroid cancer (30–50%), colorectal cancer (5–20%) and ovarian cancer (~30%) (Davies et al., 2002). Notably, cancer cells with oncogenic *ras* did not harbor mutant *B-RAF*, providing strong genetic evidence that the RAS/RAF/ERK cascade plays around with human cancers.

1.2. Signalling of RAF kinases

Structure of RAF proteins

A-RAF is the smallest isotype, at approximately 68 kDa, and C-RAF is about 74 kDa. B-RAF comprises a variety of proteins in size from 75 to 100 kDa, due to different splicing (Storm et al., 1990; Barnier et al., 1995). In general, all the RAF proteins, including different B-RAF isoforms, share a common structure with three conserved regions — two (CR1 and CR2) in the N terminal part, and the third (CR3), which encodes the kinase domain, in the C terminal part (Fig. 1.2).

The crystal structure of the B-RAF kinase domain has recently been solved (Wan et al., 2004), showing the kinase is folded into a typical conformation of active kinases. The glycine-rich loop, a flexible loop that anchors the phosphates of ATP into the catalytic cleft, makes an atypical intramolecular interaction with the activation segment, a region that lies between the invariant DFG and APE motifs and that is the site of regulatory phosphorylation events. This interaction displaces the activation segment and traps B-RAF in an inactive

conformation (Fig. 1.2). In human cancers, both the glycine-rich loop and the activation segment of B-RAF are two major hotspots of mutations leading to enhanced kinase activity.

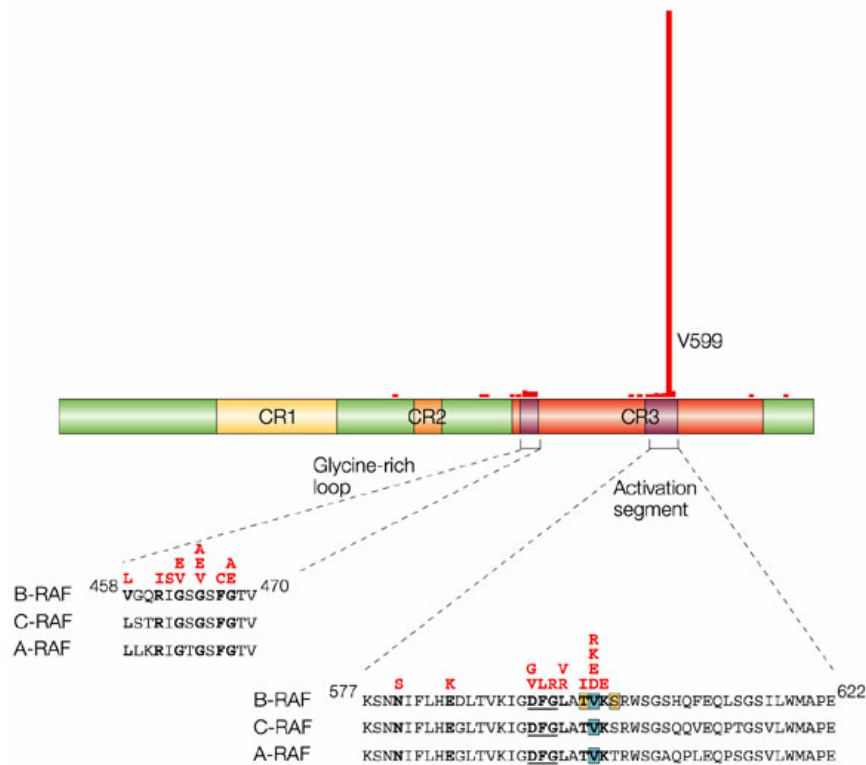


Fig. 1.2 Structure of the human RAF proteins highlighting the glycine-rich loop and the activation segment. The positions of the mutations that occur in human cancer are indicated above the structure — the length of the line provides an indication of the relative frequency with which the mutations occur. (From Wellbrock et al., 2004)

Activation of RAFs by small GTPases

In its GTP-bound and active form, RAS binds to the RAS-binding domain (RBD) and also contacts a cysteine-rich domain (CRD), both of which are located in CR1 of RAF (Wittinghofer and Nassar, 1996). As RAS is predominantly attached to the plasma membrane (Hancock, 2003), this interaction recruits RAF to the plasma membrane and initiates stimulation of its kinase activity (Fig. 1.3). Four RAS proteins (H-Ras, N-Ras, K-RasA, K-RasB) have clear differences in their binding affinities to the RBDs of the individual RAF proteins (Weber et al., 2000), which provides potential for differential regulation. Intriguingly,

the individual RAS proteins are also located in distinct membrane microdomains (Hancock, 2003). This may imply that the RAF proteins are exposed to distinct environments by engaging with different RAS isoforms.

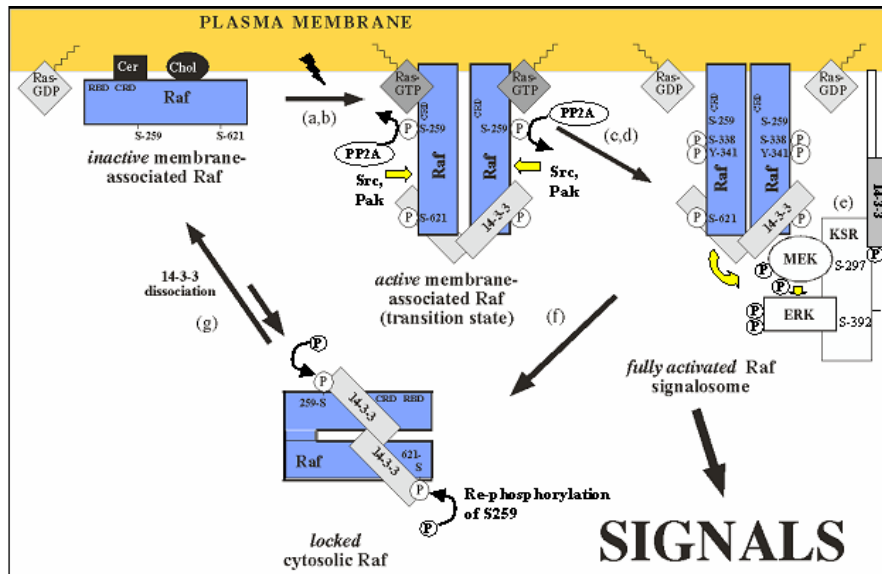


Fig. 1.3 The proposed model of C-RAF activation showing the direct involvement of RAS and 14-3-3 proteins.

The 14-3-3 adaptor/scaffold proteins can regulate the ability of RAF proteins to bind to RAS (Fig. 1.3). They bind to phospho-Serine 259 of C-RAF, located in CR2, which interferes with RAS-RAF binding (Dhillon et al., 2002; Light et al., 2002). Recently, Prohibitin, a ubiquitously expressed and evolutionarily conserved protein has been found to make direct interaction with C-RAF. This complex formation is indispensable for the membrane targeting and activation of C-RAF by RAS (Rajalingam et al., 2005). C-RAF recruitment to the plasma membrane is essential for its activation, but maybe not in all cases. Some studies have implied that the activation of C-RAF was RAS-independent (King et al., 1998; Chaudhary et al., 2000).

As another member of small GTPases, Rap1 is activated by second messengers such as calcium, diacylglycerol and cAMP, and in general by most of the extracellular signals

reported to activate RAS (Bos, 1998). Rap1 has an effector domain virtually identical to that of Ras, which is able to bind both B-RAF and C-RAF. The formation of C-RAF/Rap1 complexes does not result in C-RAF activation (Cook et al., 1993; Hu et al., 1997). In contrast, an increasing number of studies strongly suggest that Rap1 can activate B-RAF, probably because of subtle differences in the Ras-binding domains of RAF proteins (Okada et al., 1999).

Two cell types, neuronal cells and megakaryocytes, highlight the ability of Rap1 to trigger B-RAF for sustained activation of ERKs. In PC12 cells, active Rap1 (York et al., 2000; Kao et al., 2001; Wu et al., 2001) activates B-RAF, increasing the duration of ERK signaling and potentiating neuronal differentiation (York et al., 1998; Kao et al., 2001). In megakaryocytes, the sustained activation of Rap1, B-RAF and ERKs by thrombopoietin induces megakaryocytic differentiation (Garcia et al., 2001), while blockade of sustained Rap1 activation inhibits megakaryocytic differentiation and sustained ERK activation (Delehanty et al., 2003). Though the effect of Rap1 activation on ERK activity depends on the level of B-RAF expression, coupling of Rap1/B-RAF/ERK function might be regulated by cell-type-specific proteins, such as 14-3-3 (Qiu et al., 2000).

Modification of RAFs by phosphorylation

Activation and inhibition by phosphorylation and dephosphorylation is an important and conserved mechanism by which RAF kinase activity is regulated. RAF proteins are subject to complex regulation, indicated by the presence of numerous phosphorylation sites, common or unique, throughout the proteins (Fig. 1.4). Some unique differences at key individual phosphorylation sites provide many possibilities for differential regulation of B- and C-RAF.

Serine 43, Serine 233 and Serine 259 are three sites in C-RAF that suppress its activity upon phosphorylation (Wu et al., 1993; Sidovar et al., 2000; Dhillon et al., 2002; Dumaz et al., 2002; Dumaz and Marais, 2003) (Fig. 1.4). These seem to be targets of PKA, a cyclic-AMP-

dependent kinase in cells (Dumaz and Marais, 2003) but S259 is also phosphorylated by AKT/protein kinase B (PKB) (Zimmermann and Moelling, 1999). S43 phosphorylation appears to block binding of the N terminus of C-RAF to RAS (Wu et al., 1993) and phosphorylated S259 forms the core of a 14-3-3 binding site. When S233 is phosphorylated it creates another 14-3-3 binding site in C-RAF (Dumaz and Marais, 2003). Some research revealed that RAS and PP2A can cooperate to dephosphorylate S259 and activate C-RAF (Ory et al., 2003), fully overcoming the effects of PKA. However, other studies indicate that S43, S233 and S259 all contribute to C-RAF inhibition by PKA (Dumaz et al., 2002). Recently, novel phosphorylation sites at the positions of serine 296 and 301 in C-RAF, which contribute to negative regulation of C-RAF, were detected (Hekman et al., 2005).

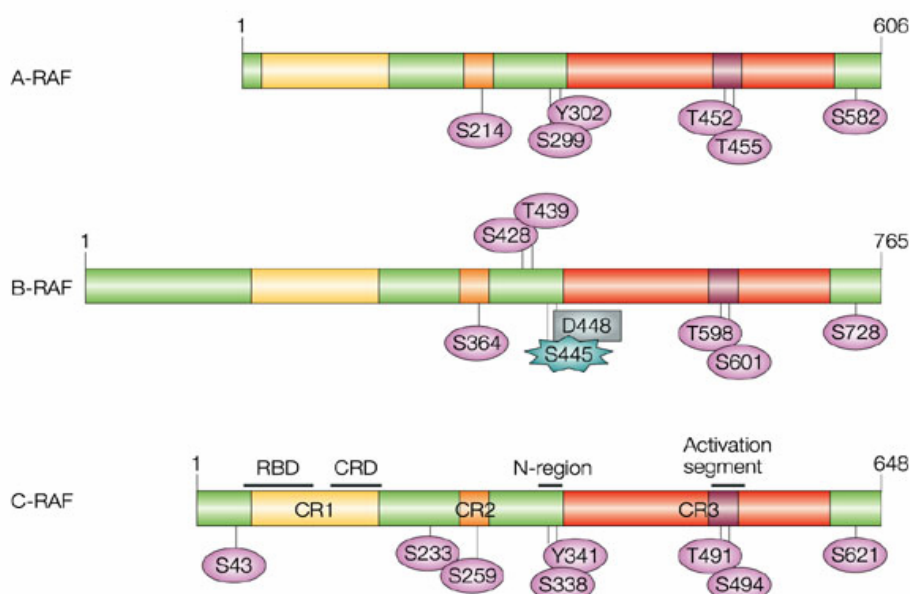


Fig. 1.4 Important phosphorylation sites of the human RAF proteins, which phosphorylation leads to activation or inhibition of RAF kinases. (From Wellbrock et al., 2004)

The five phosphorylated sites flanking or within the kinase domain, Serine 338 and Tyrosine 341 (N-region), Threonine 491 and Serine 494 (activation segment), and Serine 621

(C-terminus), stimulate C-RAF kinase activity (Fig. 1.4). Both S338 and Y341, are located at the N-terminal side of CR3 (Fabian et al., 1993; Marais et al., 1995; King et al., 1998; Mason et al., 1999) in a subdomain, known as the N-region. Negative charge within this region is essential for C-RAF kinase activity. While SRC and SRC-family kinases seem to phosphorylate Y341 in different systems (Fabian et al., 1993; Chow et al., 1995; Marais et al., 1995; Marais et al., 1997; King et al., 2001; Tilbrook et al., 2001), S338 phosphorylation can be mediated by PAK1 and PAK2, serine/threonine-specific protein kinases (King et al., 1998; Chaudhary et al., 2000; Sun et al., 2000; Zang et al., 2002). PAKs, which are activated by Rho-family GTPases (CDC42 and RAC), phosphorylate S338 and stimulate C-RAF activation in a RAC/CDC42- and PI3K-dependent manner (Sun et al., 2000). Moreover, PAKs phosphorylate S338 in the cytosol in a RAS-independent manner (King et al., 1998; Chaudhary et al., 2000; Chiloehes et al., 2001), whereas RAS- and growth-factor-stimulated S338 phosphorylation occurs at the plasma membrane in a RAS-dependent manner. Thus, there could be other unknown kinases responsible to stimulate S338 phosphorylation in a growth-factor- or RAS-dependent manner.

T491 and S494 are within the kinase domain in a region called the activation segment and their mutation blocks C-RAF activation (Chong et al., 2001). Their modification is mediated either by autophosphorylation or by catalyzation of unidentified kinases.

The third 14-3-3 binding site, made by phosphorylation of S621 in C terminus is essential for activation (Light et al., 2002; Jaumot and Hancock, 2001; Tzivion et al., 1998; Yip-Schneider et al., 2000). It is implied that this site is subject to very rapid and transient regulation (Hekman et al., 2004), indicating that dynamic recycling of the phosphate and 14-3-3 at this site might be more important than the absolute levels of phosphorylation or 14-3-3 that is bound.

Since all the five sites positively regulating C-RAF activity are conserved in A-RAF, A-RAF is activated by similar mechanisms to C-RAF (Marais et al., 1997). In B-RAF, three of

those sites, T598, S601 and S728, seem to carry out similar functions in B-RAF as their counterparts in C-RAF. Phosphorylation of the activation-segment sites T598 and S601 is essential for B-RAF activation (Zhang and Guan, 2000). Recently, it is reported that mixed lineage kinase-3 (MLK3) is necessary, indirectly, for the activating phosphorylation at T598/S601 of B-RAF (Chadee and Kyriakis, 2004).

Based on the crystal structure of the B-RAF kinase domain, T598 is buried within an intermolecular interaction interface (Wan et al., 2004). The phosphorylation of T598 would disrupt the interaction between the glycine-rich loop and the activation segment, and allow the formation of the active conformation, which provides a satisfactory explanation for how phosphorylation regulates B-RAF and by analogue presumably also C-RAF and A-RAF. The special structure also provides an explanation of why V600E is the most frequent mutation of *B-RAF* in human cancers: This amino acid exchange is sufficient for destabilizing the interaction between the glycine-rich loop and the activation segment (Wan et al., 2004).

By contrast, the N-region-mediated regulation of B-RAF is quite different. First, the position equivalent to Y341 of C-RAF is occupied by an aspartic acid, D448 in B-RAF. Then, Ser 445 of B-RAF corresponding to S338 of C-RAF is constitutively phosphorylated, unlike in C-RAF (Mason et al., 1999). As a result, the N-region in B-RAF carries a constant negative charge and consequently B-RAF has strongly elevated basal kinase activity compared with other RAFs (Mason et al., 1999). Therefore, B-RAF seems to require only RAS-mediated membrane recruitment for activation. The unique difference may account for the fact that *B-RAF* is frequently mutated in human cancer, instead of *A-RAF* or *C-RAF*.

Interaction of B-RAF and C-RAF

C-RAF:B-RAF heterodimerization has been observed in cells before (Tzivion et al., 1998; Weber et al., 2001), indicating the importance of their direct interaction. In 2004, Wan and his colleagues studied several mutant forms of B-RAF with low kinase activity and found that

these oncogenic B-RAFTs can stimulate C-RAF activity, which then signals to MEK and ERK. Surprisingly, further work revealed that in normal cells wild type B-RAF can efficiently activate C-RAF through 14-3-3 mediated heterooligomerization (Garnett et al., 2005). However, wild-type B-RAF and C-RAF form a complex in a RAS-induced way, whereas mutant forms of B-RAF bind to C-RAF constitutively.

This new paradigm of RAF signalling, RAS→B-RAF→C-RAF→MEK→ERK, appears to contribute to signaling to MEK downstream of EGF. However, ERK activation by growth factors is severely compromised in B-RAF but not C-RAF null mouse embryo fibroblasts (Wojnowski et al., 2000; Huser et al., 2001; Mikula et al., 2001; Pritchard et al., 2004), suggesting that C-RAF activation by B-RAF might account for total B-RAF-induced ERK activation to a small extent. One outcome for the unexpected facet of RAF signaling could be that B-RAF can modify MEK activity through C-RAF to provide subtle regulation of signaling intensity or duration (Garnett et al., 2005).

Regulation of RAFs by Scaffold proteins

Scaffold proteins have an important role in regulating RAFs through stabilizing and coordinating interactions between the individual components. Several scaffolds, such as kinase suppressor of RAS (KSR, a 'pseudo-kinase'), the multidomain protein connector-enhancer of KSR (CNK) and the leucine-rich-repeat protein suppressor of Ras mutations-8 (SUR8), enhance the efficiency of signalling between C-RAF and MEK or between RAS and C-RAF. KSR presents MEK to C-RAF at the membrane and then recruits ERK for MEK-mediated phosphorylation (Denouel-Galy et al., 1998; Morrison, 2001; Anselmo et al., 2002) (Fig. 1.3). CNK binds to C-RAF and cooperates with RAS to stimulate C-RAF activation (Anselmo et al., 2002; Lanigan et al., 2003). In addition, SUR8 seems to form a ternary complex with C-RAF and RAS that enhances signalling through the pathway (Li et al., 2000).

Two other scaffold proteins, RAF kinase inhibitor protein (RKIP) and the Sprouty-related protein (Spred), inhibit the MAPK pathway (Yeung et al., 1999; Wakioka et al., 2001). RKIP can bind RAF, MEK and ERK, but RKIP/RAF and RKIP/MEK interactions are mutually exclusive (Yeung et al., 2000). The RAF and MEK binding sites on RKIP overlap and exclude each other from binding by steric interference, so RKIP functions by inhibiting the formation of RAF and MEK in the same signalling module. As a potent inhibitor of the ERK pathway (Wakioka et al., 2001), Spred inhibits the ERK pathway downstream of RAS and is able to associate with RAF. Binding of Spred to Ras does not affect activation of RAS or the recruitment of RAF to the membrane. In a word, enhancement and inhibition of RAF signalling by scaffold proteins provides another level to the diversity of RAF regulation.

MEK–ERK activation by RAF kinases

The MEK–ERK kinase cascade is the only widely accepted effector of RAF proteins. MEK proteins, as direct substrates of RAFs, are activated by phosphorylation of two serine residues within their activation segments (S217 and S221 in MEK1) and in turn phosphorylate ERK1 and ERK2 on threonine and tyrosine residues within their activation segments (T202/Y204 in ERK1).

In cell extracts, B-RAF binds to and phosphorylates MEK1 and MEK2 more efficiently than do either A-RAF or C-RAF (Marais et al., 1997; Papin et al., 1996). Cell-fractionation studies show that the main MEK kinase is B-RAF but not C-RAF (Catling et al., 1994; Jaiswal et al., 1994). Immunodepletion of B-RAF from brain lysates results in a 96% loss in RAS-associated MEK1 activity (Moodie et al., 1994). In comparison, an inducible form of B-RAF stimulates more robust and rapid ERK activity than similar C-RAF and A-RAF constructs, while A-RAF is the least effective (Pritchard et al., 1995). Consistently, mouse embryonic fibroblasts from *B-RAF*^{-/-} mice have severely compromised ERK activity (Wojnowski et al., 2000; Pritchard et al., 2004), whereas ERK activation is relatively normal

in mouse embryonic fibroblasts from *A-RAF*^{-/-} and *C-RAF*^{-/-} mice (Huser et al., 2001; Mikula et al., 2001; Mercer et al., 2002). Among four different isoforms of B-RAF, resulting from complex alternative splicing (Barnier et al., 1995), the presence of exons 8b and 10 modulates both MEK activating activity and oncogenicity of B-RAF (Papin et al., 1998). Strikingly the sequence encoded by exon 10 enhances the affinity for MEK, the basal kinase activity, as well as the mitogenic and transforming properties of B-RAF.

An elegant study of the contribution of B-RAF and C-RAF to B-cell receptor (BCR) signalling in DT40 B-cell, showed that B-RAF and C-RAF are activated with different kinetics and cooperate for many downstream effects (Brummer et al., 2002). C-RAF was dispensable for BCR-mediated ERK activation, while the ablation of B-RAF caused a reduced and shortened activity of ERK. However, the B-RAF/C-RAF double knockout resulted in an almost complete loss of ERK activation and severely reduced expression of the downstream transcriptional targets c-Fos and Egr-1. Only the activation of nuclear factor of activated T cells, NFAT, was mainly dependent on B-RAF.

All these observations suggest that B-RAF is the main activator of MEK in cells and its primary function is to activate MEK, either directly or in cooperation with C-RAF, while C-RAF and A-RAF only signal to fine-tune the levels and/or duration of ERK activity and therefore to determine cell fate such as proliferation and differentiation. Because they have diverged significantly during evolution, A-RAF and C-RAF have gained other functions described below, which they execute in a MEK-independent and possibly a kinase-independent manner.

Other downstream targets of RAFs

Besides MEK1 and MEK2, several studies have indicated that mammalian RAF proteins might have other effectors. One such candidate is the transcription factor nuclear factor (NF)- κ B (Li and Sedivy, 1993; Janosch et al., 1996). C-RAF seems to be able to activate NF- κ B in

an indirect way and without requirement of MEK–ERK signaling (Fig. 1.1), as a dominant-negative version of MEK does not block C-RAF-mediated NF- κ B activation (Baumann et al., 2000). Other possible substrates for C-RAF are the phosphatase CDC25C (Galaktionov et al., 1995) and the tumour-suppressor protein retinoblastoma (RB) (Wang et al., 1998), both of which are regulators of the cell cycle. C-RAF-mediated phosphorylation of these substrates has been shown to affect their activity.

C-RAF and B-RAF have been reported to bind to Bag1, an anti-apoptotic protein that binds to another survival factor called Bcl-2 (Wang et al., 1996a; Wang et al., 1996b; Gotz et al., 2005). In addition to associating with Bcl-2, Bag1 may act as a scaffold protein that present C-RAF, and possibly B-RAF, at the mitochondrial surface, and mediate the interaction between C-RAF and the pro-apoptotic protein BAD (Fig. 1.1). This allows C-RAF to phosphorylate BAD, another putative substrate, and thereby stimulate cell survival (Troppmair and Rapp, 2003).

Further investigation demonstrated that C-RAF has kinase-independent scaffolding functions to regulate important pathways that control both apoptosis and cytoskeletal dynamics. The protein kinase, apoptosis signal-regulating kinase-1 (ASK1), is an inducer of apoptosis. C-RAF binds to the N-terminal regulatory domain of ASK1 and suppresses its pro-apoptotic activity, regardless of C-RAF kinase activity (Chen et al., 2001). Moreover, C-RAF counteracts apoptosis by suppressing the activation of MST2, mammalian sterile 20-like kinase, independent of its kinase activity (O’neill et al., 2004). Impressively, the lethal phenotype in C-RAF null mice can be rescued by a version of C-RAF with severely impaired catalytic activity towards MEK (Huser et al., 2001). Therefore, C-RAF seems to protect cells from apoptosis in a kinase-independent manner, possibly functioning as a scaffold or adaptor for proteins such as ASK1 and MST2.

Another recent study has revealed that C-RAF has a scaffolding function in the regulation of the Rho pathway (Ehrenreiter et al., 2005). Ras-related GTPases, RhoA, RhoB

and RhoC, associate with several effectors that regulate transcription, cell cycle, cytokinesis and the cytoskeleton (Schwartz, 2004). In *C-RAF*^{-/-} cells the migration defect was traced to the hyperactivation and mislocalization of Rho-dependent kinase ROK α /ROCK2 (Rho-kinase/Rho-associated protein coiled-coil forming kinase), and could be corrected by a catalytically inactive form of C-RAF. C-RAF was found to associate with ROK α /ROCK2, presumably controlling its activity and its correct subcellular localization (Ehrenreiter et al., 2005). By contrast, *B-RAF*^{-/-} fibroblast cells show increased migration, resulting from disruption in B-RAF-mediated and ERK-dependent regulation of the ROCKII/LIMK/cofilin pathway (Pritchard et al., 2004). Though several A-RAF specific partners, such as CK2 β , M2-PK, hTOM and hTIM have been reported (Hagemann and Rapp, 1999), so far it is unclear whether A-RAF has any other cellular targets.

1.3. Biological importance of RAFs

Expression and localization of individual RAFs

Early studies established that *C-RAF* mRNA is ubiquitously expressed, whereas *A-RAF* mRNA is expressed particularly highly in urogenital organs and *B-RAF* expression more restricted to neuronal tissues (Storm et al., 1990; Barnier et al., 1995). Subsequent studies have shown that A-RAF expression is generally ubiquitous in embryonic and adult mouse tissues (Luckett et al., 2000), and B-RAF also expressed in a wide range of tissues, although at considerably lower levels than in neuronal tissues (Wojnowski et al., 2000).

Notably, in adult mice the *B-RAF* gene encodes at least 10 different isoforms resulting from complex alternative splicing (Fig. 1.5), which display tissue-specific expression (Eychène et al., 1992; Barnier et al., 1995). They differ by the presence of alternatively spliced exons 8b and 10, or the absence of the middle part of exon 3 (unpublished data). In the shortest isoforms the NH₂-terminus is probably truncated. The sequence encoded by exon 10 is found only in B-RAF isoforms from neural tissues.

Indeed, RAF kinases are localized to different subcellular compartments. Both A- and C-RAF show stable or transient localization to the mitochondria (Wang et al., 1996a; Majewski et al., 1999; Nantel et al., 1999; Yuryev et al., 2000). In neurons where B- and C-RAF are both expressed, B-RAF is localized to neurite processes and C-RAF is perinuclear (Morice, et al., 1999). This localization may be due to isoform-specific lipid or protein-binding partners, which recruit RAF to distinct membrane rafts.

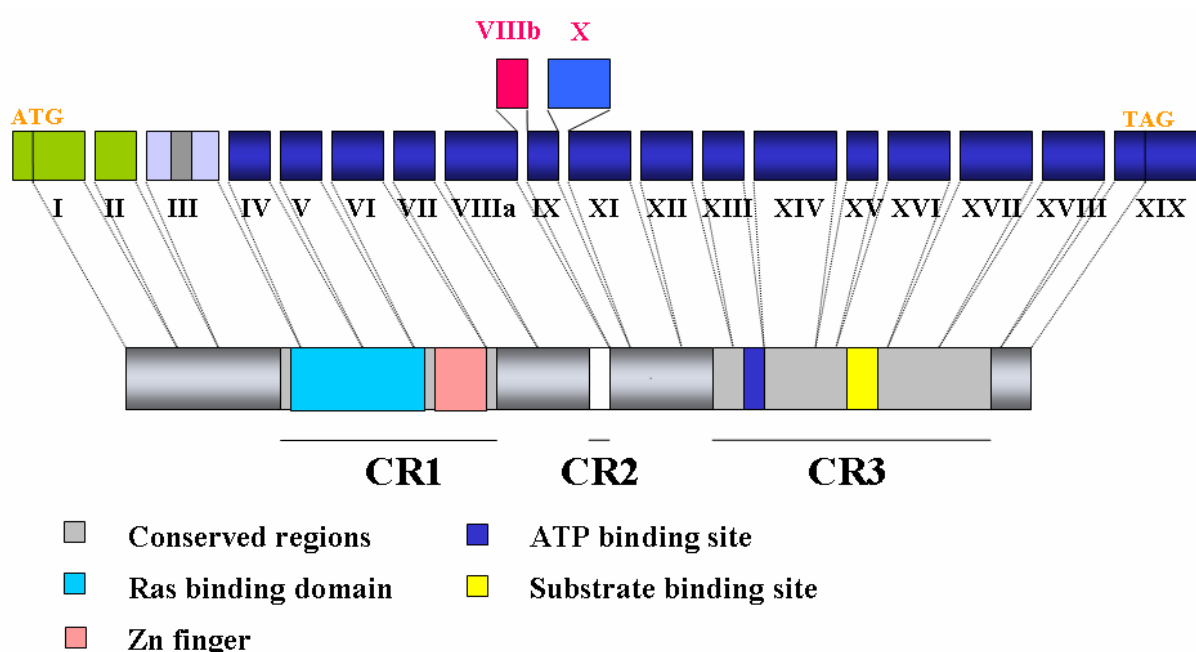


Fig. 1.5 Splicing of the murine *B-RAF* gene. There are at least 10 different isoforms in adult mice, due to complex alternative splicing in the N terminus, the middle part of exon 3, exon 8b and exon 10.

Physiological roles of RAF isotypes

A-RAF^{-/-} mice have neurological defects with some variation, depending on genetic background (Pritchard et al., 1996). In an inbred background, they die 7-21 days post partum from megacolon caused by a defect in visceral neurons that control bowel contractions, whereas mutant mice in an outbred background survive to adulthood, but still feature defects in proprioception and abnormal movements. This phenotype resembles Neurotrophin-3 (NT-3)-deficient mice (Kirstein and Farinas, 2002), suggesting that A-RAF is involved in a NT-3-

mediated neuronal survival pathway. No apparent deficiency in embryonic development is observed, consistent with the finding that the lack of A-RAF did not affect the regulation of ERK in mouse embryonic fibroblasts (MEFs) (Mercer et al., 2002).

Due to widespread apoptosis throughout the embryo, C-RAF-deficient mice die in midgestation (Wojnowski et al., 1998; Huser et al., 2001; Mikula et al., 2001). The severity of the phenotype was relieved with the outbred genetic background. The unusual observation that ERK activation by growth factors was not compromised in *C-RAF*^{-/-} MEFs, implied that C-RAF plays an indispensable role for survival, probably in a kinase-independent way. The *C-RAF*^{FF/FF} knockin mouse model with Y340FY341F mutations further confirmed this hypothesis to a certain extent, in that the mice which express a C-RAF mutant that is refractory to growth factor stimulation, could rescue the knockout phenotype, resulting in viable and apparently normal mice (Huser et al., 2001).

Since the *C-RAF*^{-/-} phenotype resembles that of *k-ras*^{-/-} mice, C-RAF seemingly is a main effector of K-Ras, with a major task to restrain the function of proapoptotic pathways, such as Fas signalling. Indeed, C-RAF null MEFs exhibited increased sensitivity to Fas-induced apoptosis (Huser et al., 2001; Mikula et al., 2001), and the anaemia in *C-RAF*^{-/-} animals was associated to the elevation of caspase activity that accelerated erythroid differentiation leading to depletion of erythroid progenitor cells (Kolbus et al., 2002). Some effectors like BAD, distinct from MEK and ERK, may mediate C-RAF's antiapoptotic function (Troppmair and Rapp, 2003).

B-RAF null mice die in midgestation due to haemorrhage caused by massive apoptosis of endothelial cells, together with some neurological abnormalities, namely disturbed growth and differentiation of the neuroepithelium (Wojnowski et al., 1997). Especially *B-RAF*^{-/-} mice show severely affected ERK activation (Wojnowski et al., 2000), implying that B-RAF plays its essential role at least partially, if not exclusively, through downstream ERK signaling. Indeed, disruption of the *Erk2* locus leads to embryonic lethality early in mouse development

and some dramatic defects in various tissues (Hatano et al., 2003; Saba-El-Leil et al., 2003; Yao et al., 2003).

Primary neuronal culture experiments suggested that B-RAF has an essential and specific function in mediating survival of sensory and motoneurons during development, possibly related with upregulation of IAP proteins which are downstream regulators of neuronal survival in response to neurotrophic factors (Wiese et al., 1999; Wiese et al., 2001). Recently enhanced cell death in the forebrain of *B-RAF^{-/-}* embryos has been observed, comparable to that in *bag^{-/-}* genotype (Gotz et al., 2005). In addition, analysis of *B-RAF^{-/-}* mice modified by the mixed background, together with directed differentiation of B-RAF deficient ES cells, identified a role for B-RAF during hematopoietic progenitor cell development as well as during megakaryocytopoiesis (Kamata et al., 2005).

On the basis of the available data, it is rational to expect that B-RAF has important and probably complex isotype- or isoform-specific roles during mouse embryogenesis after midgestation, particularly in development of central nervous system (CNS).

In order to elucidate the interactive relation for functions of B-RAF and C-RAF in embryonic development, complex mutants in both *B-RAF* and *C-RAF* loci were obtained and analyzed (Wojnowski et al., 2000). The loss of one additional allele (*C-RAF^{-/-}/B-RAF^{+/-}* or *C-RAF^{+/-}/B-RAF^{-/-}*) increased dramatically the extent of abnormalities and led to the death of 90% of the embryos before E10.5. Surprisingly, the disruption of all four copies in two loci abrogated the differentiation of most embryonic lineages, but had no effect on cell proliferation and implantation of the embryo. These data implied that B-RAF and C-RAF share an indispensable role to drive subsequent development after blastocyst stage. In the mice deficient of both A-RAF and C-RAF, a more severe phenotype than single null mutations of either gene appeared (Mercer et al., 2005). They die at E10.5, with a generalized reduction in proliferation. C-RAF and A-RAF have a combined role in controlling

physiological transient ERK activation as well as maintenance of cell cycle progression at its usual rate.

Cellular function of individual RAFs

Accurate regulation of ERK by RAFs is crucial to the balance of biological responses that a cell can make, with both the intensity and duration of ERK activity being important. For example, Platelet-derived growth factor (PDGF)-induced proliferation requires sustained ERK activity in fibroblasts (Weber et al., 1997), but when RAF is manipulated to induce strong ERK signalling, cell-cycle arrest occurs owing to the transcriptional induction of cell-cycle inhibitors such as p21^{Cip1} (Woods, 1997; Kerkhoff and Rapp, 1998).

In ventricular myocytes, acidic fibroblast growth factor activates C-RAF but not A-RAF, whereas endothelin-1 activates both isoforms (Bogoyevitch et al., 1995). Furthermore, stimulation of ventricular myocytes with TPA induces sustained A-RAF activity, but C-RAF is only transiently activated. In endothelial cells, where C-RAF is linked to survival, basic fibroblast growth factor seems to induce C-RAF activity predominantly through the phosphorylation of S338, whereas vascular endothelial growth factor stimulates C-RAF activation predominantly through Y341 phosphorylation (Alavi et al., 2003). Intriguingly, interleukin-3 activates A-RAF in primary mouse bone-marrow cells in a PI3K-dependent manner, whereas C-RAF activation in this system is independent of PI3K (Sutor et al., 1999).

In neuronal cells, epidermal growth factor preferentially activates C-RAF, whereas nerve growth factor preferentially activates B-RAF (Corbit et al., 2000; Kao, 2001). As a result, C-RAF-induced transient ERK activity leads to proliferation, whereas B-RAF-induced sustained activity leads to differentiation (Marshall, 1995). Stimulation by NGF in PC12 cells requires internalization of TrkA (York et al., 2000) to intracellular vesicles containing Rap1, B-RAF, MEK and ERK (Wu et al., 2001). Though several *in vitro* studies strongly implicate RAS–

RAF–ERK in the regulation of axon extension at least for peripheral neurons, the issue of which isotype of RAFs is required for axon growth remains unclear (Markus et al., 2002).

1.4. Experimental design and aim of the project

Potential role of B-RAF in forebrain development

Unlike the other isoforms, B-RAF has been shown to have an important function for normal CNS development, at least for neural cell survival in forebrain and spinal cord (Wojnowski et al., 1997; Wiese et al., 2001; Gotz et al., 2005). No specific other role has yet been assigned to B-RAF in mouse development after midgestation, when the majority of brain development occurs, because the lethality of *B-RAF*^{-/-} mice between E10.5 and E12.5 precludes an opportunity to further analyze its function at a later stage (Wojnowski et al., 1997).

During mammalian CNS development, the neocortex arising from the dorsal telencephalon will undergo rapid expansion by midembryogenesis so that it will become the predominant brain structure. As development proceeds, the neocortex is partitioned into anatomically distinct areas along the A/P and mediolateral axis. For example, the motor and sensory cortices develop in the anterior and the visual cortex develops more posterior (Monuki and Walsh, 2001). Neurons of the neocortex will also be organized into six distinct layers running from the lumen of the neural tube to the margin of the cerebral wall (McConnell, 1995). These cell arrangements have functional consequences, since neurons will develop synaptic connections according to the position they occupy within the neocortical areas and layers (McConnell, 1995).

The mammalian forebrain is derived from a monolayer of germinal neuroepithelial cells, lying near the lateral ventricle in a layer known as the ventricular zone (VZ). They are also called self-renewing multi-potent progenitors, or neural stem cells (NSCs), because of their abilities of self-renewal and differentiation into neurons and glia. These most immature progenitor cells generate mitotic and lineage-restricted intermediate progenitor cells.

Postmitotic neurons are generated between embryonic day 10.5 (E10.5) and E17 from cortical progenitors undergoing a maximal of 11 cell cycles (Takahashi et al., 1999). Upon one division, a neurogenic progenitor cell in the ventricular zone (VZ) can produce one proliferating progenitor and one postmitotic neuron. The neocortex is a highly organized structure of six layers, which are formed by sequential waves of postmitotic neurons that migrate away in radial direction from the germinal zone towards the pial surface. The first wave of migrating neurons establishes the preplate (PP), and the second wave of neurons subsequently splits the PP into a superficial marginal zone (MZ) and a deeper subplate, through the formation of a cortical plate (CP) in the middle. Thereafter, sequential waves of cortical neurons migrate past their predecessors and finally position themselves underneath the MZ to expand the CP. Hence, the deeper layers of the CP are occupied by early-born neurons, while the superficial layers are formed by the later-born neurons, featuring the ‘inside-out’ generation of the cortex (Angevine and Sidman, 1961).

It has been shown that growth and patterning of the neocortex are strictly dependent on localized production of instructive signals, such as growth factors and neurotrophins (Dono, 2003; Medina et al., 2004), acting on the cortical cells. Moreover, active ERK signalling appears in CNS area including forebrain (Corson et al., 2003), and MEK–C/EBP (mitogen-activated-protein-kinase kinase and CCAAT/enhancer-binding protein) pathway plays a role in the promotion of growth factor-mediated cortical neurogenesis (Menard et al., 2002). All of them strongly suggest that RAF family, most promisingly B-RAF, is involved in regulation of survival, growth and differentiation of developing forebrain.

Rescued B-RAF null mice to be analyzed

In order to elucidate the role of B-RAF in developing brain as well as other tissues, *B-RAF^{KIN/KIN}* mice has been created in our group, which express a chimeric RAF but not naive B-RAF in the *B-RAF* locus (Tyrsin, Ph.D. thesis) (Fig. 1.6). The artificial kinase combines the

extra N terminus of B-RAF with all the domains of A-RAF, aimed to rescue the early lethality by mimicking a hypomorphic B-RAF with minimal kinase activity. As expected, the mutant mice in CD-1 background were protected from endothelial apoptosis and survived beyond midgestation, showing no obvious developmental defects. Importantly, motoneurons in the spinal cord and the progenitors in the forebrain were also rescued from death, which indicated overall prevention of abnormal apoptosis in neural cell lineages. Apparently, these knockin mice provide the opportunity to discover the proliferation- and differentiation-oriented effects of B-RAF in development of brain and spinal cord.

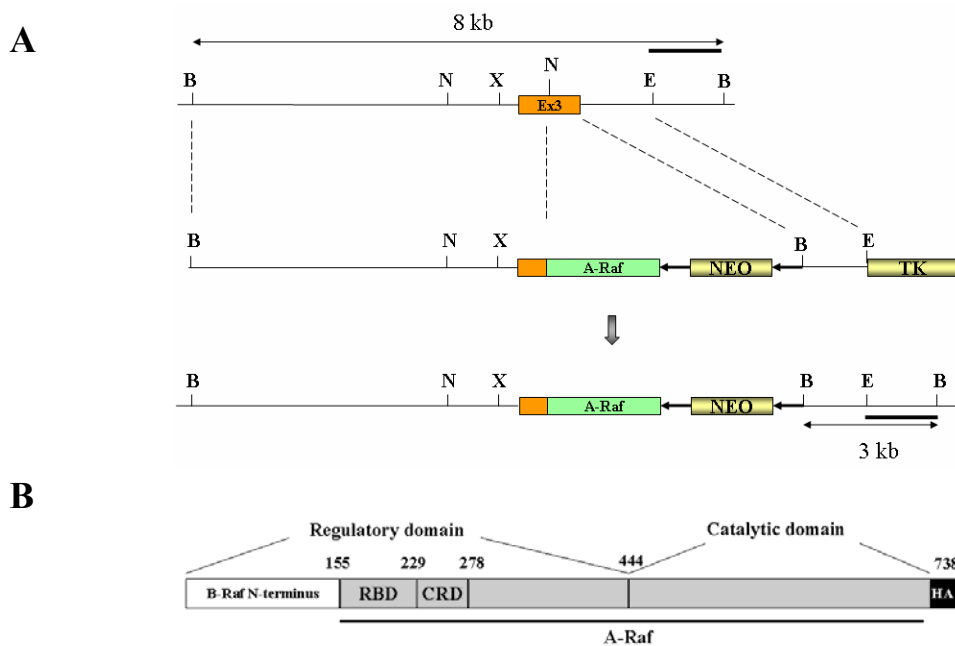


Fig. 1.6 The design for generation of *B-RAF*^{KIN/KIN} mice. **A.** Targeting strategy of the *B-RAF* locus. **B.** The chimeric protein combined the extra N terminus of mouse B-RAF and all the domains of A-RAF. (Modified from Tyrsin, Ph.D. thesis)

Using this rescued B-RAF null mice, we planned to explore a potential role of B-RAF in embryonic forebrain through a detailed investigation of *B-RAF*^{KIN/KIN} animals focusing on cortical development, a complex process in which extrinsic and intrinsic factors modulate the sequential generation of neurons and glia from precursors after successive rounds of division.

Conditional B-RAF KOs to be generated

In conventional gene targeting, disruption of target gene is already present in the germ line, thus affecting all tissues during the entire lifespan of the resulting mouse. Incidence of an embryonic lethal phenotype, existence of unwanted pleiotropic side effects and appearance of complicated accumulative phenotype are the most disadvantageous to the detailed discovery of the endogenous gene function. Using conditional KO models, allowing the deletion of genetic material/gene function in selected cells at a specific time, one can efficiently avoid embryonic lethality, prevent unwanted pleiotropic side effects and exclude accumulative compensatory developmental changes starting from the earliest developmental stage.

The flexible use of site-specific recombinases such as Cre and the successful development of the reversible tetracycline-based switch have proved to be powerful avenues for creating conditional loss-of-function mouse models (Gossen and Bujard, 2002). In a certain mouse line, where two recombinase recognition sites, loxP are neutrally introduced in the intronic sequence around essential exon(s) of a target gene, tissue-specific transgenic Cre expression will lead to genomic deletion of flanked-by-loxP (floxed) exon(s) and thus functional silencing of this targeted gene in a spatial way. On the other hand, when tetracycline-regulatory system, composed of transactivator unit and responder unit, is incorporated into an endogeneous gene locus as a switch ('knockin'), timed administration or depletion of doxycycline (Dox) can turn off endogenous expression of this target gene in a temporal way, depending on the transactivator type (Shin et al., 1999; Bond et al., 2000).

To study the *in vivo* function of B-RAF in adult mice and uncover unknown roles in embryonic neurogenesis as well as other morphogenesis, conditional *B-RAF* knockouts would be the ideal models. Following the above strategies, generation of *floxed B-RAF* and *tetracycline-regulated B-RAF* mouse lines was to be attempted in order to obtain a tool for the detailed examination of B-RAF in CNS development.

2. RESULTS

Part I. Analysis of B-RAF null mice

2.1. Developmental expression of B-RAF kinase in embryonic forebrain

In the forebrain of *B-RAF*^{-/-} mice maintained on the inbred strain C57Bl6, there was enhanced cell death during midgestation (Gotz et al., 2005); in addition endothelial cell death also occurred during midgestation leading to the lethality around E11.5 (Wojnowski et al., 1997). No specific other role beyond maintenance of survival has yet been assigned to B-RAF in complicated forebrain development after midgestation, due to the embryonic death. The continuous expression of B-RAF in embryonic forebrain is indication of an essential role of B-RAF in neural cells after they have passed through the critical phase of naturally occurring cell death. To elucidate the role of B-RAF in development of central nervous system and other organs, *B-RAF*^{KIN/KIN} mice have been created in our group, which are B-RAF deficient but express a chimeric protein consisting of the unique N terminus of B-RAF and all the domains of A-RAF in the *B-RAF* gene locus (Tyrsin, Ph.D. thesis). In contrast to *B-RAF*^{-/-} (KO) mice, *B-RAF*^{KIN/KIN} (KIN) mice in CD-1 background survived after midgestation because their endothelial cells were protected from apoptosis. More importantly, overall prevention of abnormal neural apoptosis made this animal a useful model to study proliferation- or differentiation-oriented function of B-RAF other than its survival effects in forebrain development.

Using a specific antibody against the C terminus of B-RAF, we detected no B-RAF protein in the KIN forebrain lysates, while expression of B-RAF was clearly observed in WT from E12.5 to E16.5 (Fig. 2.1). Western blot analysis with an antibody against the C terminus of A-RAF demonstrated that KIN animals expressed the chimeric RAF, composed of the unique N terminus of B-RAF and most the parts of A-RAF, whereas the steady-state level of endogenous A-RAF in KIN was the same as in the control (Fig. 2.1). Notably, the expression

level of the chimeric RAF was lower than that of endogenous A-RAF in *B-RAF*^{KIN/KIN} forebrain, detected by the same antibody.

It is known that in adult mouse tissues such as cerebrum and cerebellum, the *B-RAF* gene encodes different isoforms by the presence or absence of alternatively spliced exons 8b and 10 (Barnier et al., 1995). Intriguingly, the sequence encoded by exon 10 is found only in B-RAF isoforms from neural tissues. Therefore, the expression of B-RAF isoforms remains to be examined in embryonic forebrain. In accordance to endogenous expression, a certain isoform of B-RAF can be selected for the rescue experiments to dissect out the isoform-specific role of B-RAF in growth and patterning of cerebral cortex.

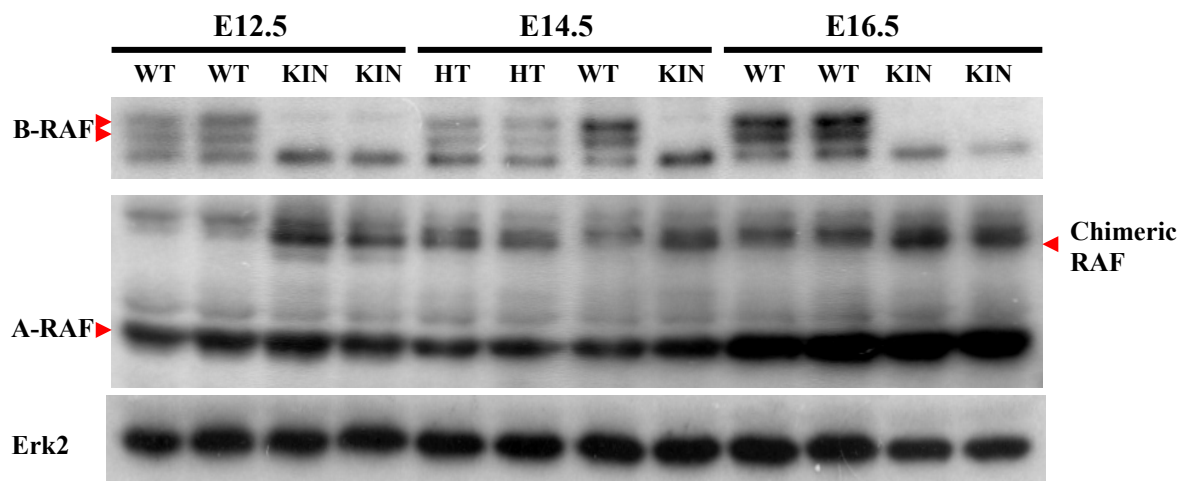


Fig. 2.1 Expression of RAF kinases in developing forebrain of mouse embryos. Proteins from forebrain extracts were separated on denaturing polyacrylamide gels, transferred to nitrocellulose membrane and treated with the antibody against the C terminus of B- or A-RAF. Chimeric RAF was detected with the anti-A-RAF antibody, as expected. Erk2 immunoblot was used as protein loading control.

RT-PCR to amplify selectively exon10-containing isoforms detected their expression in developing forebrain, but two primers amplifying from exon 8a to exon 11 failed to obtain the signal from exon 10-containing transcripts in total *B-RAF* mRNA (Fig.2.2). Thus, this result showed that there was the low percentage of exon 10-containing isoforms in total *B-RAF* transcripts at the examined stages.

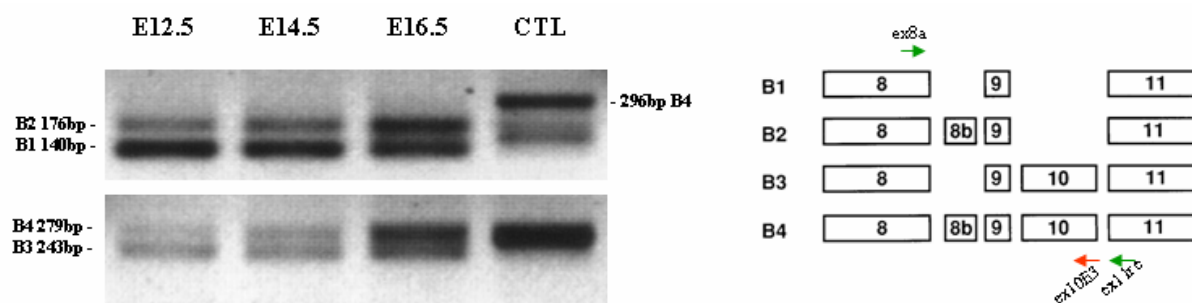


Fig. 2.2 The exon10-containing isoforms in total *B-RAF* transcripts of forebrain were detected in RT-PCR not by two primers amplifying from exon 8a to exon 11 (upper panel), but by those selectively from exon8a to exon10 (lower panel). The scheme (right) showed 4 different B-RAF isoforms in terms of splicing of exons 8b and 10. cDNA was synthesized from 0.05 μ g RNA by reverse transcription, and amplified with correspondent primers in 35 cycles. PCR control reaction without RT yielded no detectable fragments, and the amount and quality of cDNA were verified by amplification for β -actin (data not shown). CTL, cerebellum at postnatal day 5.

2.2. Unimpaired self-renewal NSCs in B-RAF deficient forebrains at E10.5

Neural stem cells (NSCs) with self-renewal and multipotent developmental properties, arising from a single layer of neuroepithelium after closure of the neural tube, play key roles in brain development. Stem cells undergo continuous division to generate the appropriate progenitors, which are destined for either neuronal or glial lineage. In the cerebral cortex, the majority of neurons are generated before astrocyte formation. It should be noted, so far there were only some molecular markers such as Nestin, Musashi1 and Sox1, selective rather than specific for NSCs (Okano, 2002). Based on the analysis of adherent clone production, estimates of NSC abundance for telecephalon from E10 mouse range from 5 to 20% (Temple, 2001).

The establishment of clonogenic expansion of neural stem cells by neurosphere formation (Reynolds and Weiss, 1992), as one of the major breakthroughs of CNS stem cell biology, enabled us to define the NSCs experimentally and to quantify the multilineage potency and self-renewing ability of these cells. To determine if neural stem cells in *B-RAF* deficient forebrains have been impaired in the beginning, *in vitro* neurosphere assay was done using the protocol with some modification, described by Wachs et al. (2003). Since

telencephalic neurogenesis just starts around E10.5, and *B-RAF*^{-/-} embryos are still viable at E10.5, we compared neural stem cells from forebrains of WT, KO and KIN embryos at this stage. Dissociated telencephalic cells were suspended with Neurobasal medium, containing 2% B27 Supplement, 20 ng/ml each of bFGF and EGF, 1% L-Glutamine, and 1% Penicillin/Streptomycin, and then 20,000 cells in 0.5 ml medium plated into one well of 24-well suspension culture plates in duplicate.

In the same conditions, suspension cultures from each genotype proliferated in the presence of bFGF and EGF, and formed typical neurospheres. There was no significant difference between the mutant groups and the control in terms of the frequency and size of primary neurospheres ((Fig.2.3A, C). Upon generation of secondary neurospheres, NSCs with different genotypes showed their similar ability of self-renewal (Fig.2.3B). Under differentiation conditions, both the *B-RAF*^{-/-} and *B-RAF*^{KIN/KIN} neurospheres were able to generate all three neural populations: neurons, astrocytes and oligodendrocytes, which were marked by neuron-specific β III tubulin (TuJ-1), glial fibrillary acidic protein (GFAP) and ganglioside O4 antigens respectively, as the wild-type control (Fig.2.4).

2.3. Affected neocortical development in *B-RAF*^{KIN/KIN} mice

Neurogenesis in mouse neocortex starts at around E10.5 and lasts until E17 (Takahashi et al., 1999). As neurogenesis progresses, more neural progenitor cells exit the cell cycle, differentiate into postmitotic neurons and migrate into the preplate and, by dividing it into the subplate (SP) and molecular layer (ML), form the cortical plate (CP). The deep cortical layers V and VI are generated early, whereas progressively younger neurons form cortical layers IV, III, and II.

In order to evaluate whether forebrain development is affected by the lack of B-RAF, we performed extensive histological and immunohistochemical analyses focusing on the cortex

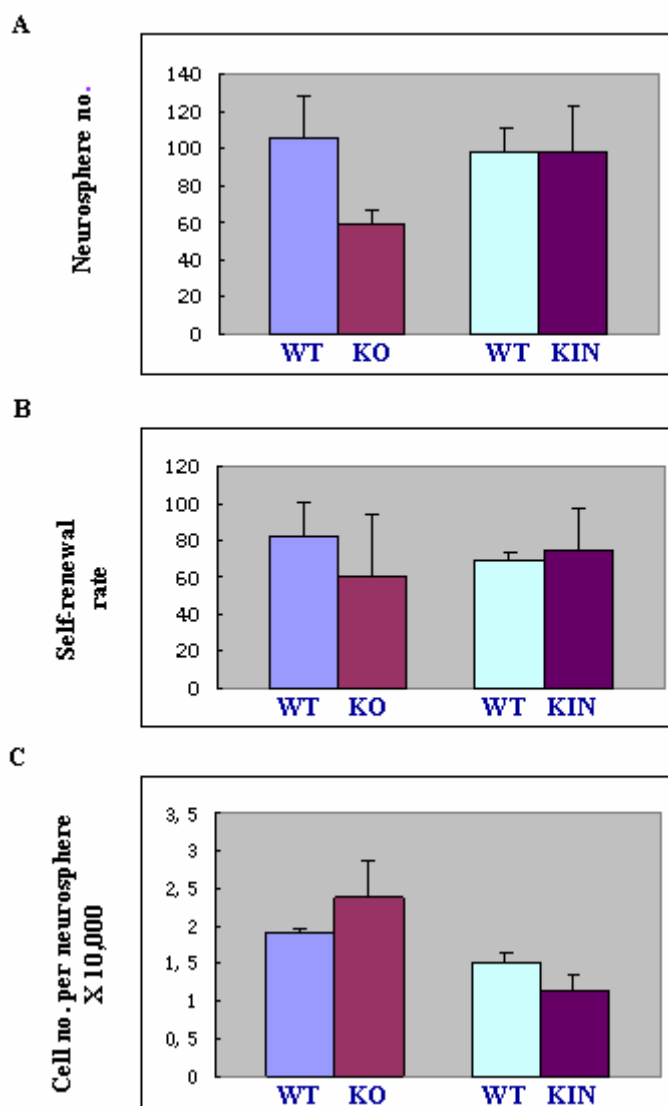


Fig. 2.3 *in vitro* neurosphere assay for neural stem cells in E10.5 forebrains. **A.** Number of primary neurospheres (\pm SD), indicating frequency of NSC in forebrain, in presence of EGF and bFGF. 20,000 cells from dissociated forebrain of individual embryos were plated and neurospheres were counted on day 12. No significant difference ($P > 0.05$) in neurosphere number between different genotypes was detected. **B.** The self-renewal ability, indexed by the average number of secondary neurospheres (\pm SD) generated by one primary neurosphere. 10,000 cells from dissociated primary neurospheres were plated and secondary neurospheres were counted on day 10. No significant difference ($P > 0.05$) in this ability between different genotypes was observed. **C.** Average size of primary neurospheres (\pm SD), showed by the total number of cells in a single neurosphere. No significant difference ($P > 0.05$) in the neurosphere size was found.

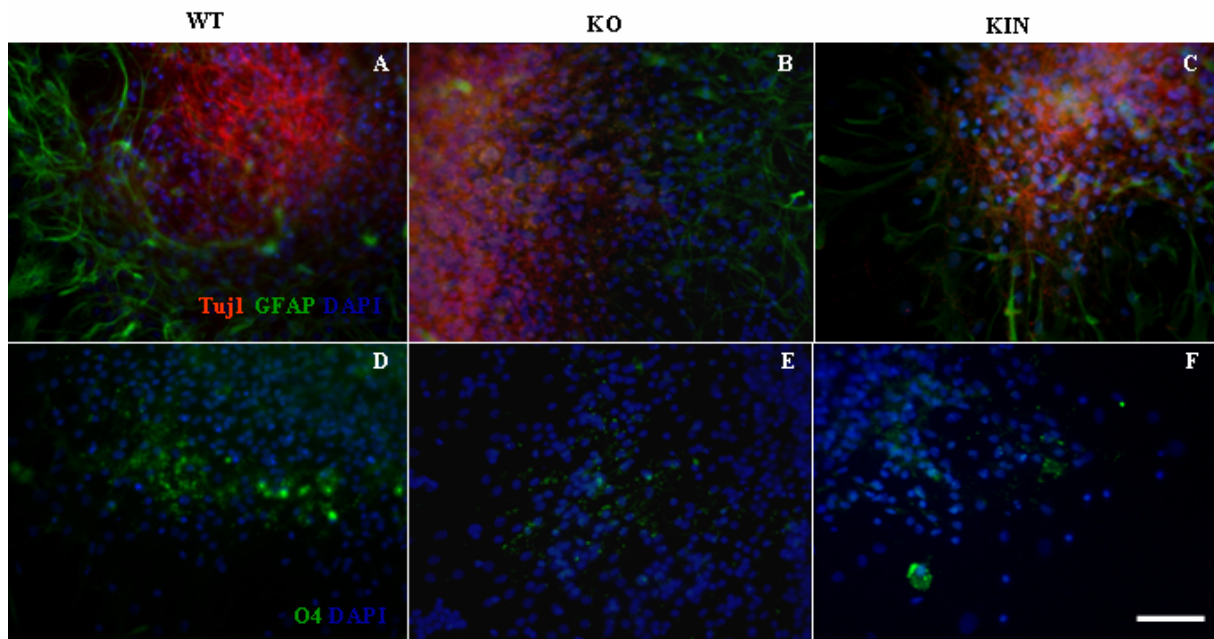


Fig. 2.4 *in vitro* differentiation of primary neurospheres in adherent culture. Primary neurospheres were grown under differentiation conditions for 14 days, fixed and stained for TuJ-1 (postmitotic neurons, red, A-C), GFAP (astrocyte, green, A-C), O4 (oligodendrocyte, green, D-F) and DAPI (cell nuclei, blue, A-F). The neurospheres from different genotypes maintained the ability to differentiate into various different cell types. Scale bars,(A-F)100 μ m.

which develops in a coordinated process of neuronal production and migration in WT and *B-RAF^{KIN/KIN}* embryos starting at E10.5.

To quantitatively assess early neuronal birth in *B-RAF^{KIN/KIN}* and control forebrains, we performed immunostaining for TuJ-1 (β III tubulin), the earliest marker of postmitotic neurons (Lee et al., 1990; Ferreira and Caceres, 1992). Corresponding serial sagittal sections of *B-RAF^{KIN/KIN}* and littermate control brains at E10.5 and E12.5 were stained with the anti-TuJ-1 antibody. No significant differences were found in the thickness and distribution of the TuJ-1 positive cells in *B-RAF^{KIN/KIN}* compared to wild-type littermates at this stage (Fig. 2.5 A-D).

The progressive change in the intensity of TuJ-1 expression defines the degree of maturation of these layers, more intense in SP and ML than in CP, in neocortex. At E16.5,

there was some apparent phenotypic change in *B-RAF*^{KIN/KIN} forebrain: Laminated structure was tightly packed and stratification of cortical neurons disorganized, compared to in WT (Fig 2.5 E-H). While the distance between the top of the SP and the pial surface was reduced nearly twofold (127µm in *B-RAF*^{KIN/KIN} embryos compared with 246µm in control cortex), the total width was reduced by only 16% (497µm in *B-RAF*^{KIN/KIN} embryos compared with 592µm in control cortex). An increase in the density of TuJ-1 positive signal covering SP and the intermediate zone (IZ) of *B-RAF*^{KIN/KIN} embryos was observed (Fig. 2.5 G, H).

This kind of cortical phenotype persisted and was even more pronounced in the cortex of postnatal viable animals (P19) (Fig. 2.6 A, B). The stratification of the cortical neurons appeared to be disorganized, without a clear boundary between cortical layers II and III in the KIN mice, compared to the wild-type littermates. The thickness of layers II–IV was reduced and the neurons, identified by NeuN labeling, were packed more densely in these cortical layers, compared to control cortex (data not shown).

To further characterize the effects of loss of B-RAF signalling during neocortical development, we examined specific populations of cortical neurons in brain sections of *B-RAF*^{KIN/KIN} and control mice at postnatal day 19 (P19) by immunostaining. The expression of Brn-2, a POU domain transcription factor expressed in pyramidal projection neurons of layers IV-II, was nearly completely lost in the *B-RAF*^{KIN/KIN} somatosensory and visual cortex areas (Fig. 2.6 C,D), whereas in the more anterior cortex, Brn-2 expression was reduced, compared to littermate controls not lacking B-RAF (data not shown).

In order to assay for the presence of an important feature of layer IV-II pyramidal neurons, the dendritic fasciculation by MAP2 staining was determined. We observed a dramatic alteration of the apical and basal cortical dendrites of *B-RAF*^{KIN/KIN} with a complete loss in the somatosensory and visual cortex areas. While in the most superficial layers dendrites appeared unfasciculated and poorly stained (Fig. 2.6 E, F), in the deepest layers

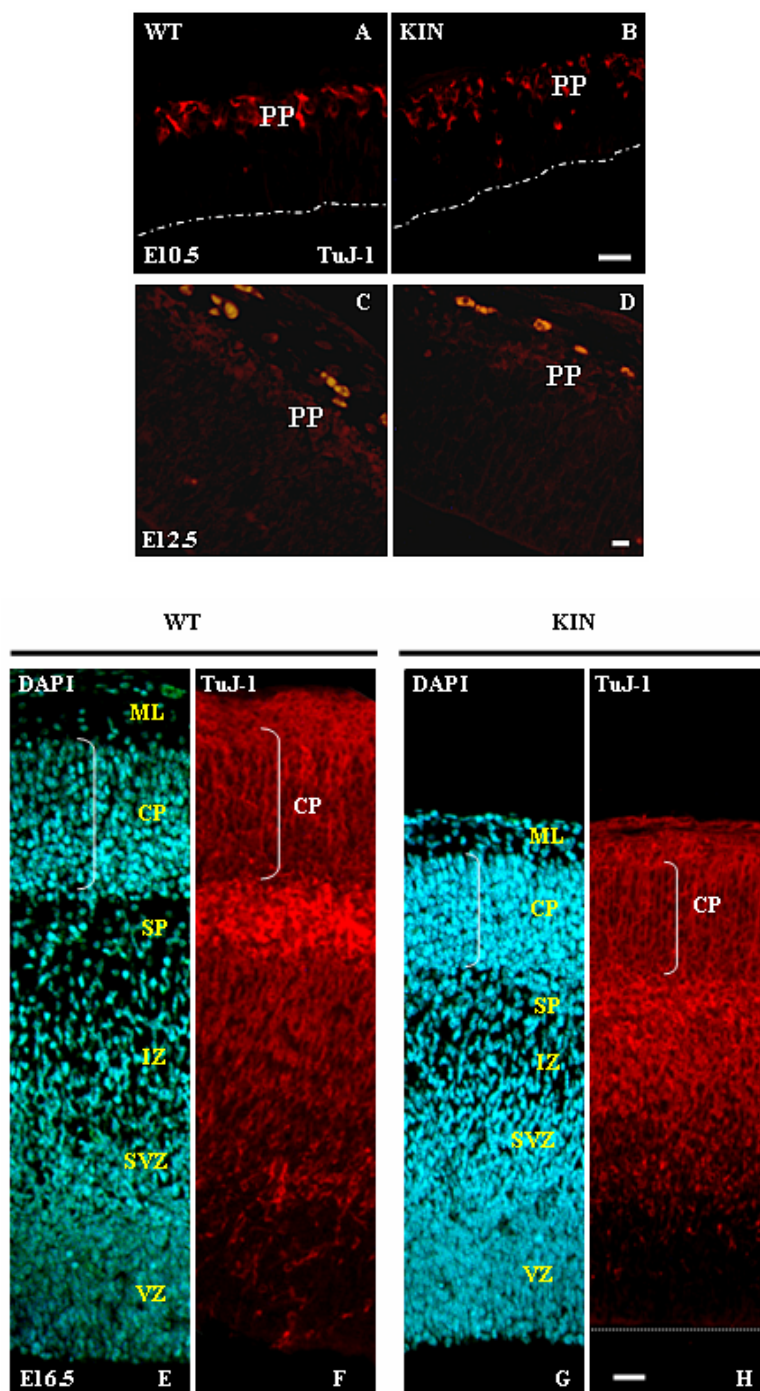


Fig. 2.5 Affected cortical development of $B\text{-RAF}^{KIN/KIN}$ mice in the late cortical plate stage. **A-D.** Localization of TuJ-1 positive postmitotic neurons in the preplate of the neocortex, noting the normal formation of the preplate in B-RAF deficient mice. **E-H.** DAPI staining and TuJ-1 immunostaining in sagittal sections of E16.5 cortices. Whereas all cortical layers were formed in $B\text{-RAF}^{KIN/KIN}$ embryos, the width of cortical plate in $B\text{-RAF}^{KIN/KIN}$ embryos was much more reduced than the total width, paralleled by an increased density of TuJ-1 positive cells. The developmental stages and genotypes are indicated. Scale bars, (A-B) 50μm, (C-D) 20μm, (E-H) 100μm.

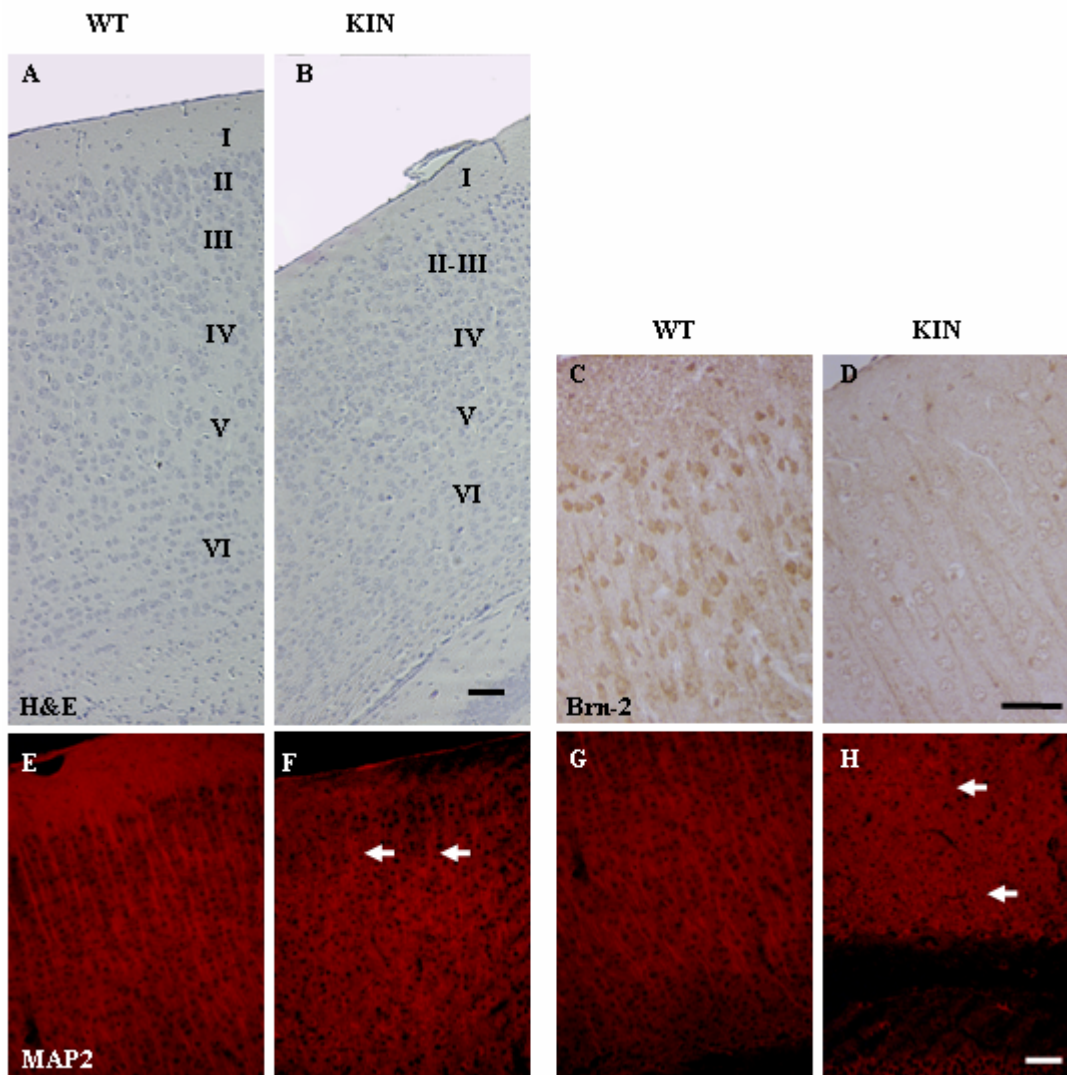


Fig. 2.6 Cortical phenotype in postnatal *b-raf*^{KIN/KIN} mice. **A,B.** H&E staining of sagittal sections of the wild-type and mutant cortex. The cell layers I-IV are indicated. **C,D.** Reduction of Brn-2 positive pyramidal neurons in the mutant. **E-H.** Loss of MAP-2 staining indicative of a loss of dendritic fasciculation (arrows) in layers II and III of mutant cortex. Scale bars, (A-B) 200 μ m, (C,D) 50 μ m, (E-H) 100 μ m.

(V–VI) staining of fibers and cell bodies was slightly reduced in *B-RAF*^{KIN/KIN} compared to controls (Fig. 2.6 G, H).

These observations may have been caused by a variety of reasons, a loss of these neurons through apoptosis, a decreased generation of new neurons, a lack of migratory cues or an impaired cell-intrinsic migratory potential of the neurons themselves. Any defect in its own or in combination would be predicted to result in the above described layering defect.

2.4. Reduced proliferation of late progenitor cells in *B-RAF*^{KIN/KIN} cortex

Because there was no increased apoptosis in *B-RAF*^{KIN/KIN} cortex from E10.5 to postnatal day 19 (data not shown), we could exclude a loss of neurons as the cause for the thinning of the cortex from E16.5 onwards. We next examined the proliferation of cortical progenitors by bromodeoxyuridine (BrdU) labelling (Fig. 2.7 A-F). Up to E13.5, there was no significant difference in the number of BrdU-labelled cells in the VZ of *B-RAF*^{KIN/KIN} embryos compared with wild-type (E10.5: 48%±3% in WT, 48%±6% in *B-RAF*^{KIN/KIN}; E13.5: 36%±4% in WT, 31%±6% in *B-RAF*^{KIN/KIN}). A slightly reduced cell proliferation in the VZ of *B-RAF*^{KIN/KIN} neocortex was observed at E14.5 that was further reduced at E16.5 (E14.5: 34.5%±0.99% in WT, 25.26%±0.31% in *B-RAF*^{KIN/KIN}; E16.5: 21.88%±0.99% in WT, 11.77%±0.31% in *B-RAF*^{KIN/KIN}) (Fig. 2.7 G).

These results indicate that B-RAF has an essential role in the proliferation of late cortical progenitor cells, and that the reduction in cortical cell production could be one cause of the hypoplastic cortex seen in the *B-RAF*^{KIN/KIN} postnatal brain.

E15.5 and E16.5 cortical progenitor cells produce neurons that make up the more superficial layers II-IV of neocortex. Our observation of reduced proliferation of late progenitor cells may explain in part the reduction in the thickness of the adult cortex in *B-RAF*^{KIN/KIN} embryos. However, the nearly complete lack of Brn-2 positive pyramidal projection neurons in postnatal *B-RAF*^{KIN/KIN} mice (Fig.2.6H) would not be consistent with an only twofold reduction in progenitor proliferation at E16.5, because we observe only a small reduction in the number of Brn-2 positive cells in E16.5 VZ, IZ and CP *B-RAF*^{KIN/KIN} mice compared to wild-type (data not shown). Therefore, we next investigated whether the migration of neurons would be disrupted.

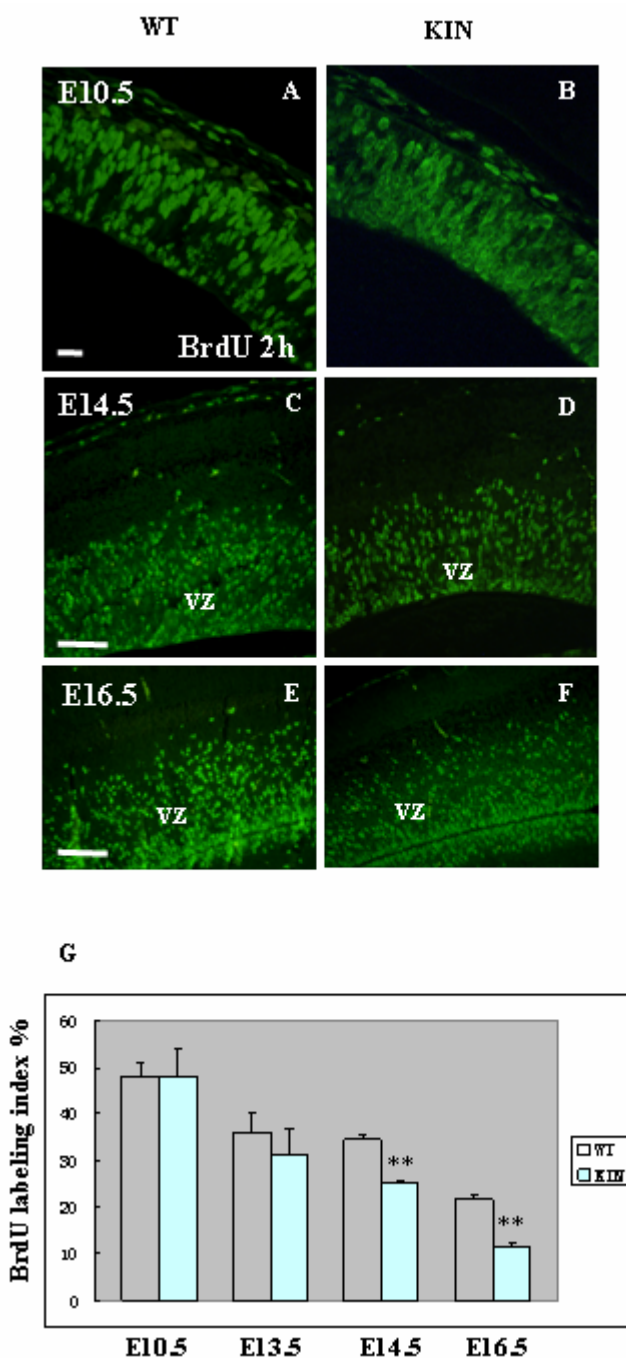


Fig. 2.7 Reduced proliferation specifically in late progenitor cells in $B\text{-RAF}^{KIN/KIN}$ embryos. **A-F.** Localization of BrdU incorporation in sagittal sections of the developing cortex, in note of impaired proliferation from E14.5 in $B\text{-RAF}^{KIN/KIN}$ embryos. **G.** Quantification of BrdU-positive cells. The developmental stages and genotypes are indicated. Scale bars, (**A, B**) 50 μm , (**C-F**) 100 μm .

2.5. Impaired migration of late-born cortical neurons in *B-RAF*^{KIN/KIN}

To assess cell migration defects of the late-born neurons we birthdated the acutely generated cortical neurons in control and *B-RAF*^{KIN/KIN} embryos with BrdU at E14.5, and analyzed the extent of their migration at E17.5. Many BrdU-labelled cells were distributed in the CP close to the ML in control embryos, while only a few labelled cells were seen in *B-RAF*^{KIN/KIN} embryos, as shown (Fig. 2.8 A, B). Significantly, the relative number of BrdU-positive cells around CP was decreased in *B-RAF*^{KIN/KIN} embryos (Fig. 2.8 C).

Correct neuronal migration requires both radial glial fibers as guiding scaffolds for migrating neurons (Rakic, 1972) and guidance cues such as Reelin secreted from Cajal-Retzius neurons that play a key role in neuronal lamination (Ogawa et al., 1995; Rice and Curran, 1999). The alignment and density of radial glial fibers, labelled with an antibody against nestin, were not altered in *B-RAF*^{KIN/KIN} (Fig. 2.8 D-G). Furthermore, neither the number of Cajal-Retzius neurons nor their expression of Reelin, as judged from immunolabeling, was changed in the cortex of *B-RAF*^{KIN/KIN} embryos (Fig. 2.8 H-K). Thus, the migration defect in the *B-RAF*^{KIN/KIN} cortex does not seem to be a consequence of a disrupted radial glial fiber system or a loss of Reelin-expressing Cajal-Retzius neurons, but most probably is caused by a cell-autonomous neuronal defect.

2.6. Attenuated activation of ERK in *B-RAF*^{KIN/KIN} telencephalon

Previous studies showed that there is little, if any, phospho-ERK1/2 in different types of B-RAF deficient cells (Wojnowski et al., 2000; Pritchard et al., 2004; Kamata et al., 2005; Brummer et al., 2002). In order to investigate the biochemical basis underlying the proliferation defects of *B-RAF*^{KIN/KIN} cortical progenitors, ERK phosphorylation was examined for *B-RAF*^{KIN/KIN} forebrain lysates and found to be significantly reduced compared to WT embryos (Fig. 2.9 A, B). At E10.5, the amount of phospho-ERK in *B-RAF*^{KIN/KIN}

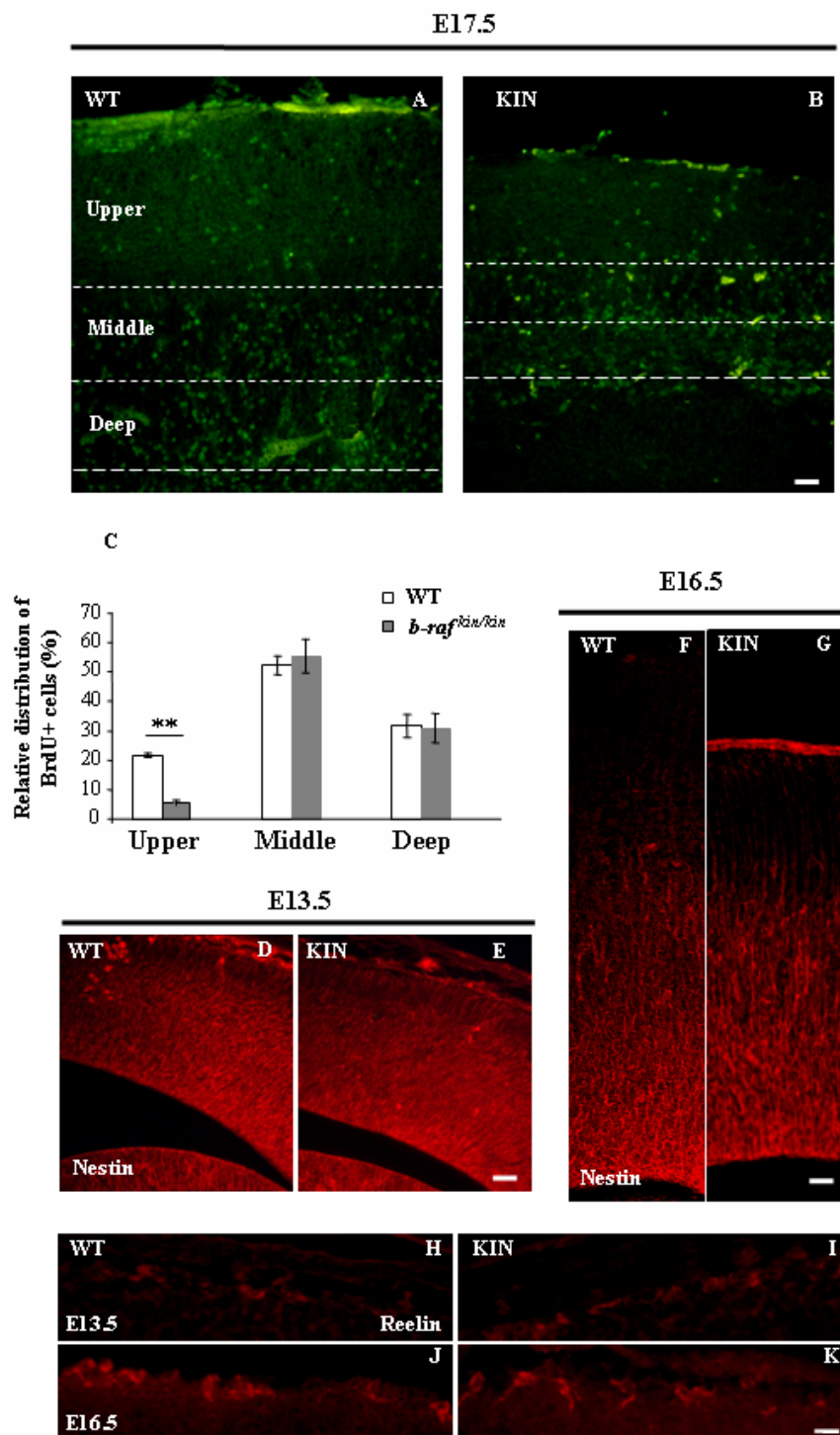


Figure 2.8 Impaired migration of late-born neurons in *B-RAF*^{KIN/KIN} mice. **A-B.** BrdU immunofluorescence of E17.5 neocortex, neuron-birthdated by BrdU at E14.5. **C.** Relative distribution of BrdU-positive cells (mean \pm SD) shows a reduction in the upper neocortex indicative of a defect in radial migration (n=3; t test p<0.01). **D-G.** Nestin staining reveals a comparable number of radial glia cells and their fibres. **H-K.** Reelin staining reveals similar numbers of Cajal Retzius neurons and the guidance cue Reelin in wild-type and in *B-RAF*^{KIN/KIN} embryos. The developmental stages and genotypes are indicated. Scale bars, (**A, B, D-G**) 100 μ m, (**H-K**) 50 μ m.

forebrains appeared slightly increased compared to *B-RAF* knockout. We also checked whether phosphorylation of AKT (PKB) was altered in *B-RAF*^{KIN/KIN} forebrain lysates, since the PI3K/AKT pathway is in parallel activated by tyrosine receptor kinases. Intriguingly, there was no apparent difference of AKT phosphorylation between those genotypes (data not shown).

A more detailed analysis of ERK activation was performed in dissociated cells of the telencephalon. Cortical progenitors isolated from E12.5 mouse forebrain were cultured in serum-free medium without exogenous growth factors only for four hours and then stimulated over a time course of 0 to 60min with bFGF, a key mediator of survival and cell migration. Consistent with the brain lysate data, both the basal and stimulated level of pERK in cultured *B-RAF*^{KIN/KIN} cells was significantly lower than that in control (Fig. 2.9 C, D). There was no apparent difference in the time course of ERK phosphorylation following stimulation.

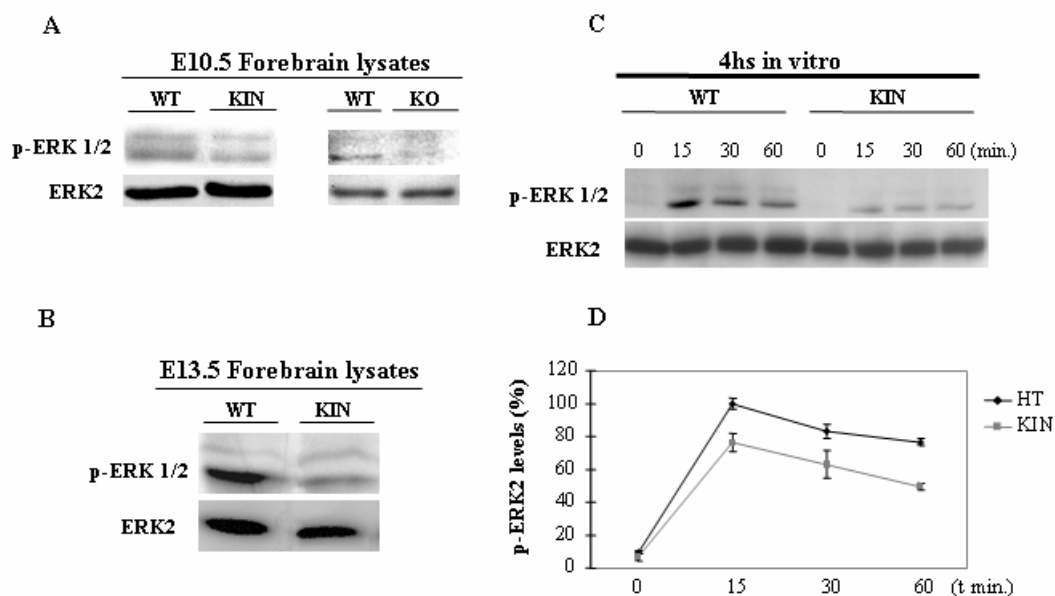


Fig. 2.9 ERK activation in *B-RAF*^{KIN/KIN} forebrain. **A-B.** Western blot for phospho-ERK from forebrain lysates. **C.** Western blot analysis in short term cultures established from E12.5 forebrain unstimulated or stimulated with basic FGF for the times indicated. **D.** Densitometric quantification of phospho-ERK levels in short term culture lysates analyzed by immunoblotting (mean \pm SD; n=3). The developmental stages and genotypes are indicated.

2.7. Abnormalities of Actin Cytoskeleton in *B-RAF*^{KIN/KIN} cortical neurons

ERK has recently been implicated as a regulator of the actin cytoskeleton in neuronal cells by transcriptional mechanisms (Harada et al., 2001) or direct phosphorylation of actin-binding proteins (Futter et al., 2005). To ask whether subcellular distribution of phospho-ERK is changed in neurons of *B-RAF*^{KIN/KIN} forebrain, we cultured cortical progenitor cells for two days on poly-D-lysine/laminin substrate in serum-free medium in the presence of bFGF to induce their neuronal differentiation and neurite outgrowth. Then, we performed immunostaining with an anti-phospho-ERK antibody. We observed that the majority of pERK is membrane-associated in wild-type cortical neurons (Fig. 2.10 A, C, D). In contrast, in *B-RAF*^{KIN/KIN} neurons, the preferential membrane localization is disrupted, with a prominent cytosolic distribution (Fig. 2.10 B, E, F). We have quantitated membrane phospho-ERK immunofluorescence and found that the ratio of membrane- versus cytosol- associated signal is only 29% in *B-RAF*^{KIN/KIN} neurons, in contrast that 88% in wild-type cortical neurons (Fig. 2.10 G).

Next, we sought to determine obvious abnormalities in the actin cytoskeleton in *B-RAF*^{KIN/KIN} cells. Staining of cortical neurons with phalloidin revealed that the membrane associated staining seen in wild-type cells is changed to a largely cytosolic distribution (Fig. 2.10 H-M). By quantitation, it was indicated that the ratio of membrane- versus cytosol-associated signal is only one-third as much in *B-RAF*^{KIN/KIN} neurons as the value in wild-type cortical neurons (Fig. 2.10 N).

2.8. p35 expression in *B-RAF*^{KIN/KIN} cortical neurons

The p35/Cdk5 (cyclin-dependent kinase 5) complex plays an important role in the proper establishment of neocortical layers. Its key targets include various instrumental proteins for cell movement, for example, N-cadherin with adhesive properties, and Actin/Tubulin as

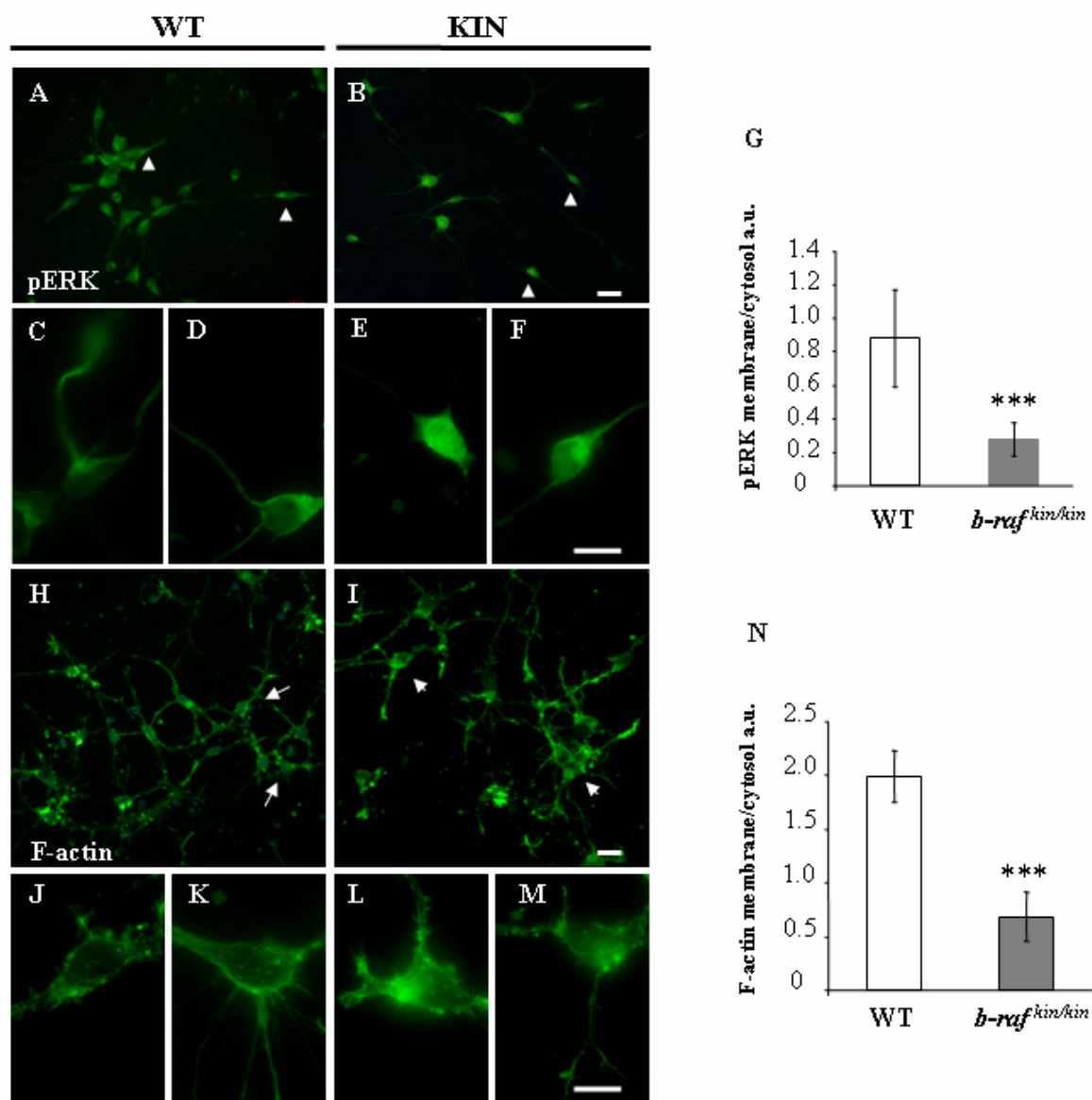


Fig. 2.10 Abnormalities in phospho-ERK localization and actin cytoskeleton in *B-RAF^{KIN/KIN}* neurons. **A-F.** Phospho-ERK immunofluorescence of cortical neurons cultured in the presence of bFGF on poly-D-lysine/laminin. **G.** Quantification of phospho-ERK immunofluorescence intensity at the membrane and non-membrane compartments (mean \pm SD; n=3; t test p < 0.001). **H-M.** F-Actin immunofluorescence of cortical neurons. **N.** Quantification of actin immunofluorescence intensity at the membrane and non-membrane compartments (mean \pm SD; n=3; t test p < 0.001). Scale bars, (**A,B,H,I**) 50 μ m, (**C-F, J-M**) 10 μ m.

cytoskeleton components (Gupta and Tsai, 2003). Recent progress on the signaling relationship between Cdk5 and the other key proteins, involved in neocortical layer formation, indicated that p35/Cdk5 may intersect with several separate and critical signaling pathways (Bielas et al., 2004).

It is very interesting to know whether cortical migration defect in B-RAF deficient mice was mediated by affected p35/Cdk5 complex. Cdk5 is expressed ubiquitously in a number of tissues, with the highest abundance in the nervous system. However, its activity is restricted to the neural tissues because of the tissue-specific expression of its main activator p35 as well as the alternative one p39 (Tsai et al., 1994; Humbert et al., 2000). We test whether expression of p35 has been deregulated in developing KIN forebrains. In Western blot, no difference in the total amount of p35 proteins was observed between KIN and WT (Fig. 2.11). However, there might be abnormal kinase activity of Cdk5 in the mutant mice at these stages, which would be answered by a Cdk5 kinase assay experiment.

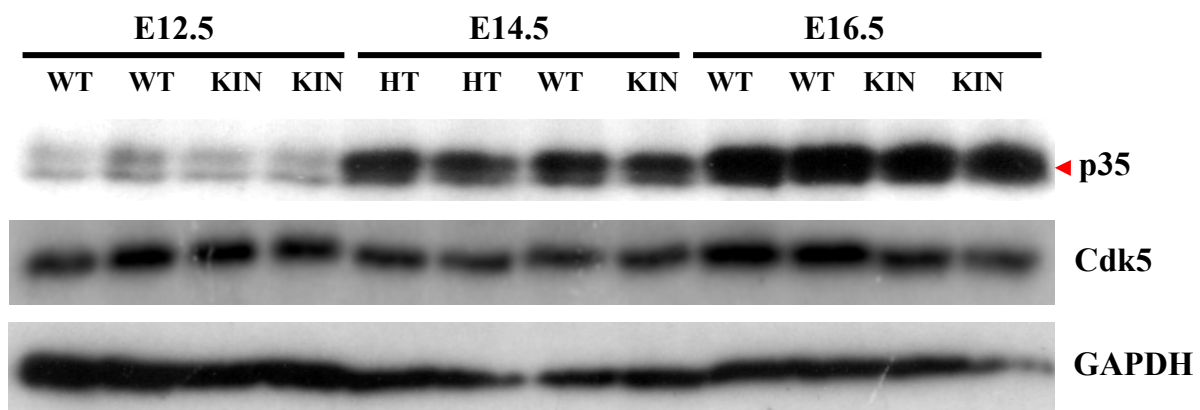


Fig. 2.11 Expression of p35, the main activator of Cdk5, in the forebrains of different littermates during neurogenesis. Western blot analysis of forebrain lysates demonstrated that p35 expression was quite similar between different genotypes.

Part II. Generation of conditional KOs

2.9. Constructing of targeting vectors for conditional KOs

To study the *in vivo* role of B-RAF in embryonic neurogenesis and postnatal brain function, conditional *B-RAF* knockouts would be the ideal tools, which can efficiently overcome those common problems from conventional knockouts, including embryonic lethality, pleiotropic side effects and accumulative compensatory changes. Two targeting strategies were employed to create conditional KOs: *floxed B-RAF* and *tetracycline-regulated (tet) B-RAF*.

The *floxed B-RAF* targeting vector (Fig 2.12) was utilized to introduce one loxP site upstream of the third exon in *B-RAF* locus, and a floxed neomycin-resistant (neo) cassette downstream of exon 3, since exon 3 is present in all of *B-RAF* splicing forms (Barnier et al., 1995) and encodes the first part of RBD domain in B-RAF protein. The construct pKSTK*neoLoxP*, containing positive (floxed PGK-neo-pA) and negative (HSV-tk-pA) selection markers, was chosen as backbone plasmid for targeting vectors. As a homology source of *floxed B-RAF* targeting vector, an 8.4kb BamHI genomic fragment encompassing the third exon of mouse *B-RAF* gene was already cloned in pBluescript KS vector, resulting in the plasmid p7.

Cut from p7 and used as 5' homologous arm, 5.2kb 5'BglII/3'SpeI-fragment containing exon3 was assembled into BamHI site upstream of neo cassette in pKSTK*neoLoxP* through two steps. In its unique XhoI site of this 5' arm, a single loxP site with short extension sequence, favorable for PCR assay, was inserted. At last, the 1.0kb 5'SpeI/3'XbaI fragment from p7 was assembled into XbaI site downstream of neo cassette as 3' homologous arm. For confirmation of homologous recombination, 5' probe was cut by BamHI-HindIII from p7, 0.5 kb in length, while 3' probe prepared by PCR using p7 template and brafgs14/gas19 primers, 0.6kb in length.

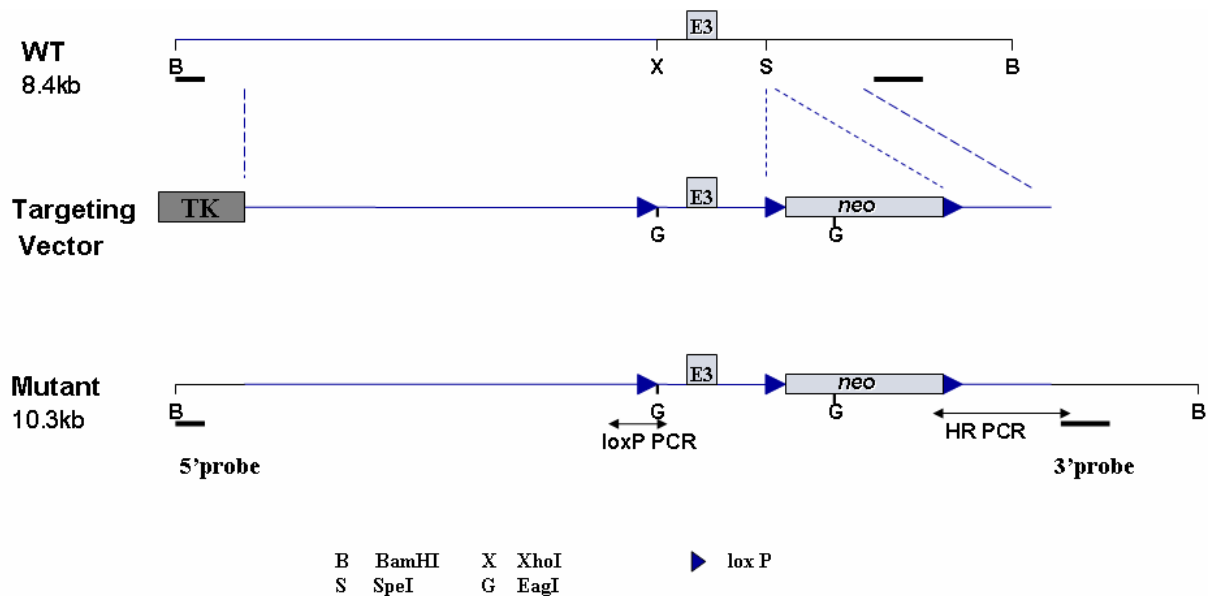
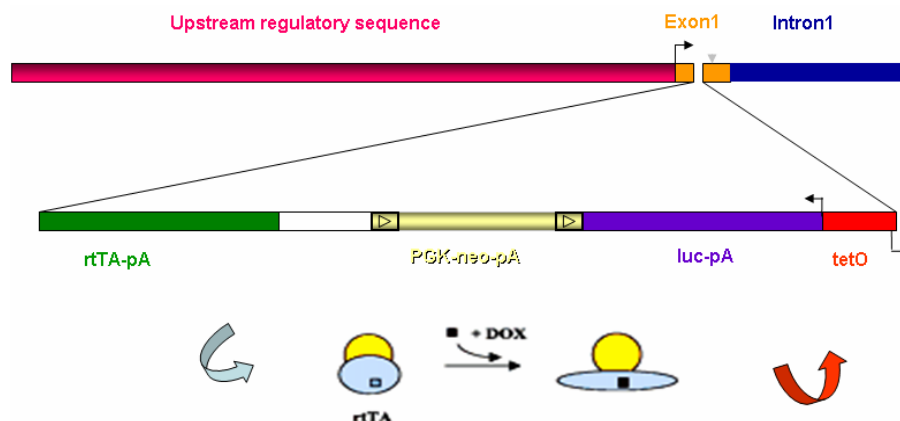


Fig. 2.12 Targeting vector for the *floxed B-RAF* locus. A single loxP site and one floxed neo cassette are introduced upstream and downstream of exon 3 (E3) in the same orientation.

In parallel, the *tet B-RAF* targeting construct was designed to insert a complete tetracycline-controlled transcription unit into the 5' untranslated region of the *B-RAF* gene, so that B-RAF expression depends on the presence of the inducer, doxycycline (Dox) (Fig. 2.13). In the homology source plasmid, L34-37 for *tet B-RAF* vector, a 9.5-kb EcoRI genomic fragment harboring the first exon of mouse *B-RAF* gene was already cloned in pUC18 vector.

Released from L34-37, 5.1kb 5'PstI/3'NotI-fragment containing the untranslated part of exon1 (5' homologous arm) was fused to rtTA coding sequence (amplified from pUhr6.2) followed by pA signal. The fusion fragment was then assembled into ClaI site upstream of neo cassette in pKSTKneoLoxP. As 3' homologous arm, the 1.2kb 5'NotI/3'EcoRV fragment with translation start was released from L34-37, and ligated to bi-directional tetO promoter harboring luciferase reporter gene (isolated from pbi5). At last, this responder unit

A



B

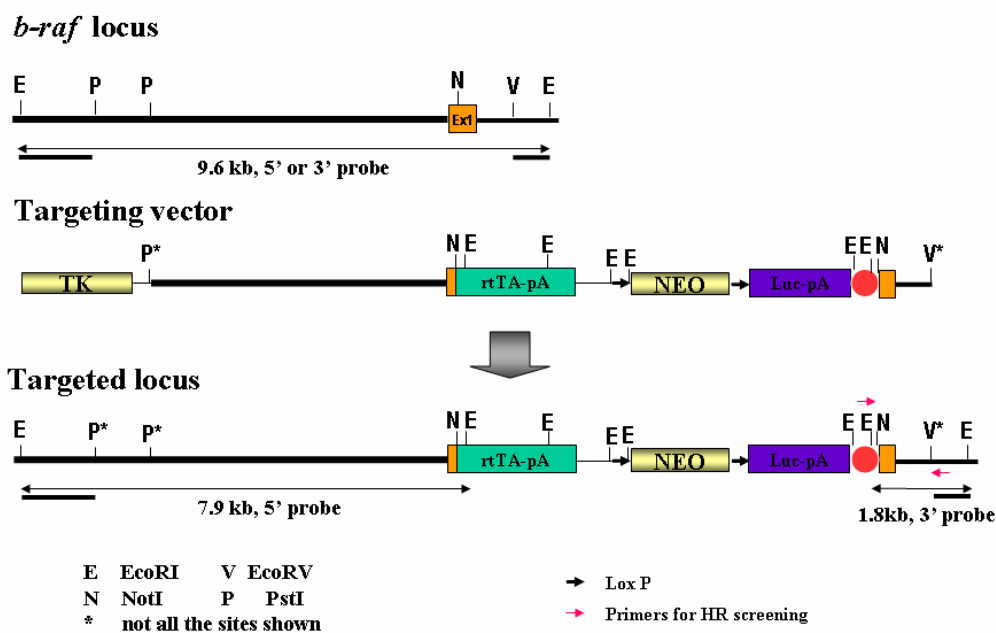


Fig. 2.13 A. The design of *tet B-RAF* locus. The endogenous *B-RAF* promoter drives expression of the transactivator *rtTA*, and then transcription of endogenous *B-RAF* gene is dependent on the presence of the inducer *Dox*. **B.** Targeting vector for *tet B-RAF* locus. *rtTA* cassette was fused to *B-RAF* promoter, and a bidirectional *tetO*-miniCMV promoter controlled luciferase reporter gene and endogenous *B-RAF*. *Neo* cassette suppressed the basal expression of responder genes.

fragment was introduced into XbaI site downstream of neo cassette. For Southern blot analysis, 5' probe was cut by EcoRI-PstI from p34-37, 1.8kb in length. Thus, 3' probe was prepared by EcoRV-EcoRI digestion of p34-37, 0.7kb in length.

2.10. Production of targeted ES clones

The *floxed B-RAF* targeting vector was linearized at the unique SalI site and electroporated into Embryonic Stem cells (ES), one R1 subclone. From two electroporations, about 200 colonies with good morphology were isolated after 350µg/ml G418 and 2µM gancyclovir double selection. Targeted clones were identified by PCR using one sense primer (neo3a) specific to the neo cassette, and the other antisense primer (Int3R+) to the genomic sequence outside the vector (see Figure 2.12). To ensure that a single loxP site upstream of exon3 did exist, PCR using primers 5XhoI and BaXh was done to selectively amplify this loxP.

Three PCR positive clones were then verified by Southern blot analysis with both 5' and 3' end probes as well as one more loxP PCR, out of which 2 targeted clones were shown in Fig. 2.14. A novel longer band corresponding to the targeted allele appeared as expected after hybridization with each probe, confirming homologous recombination of both arms.

For linearization, *tet B-RAF* targeting vector was cut at the unique SalI site and electroporated into E14 and R1 ES cells. All the good colonies (~400 from E14 electroporation due to weaker G418 selection, ~100 from R1 electroporation) were isolated and identified first by PCR using one sense primer (pCMV01) to the tetO promoter, and the other antisense one (HRP1) to the genomic sequence outside the vector (see Figure 2.13B).

Then five candidate clones (3 from E14 electroporation, 2 from R1 electroporation) were confirmed for homologous recombination by Southern hybridization with both 5' and 3' end probes (Fig. 2.15 A, B). Homologous recombination of both arms was verified by the appearance of an additional shorter band of the expected size.

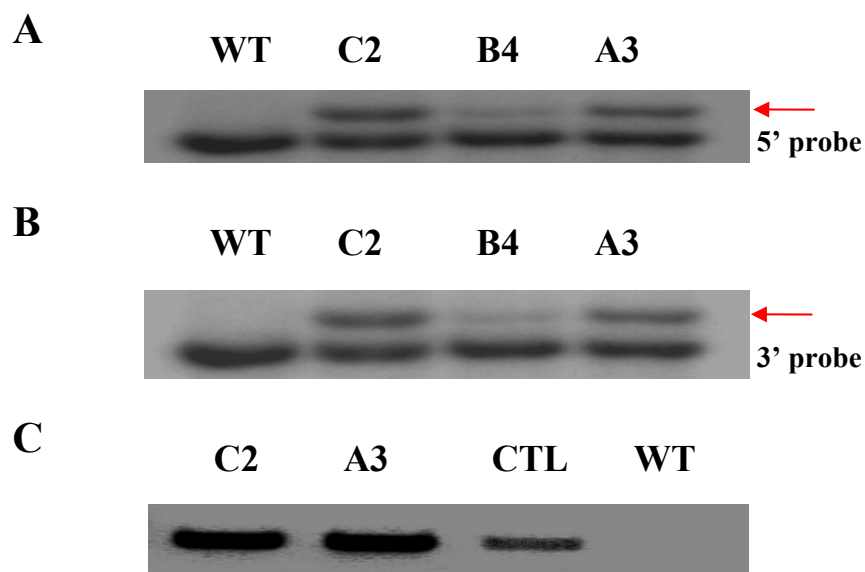


Fig. 2.14 Southern blot analysis of *floxed B-RAF* candidate clones after PCR screening. **A, B.** Homologous recombination of 5' (**A**) and 3' (**B**) arm was confirmed by Southern blot after BamHI digestion in two clones, C2 and A3, except B4. An expected longer band appeared when homologous recombination has occurred. Arrows indicate the positive bands. **C.** PCR assay for a single loxP upstream of exon 3. CTL, *floxed B-RAF* targeting vector.

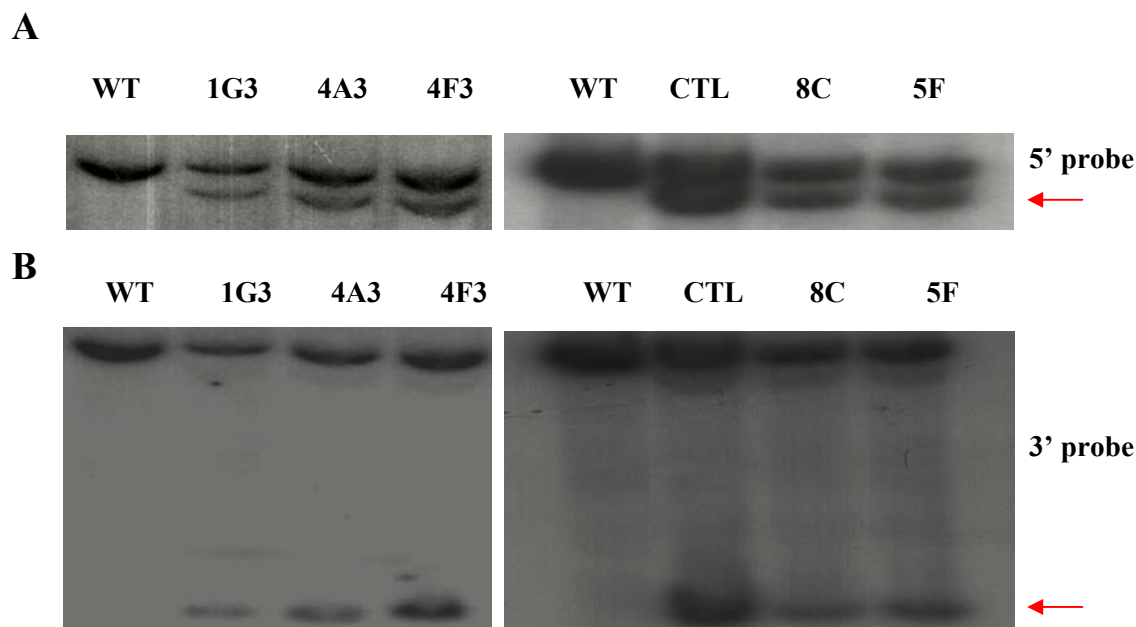


Fig. 2.15 Confirmation of homologous recombination in *tet B-RAF* targeted clones. **A.** After EcoRI restriction an additional shorter band appears when homologous recombination of 5' arm has occurred. **B.** After EcoRI restriction another shorter band appears when homologous recombination of 3' arm has happened. Arrows indicate the positive band. CTL, 1G3 used as positive control.

2.11. Test of Cre/loxP system and tet-switch in targeted clones

In the mutant allele targeted by *floxed B-RAF* vector, a single LoxP site and one floxed neo cassette were introduced (see Fig. 2.12). In the resulting germline animals, at first floxed neo cassette has to be deleted by germline-specific Cre activity, because of its potential interference with the expression of B-RAF. Then in the target tissue, floxed exon 3 should be excised by tissue-specific Cre activity. Before the *in vivo* genetic engineering (Fig. 2.16A), it is very desirable to verify that Cre-mediated site-specific recombination occurs in ES cells.

Therefore, a powerful recombinant Cre recombinase, His-TAT-NLS-Cre (HTNC), was transduced into the targeted ES cells (Peitz et al., 2002). Those ES cells were incubated in 2 μ M HTNC-containing medium for 20 h. 3 days later, PCR analysis of genomic DNA demonstrated that two crucial types of Cre-mediated recombination, deletion of neo cassette and total deletion, were achieved in some transduced cells (Fig. 2.16 B, C). In the control, incubated in normal medium, no special band was observed, indicative of enzymatic effect of HTNC. After subcloning the transduced cell pool, single colony with either deletion of neo cassette or total deletion was obtained (data not shown).

To test the efficacy of the tet system, the targeted ES cells carrying a *tet B-RAF* allele were grown in the presence or absence of Dox. 2 days later, total RNAs and cell lysates were prepared from the cell culture. The tightly controlled expression of B-RAF mRNA and protein from *tet B-RAF* allele by tet-switch was confirmed by RT-PCR and Western blot. To be sure of detecting the mRNA transcribed from the targeted allele, RT-PCR with one sense primer, corresponding to transcribed sequence of responsive miniCMV promoter, and one antisense primer for *B-RAF* gene was performed. In all tested clones the expression of mRNA was regulated in a dox-on style (Fig. 2.17 A). The increased expression of B-RAF protein in the presence of Dox was confirmed by Western blot using the polyclonal antibody against C terminus of B-RAF (Fig. 2.17 B).

As expression of the luciferase reporter gene is coupled with that of *B-RAF* gene in *tet B-RAF* allele, luciferase assay would provide additional quantitative information for tet-switch. Without Dox administration, luciferase activity in *tet B-RAF* targeted cells is comparable to the background (Fig. 2.17 C). In contrast, Dox induced more than 100-fold luciferase activity in *tet B-RAF* cells.

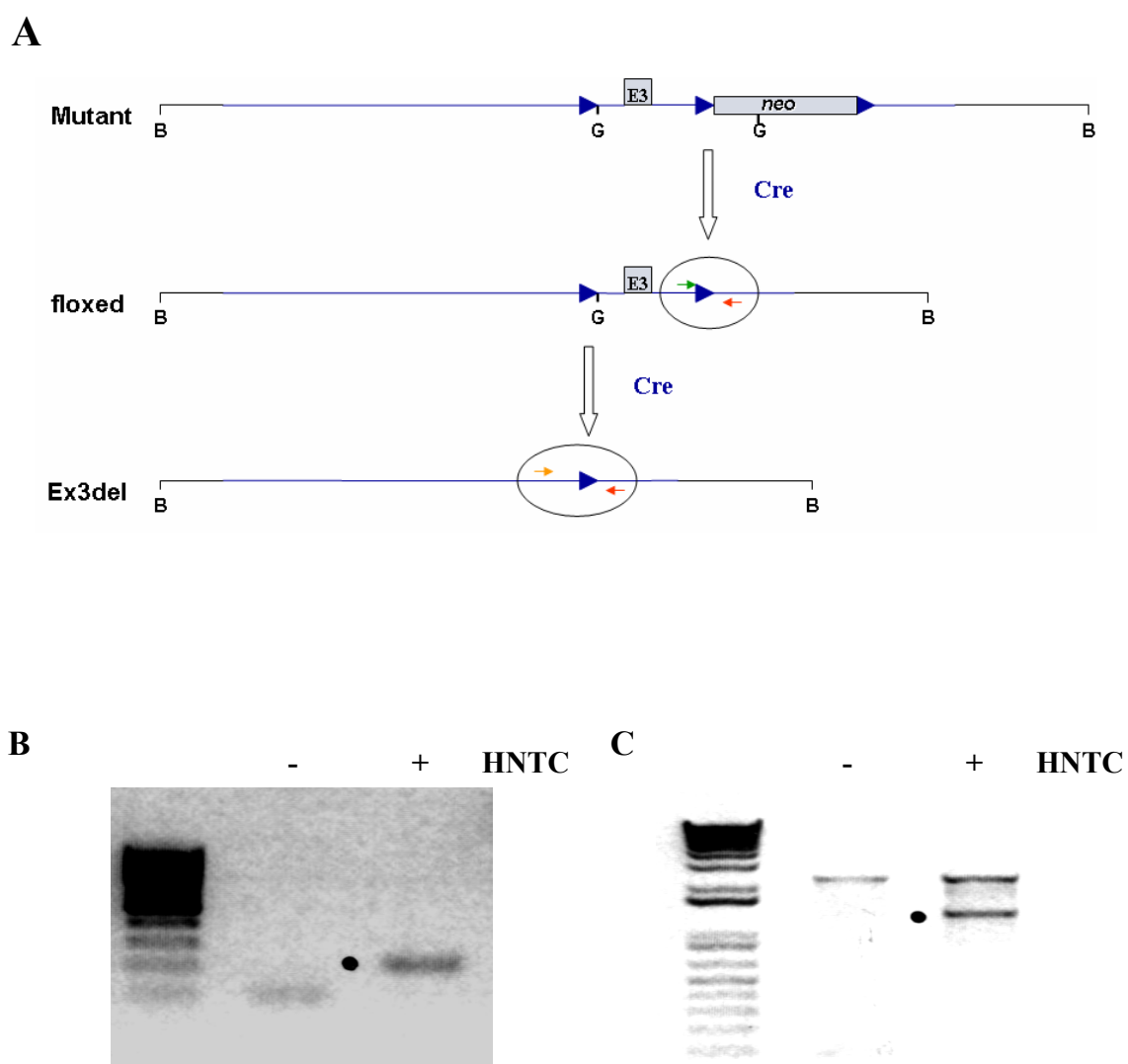
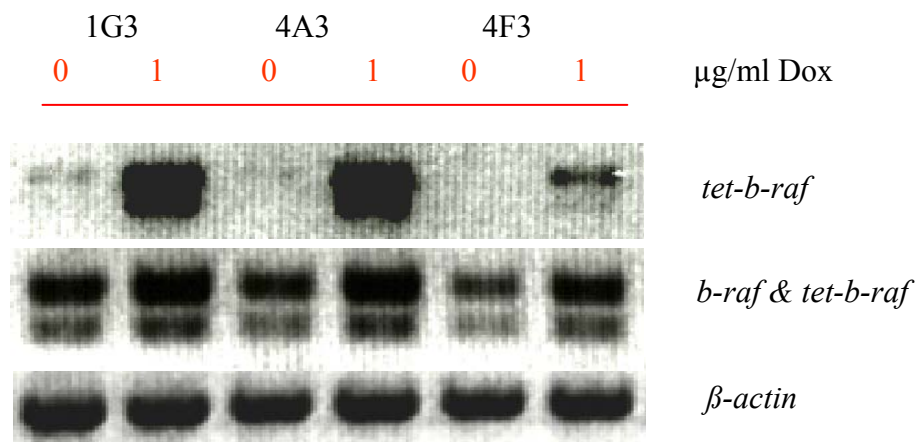
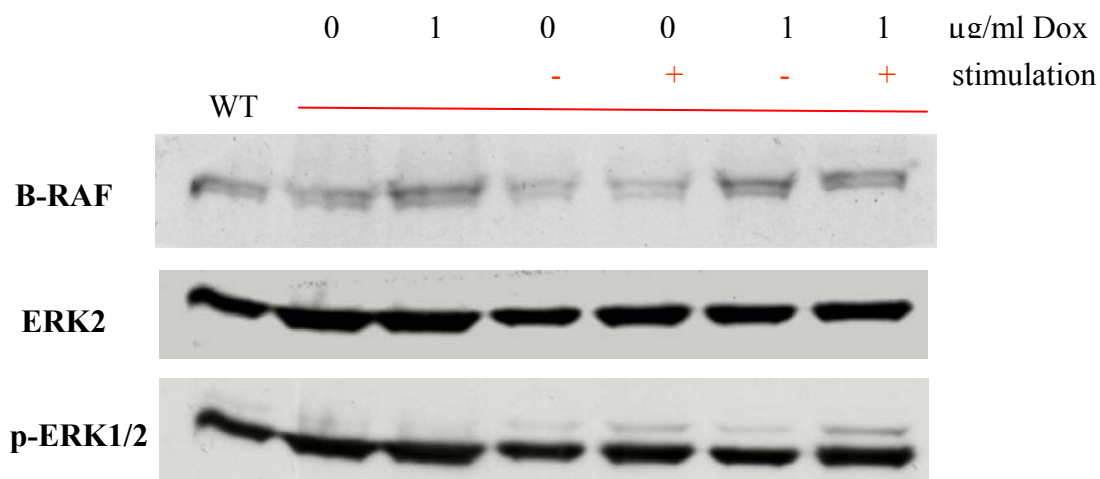


Fig. 2.16 Examination of Cre/loxP system in targeted cells by *floxed B-RAF* vector. **A.** Cre-mediated site-specific recombination in the mutant allele, leading to *floxed B-RAF* allele and *exon3-deleted (ex3del)* allele. **B.** PCR assay for *floxed B-RAF* allele resulting from neo deletion. **C.** PCR assay for *ex3del* allele resulting from total deletion. Black dots indicate the positive bands.

A



B



C

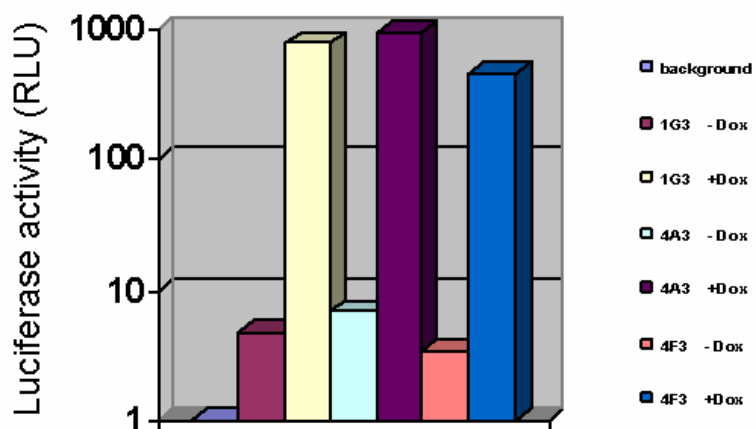


Fig. 2.17 Test of tet-switch in *tet B-RAF* targeted clones. **A.** RT-PCR detected Dox-induced expression of B-RAF mRNA from *tet B-RAF* allele, and increased expression of total mRNA from both alleles in a dox-on style. cDNA was synthesized from 0.05µg RNA by reverse transcription, and amplified in 35 cycles. PCR control reaction without RT yielded no detectable fragments. **B.** Western blot analysis showed increased expression of total B-RAF protein and normal ERK phosphorylation in presence of Dox. For stimulation, the cells were starved with serum/LIF-free medium for 24 h and then stimulated by LIF (1:200) for 15 min. A representative result from the clone, 1G3. **C.** Luciferase assay indicated that tet-switch worked well with low basal activity (-Dox) and sufficient inducibility (+Dox). RLU, relative luciferase unit. background, wildtype cell lysate.

2.12. Chimera formation and mating for germline transmission

Three targeted clones by *floxed B-RAF* targeting vector were taken for injection experiments. Using micromanipulator and dissecting microscope, ES cells were injected into 3.5 day-old B6D2F1 blastocysts, 10-15 cells/blastocyst. Those injected blastocysts were implanted into the uterus of pseudopregnant NMRI foster mother, 8-20 blastocysts/mouse. The chimeric males with different degree of ES cell contribution in coat colour were obtained and those with more than 50% were bred with C57Bl6 female mice until 50 pups were born (Table 1, Fig. 2.18A). The germline transmission was determined first by agouti color of F1 offspring after the cross. So far, no germline transmission was observed. Recently, other 11 new targeted clones have been identified and included in the injection list.

Theoretically, a chimeric group derived from high potential ES (XY) cells would consist of males only. In practice, the sex ratio (male versus female) of a chimeric group varies from 50:50 to 100:0 depending on the quality of ES cells, and reflects the quality of ES cells and obviously the likelihood of germline transmission for this group (Fedorov et al., 1997). From the targeted clone A3, 3 female chimeras of low degree together with 3 highly chimeric males were obtained, indicating that this clone lost some partial potential to colonize the genital ridge in mosaic embryos (Table 1).

Five targeted clones by *tet B-RAF* targeting vector were used for blastocyst injection. Following the same protocol, the highly chimeric males (50-100% in coat colour) were formed only from targeted R1 ES clones, and then mated with C57Bl6 female mice (Table 1, Fig. 2.18B). Till now, germline transmission was still on the way. As the most significant factor in this experiment is the contribution of targeted ES cells to the germ-line cells, we plan more targeting experiments to acquire more positive clones for germline transmission.

In order to determine whether the dox-on switch works *in vivo*, we took some highly chimeric male to do luciferase assay in various types of tissues, after feeding of Dox food for two weeks. Highest induction of responder gene in brain as well as substantial induction in other tissues suggested that tet-switch in *tet B-RAF* allele is able to function well in the animal model (Fig.2.18 C).

Table 1. Chimera formation of targeted ES clones

ES cell clone	Pups born	chimeras	male/ female		agouti coat colour (in %)				sterile
					< 25	25-49	50-75	76-100	
<i>floxed b-raf</i>									
A3 (R1)	10	6	m	3	-	-	-	3	-
			f	3	1	1	1	-	-
C2 (R1)	0*								
A2n (R1)	9	1	m	1	-	-	-	1	-
<i>tet b-raf</i>									
1G3 (E14)	4	2	m	2	-	2	-	-	-
4A3 (E14)	29	2	m	2	2	-	-	-	-
4F3 (E14)	0*								
5F (R1)	19	11	m	8	-	2	2	4	2
			f	3	-	-	3	-	-
8C (R1)	37	15	m	10	2	2	-	6	1
			f	5	3	-	1	1	1

* No viable postnatal mice after several times of injection. All clones were injected into B6D2F1 hybrid blastocysts.

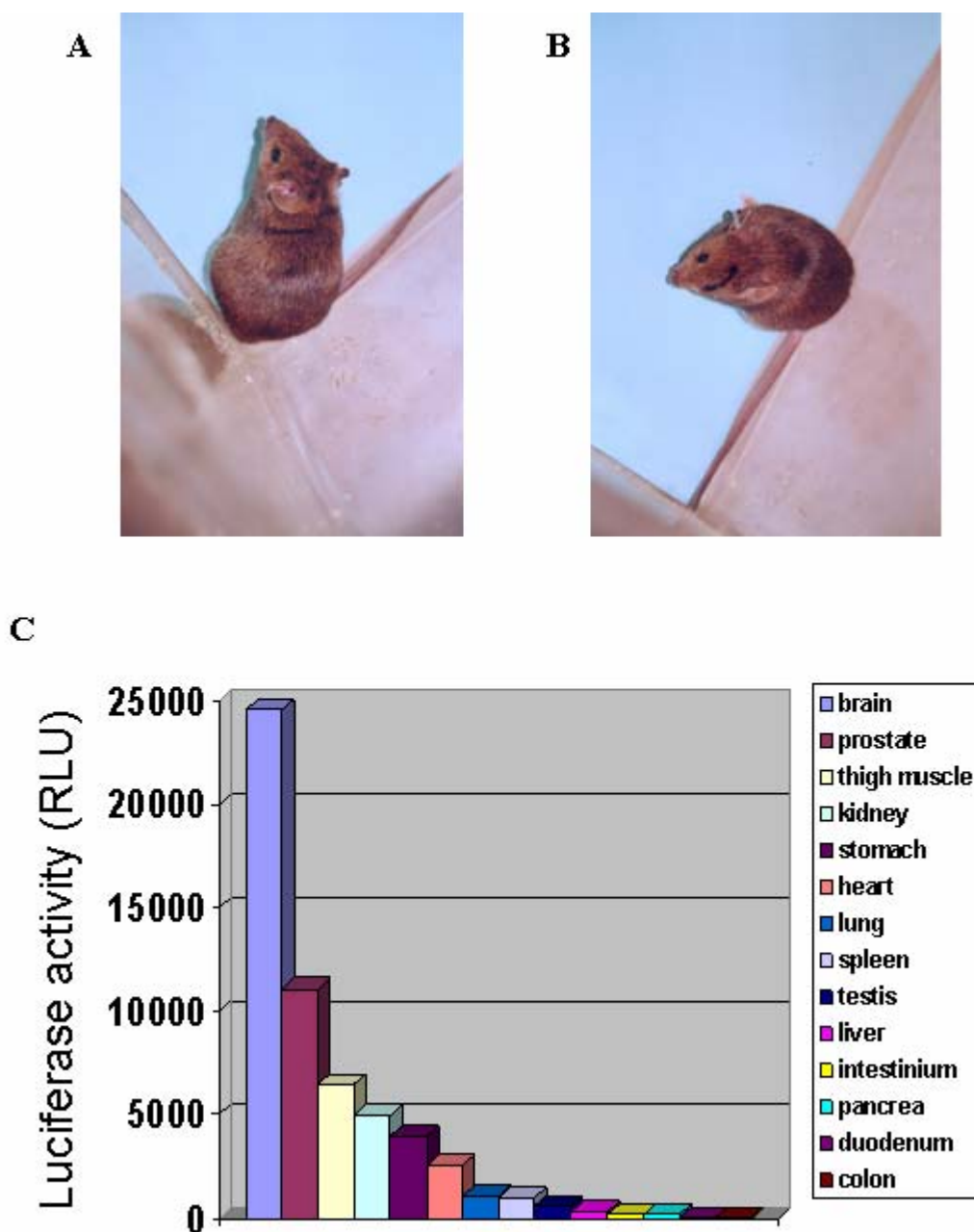


Fig. 2.18 Resultant chimeras from blastocyst injection. **A.** A fertile chimeric male with high contribution of targeted ES cells by *floxed B-RAF* vector. **B.** A fertile male with high chimerism from blastocyst injection of *tet B-RAF* ES cells. **C.** Luciferase assay of tissue lysates from dox-fed highly chimeric male, derived from *tet B-RAF* ES cells, indicating highest induction of responder gene in brain and substantial induction in other tissues. A representative result was shown. RLU, relative luciferase unit.

2.13. Preparation for a tetracycline-regulated B-RAF transgene line

Since conventional *B-RAF* deficient mice are available, introduction of a well-designed transgene with a switch to regulate expression of B-RAF cDNA gene seems to be a practical and effective way, as an alternative to making of *tet B-RAF* mouse line.

A similar design to *tet B-RAF* targeting vector was adopted into this transgenic construct, called tet-BrafEGFP (Fig. 2.19A). The long fragment, including 3kb *B-RAF* promoter element, promoterless rtTA cassette, complete neo cassette and tetO promoter with luciferase reporter gene, was released from *tet B-RAF* targeting vector, then assembled with human B-RAF full-length cDNA, which in-frame fused with EGFP coding sequence followed by pA signal. By this vector, B-RAF with EGFP fluorescence is expected to express in an endogenous way, depending on the presence of Dox.

To confirm the fusion of B-RAF and EGFP, NIH3T3 with constitutive tTA expression were transiently transfected with a middle-size responder plasmid pbi-BrafEGFP. In the positive cells, an intensive fluorescence was prominent, and more importantly, its distribution is in cytosolic component, which is actually different from that of pure EGFP (Fig.2.19 B, C).

This vector was linearized with Sall and used for oocyte injection. The transgenic mouse line is being generated hopefully.

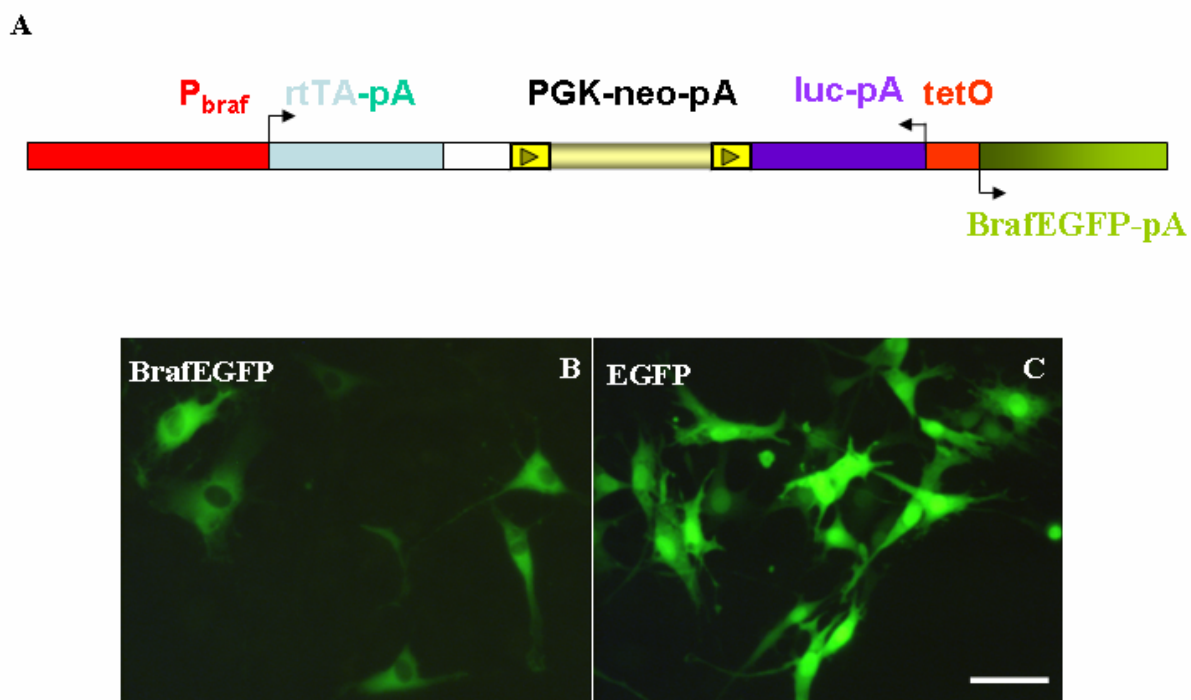


Fig. 2.19 Design of a tetracycline-regulated B-RAF transgene. **A.** The construct of tetracycline-regulated B-RAF transgene with EGFP tag. **B.** Subcellular distribution of fusion protein of B-RAF and EGFP. **C.** Subcellular distribution of pure EGFP. Scale bars, (**B,C**) 100 μ m.

3. DISCUSSION

Using $B\text{-RAF}^{KIN/KIN}$ mice expressing an artificial RAF, composed of the unique N terminus of mouse B-RAF and all the domains of human A-RAF, from the $B\text{-RAF}$ locus, we could for the first time explore the role of B-RAF in embryonic and postnatal forebrain. Through a detailed investigation of these animals in concentration on cortical development, we observed that in the mutant mice, proliferation of neural progenitors was reduced and migration of cortical neurons was impaired during neocortex neurogenesis, suggesting an important role for B-RAF in neuronal production and migration.

To study the *in vivo* role of B-RAF in embryonic neurogenesis and postnatal brain function, we attempted to establish conditional $B\text{-RAF}$ knockouts as novel animal models. Based on the efficient use of Cre/loxP system and tet-switch, generation of *floxed B-RAF* and *tetracycline-regulated (tet) B-RAF* mouse ES cell lines was performed. After blastocyst injection of the modified ES cell clones, high-grade chimeric mice have been obtained and hopefully bred for germline transmission.

3.1. $B\text{-RAF}^{KIN/KIN}$ animals as rescued B-RAF null mice

Because the lethality of $B\text{-RAF}^{-/-}$ mice between E10.5 and E12.5 precludes an opportunity to further analyze its function at a later stage (Wojnowski et al., 1997), $B\text{-RAF}^{KIN/KIN}$ animals, as B-RAF null mice rescued by an artificial RAF, had been already created in our group (Tyršin, Ph.D. thesis), in order to elucidate the role of B-RAF in developing brain as well as other tissues after midgestation. Aimed to rescue the early lethality by mimicking a hypomorphic B-RAF with minimal kinase activity, the artificial kinase combines the extra N terminus of B-RAF with all the domains of A-RAF, since A-RAF is the least effective MEK activator of the RAF family (Pritchard et al., 1995). By use of a knockin strategy, the chimeric RAF was expressed under the endogenous $B\text{-RAF}$ promoter instead of naive B-RAF.

As expected, the mutant mice in CD-1 background were protected from endothelial apoptosis and survived beyond midgestation, showing no obvious developmental defects (Camarero et al., manuscript). More importantly, neural cells in their spinal cord and forebrain were also rescued from death, providing the opportunity to discover the proliferation- and differentiation-oriented effects of B-RAF in CNS development.

In normal embryonic forebrain, B-RAF protein expression was maintained at a similar level at different developmental stages, while the amount of A-RAF increased apparently at E16.5 (Fig.2.1). The isotype-specific pattern implicated that B-RAF may have a basic function to support survival, growth and differentiation of most neural cell lineages in forebrain, whereas A-RAF is probably more important for relatively mature neurons.

No B-RAF but chimeric RAF was detected in *B-RAF^{KIN/KIN}*, confirming the substitution of natural B-RAF by the artificial kinase. The endogenous *A-RAF* expression was not affected, compared to the wildtype. Provided that the amount of the chimeric protein was much lower than that of natural A-RAF (Fig.2.1), it is most likely that the observed phenotype is the result from disruption of the complete B-RAF role, but not from interference with endogenous A-RAF function. In fact, embryonic development is quite normal even under the ablation of A-RAF (Pritchard et al., 1996).

In adult mouse cerebrum, there are several B-RAF isoforms differing in the presence or absence of alternatively spliced exons 8b and 10 (Barnier et al., 1995). Since isoforms containing amino acids encoded by exon 10 are specifically expressed in neural tissues, their expression during forebrain development is more interesting. By RT-PCR a minor level of exon 10-containing transcripts among total *B-RAF* transcripts was detected in WT forebrain from E12.5 to E16.5 (Fig.2.2). Though there was the low percentage of exon 10-containing isoforms at the examined stages, their importance for developing forebrain is perhaps not trivial. In principle, a certain isoform of B-RAF can be selected for the rescue experiments to

dissect out the isoform-specific role of B-Raf in embryonic cerebral cortex.

3.2. NSCs in forebrain during midgestation stage

The result of *in vitro* assay for neural stem cell at E10.5 forebrains demonstrated that at least at this stage NSCs in *B-RAF* KO and KIN are apparently unimpaired in terms of their relative frequency, and their abilities of self-renewal, proliferation and differentiation (Fig.2.3, Fig.2.4). Indirectly it means that neural induction and early patterning of the neural plate is not dependent on B-RAF specific signalling.

The investigation on interaction of neural stem cells with their local extracellular microenvironment or niche has made clear that, neural stem cell expansion and differentiation are regulated by environmental factors, such as vascular endothelial growth factor, synthesized in the stem cell niche (Breier and Risau, 1996; Shen et al., 2004). The normal maintenance of NSCs in B-RAF null forebrains at E10.5 is probably due to no severe change in their local extracellular microenvironment. At least till E10.5 there is yet no apparent apoptosis of endothelial cells in *B-RAF* KO.

Neurosphere culture develops a three-dimensional structure, remarkably similar in extracellular matrix (ECM) composition and distribution of cellular phenotypes to the developing CNS, and can be used as a model for the developing neuroepithelium (Campos et al., 2004). However, there seemed no apparent cell death during neurosphere formation and differentiation of *B-RAF*^{-/-} NSCs, as observed in the forebrain (Gotz et al., 2005), implying that *in vitro* neurosphere culture is somewhat different from *in vivo* neural development.

3.3. Cortical defect in neocortex development

In the mouse cortex, neurons are generated between embryonic day E10.5 and E17. The mitotic neuronal progenitor cells are derived from the most immature progenitor cells (NSCs),

and generate postmitotic neurons after a maximal of 11 cell cycles (Takahashi et al., 1999). The neocortex with a structure of six layers is then formed by sequential waves of postmitotic neurons that migrate in the radial direction from the germinal zone towards the pial surface.

After the preplate (PP) is split into a superficial marginal zone (MZ) and a deeper subplate by a newcomer, cortical plate (CP), sequential waves of cortical neurons migrate past their predecessors and finally position themselves underneath the MZ to expand the CP, in the ‘inside-out’ layering way (Angevine and Sidman, 1961). Two different modes of radial migration have been described for newly generated neurons (Nadarajah and Parnavelas, 2002). In the early phases of neocortical layer development, neurons move their cell soma towards a leading process that is stably attached to the pial surface, in a mode called somal translocation. Later on when the cortex has grown in size, neurons migrate along radial glial fibers maintaining their overall cell length, by a movement named glia-guided locomotion.

In KIN embryos, cortex development goes through the preplate stage and the early cortical plate stage, indicated by the proper formation and splitting of the preplate (Fig.2.5 A-H). In the late cortical plate stage starting from E14, there were apparent cortical defects in *B-RAF^{KIN/KIN}* forebrain: Laminated structure was tightly packed, stratification of cortical neurons disorganized, and TuJ-1+ conjunction between CP and SP obscurely-defined (Fig.2.5 E-L). During neuronal maturation, the final stage of cortical development, this kind of phenotype was remained and pronounced in the postnatal mice. Loss of B-RAF led to appearance of densely packed layers IV-II, severe loss of pyramidal projection neurons with Brn-2 marker, and disruption of dendrite formation in these upper layers (Fig.2.6).

In further analysis, BrdU labelling experiments showed that from E14.5 to E16.5 cell proliferation in VZ of the mutant mice was increasingly reduced (Fig.2.7). Decrease in cortical progenitor proliferation suggested insufficient expansion of neuron-restricted progenitors and reduced production of newly generated postmitotic neurons in B-RAF null

mice. More strikingly, BrdU birthdating experiments revealed that the late-born cortical neurons failed to migrate properly by glia-guided locomotion (Fig.2.8), which looked like ongoing migration defect (Bielas et al., 2004). Therefore, affected ongoing migration and then incorrect positioning is promisingly responsible for the observed cortical defects. Besides that, possible maturation disability of those normally-positioned neurons, including expression of the Brn-2 and MAP2 markers, due to B-RAF deficiency, might in part contribute to the phenotype in postnatal KIN.

3.4. Progenitor proliferation associated with ERK activation

Although ERK phosphorylation in the KIN progenitors, untreated or bFGF-stimulated, was reduced already from E10.5 onwards (Fig. 2.9), there was not yet any obvious immediate effect on proliferation. Only from E14.5, we observed significant reduction in progenitor proliferation (Fig.2.7), indicating that cell proliferation is more sensitive to B-RAF/ERK signalling at the later stage.

Since MEK-ERK-RSK-C/EBP pathway plays an essential role during growth factor-regulated cortical neurogenesis (Menard et al., 2002), the disrupted ERK activity in rescued B-RAF null mice maybe deregulated the downstream factor C/EBP, leading to affected pool expansion and neuronal birth of cortical progenitors.

In an *in vitro* analysis for cortical progenitors (Barnabe-Heider and Miller, 2003), it is demonstrated that inhibition of MEK had no effect on progenitor proliferation, monitored by BrdU incorporation after an overnight pulse in presence of FGF2, which could reflect the actual difference between *in vitro* and *in vivo* systems.

3.5. Affected neuronal migration probably due to cell autonomous defect

Four distinct phases have been discerned in locomotion at this time of corticogenesis: initial

radial migration, arrest of migration in the subventricular zone, migration back towards the ventricle and finally, secondary migration to the appropriate layer (Noctor et al., 2004). What step in migration is specifically impaired cannot be concluded from static histological analysis but would require time-lapse imaging of slice cultures.

Immunohistochemistry results suggested that the migration defect is most likely caused in a cell autonomous way, in respect that there was no visible damage in radial glia scaffold or guidance cue such as reelin (Fig.2.8). In the primary culture of dissociated cells from E12.5 KIN forebrain, we observed altered subcellular localization of pERK and disrupted actin cytoskeleton in freshly born neurons (Fig.2.10). There is a dramatic decrease in the amount of phospho-ERK present at the cell surface membrane of *B-RAF^{KIN/KIN}* cortical neurons, and a much higher degree of F-actin relocalization into the cytosol.

Lack of B-RAF, the upstream activator of ERK, led to an increase in the migration of fibroblasts in conjunction with a reduction at the level of F-actin, suggesting that B-RAF acts via the ROCKII/LIMK/cofilin pathway to maintain actin stress fibers in fibroblasts (Pritchard et al., 2004). In contrast, the migration defect of *C-RAF^{-/-}* fibroblasts was traced to the hyperactivation and mislocalization of Rho-dependent kinase ROK α /ROCK2, demonstrating a scaffolding function of C-RAF involved in the Rho pathway to regulate cell migration (Ehrenreiter et al., 2005). Moreover, a role of C-RAF in epithelial cell adhesion and migration has been uncovered, and Prohibitin is instrumental for the RAS activation of C-RAF in the signalling pathway induced by epidermal growth factor (Rajalingam et al., 2005).

Considering that cortical neurons migrate along radial glial fibers and that their migration modes are more complex than other types of cells, the mechanistic details how B-RAF controls cortical migration may be specific and complicated. ERK has been identified to alter neurite growth by several mechanisms, including the transcriptional induction of the Cdk5 activator p35 through Egr1 in PC12 cells (Harada et al., 2001), activation of

phospholipase D2 in PC12 cells (Watanabe et al., 2004) and direct phosphorylation of the actin-binding protein spinophilin (Futter et al., 2005). Together with the observation of inappropriate ERK cellular distribution in the mutant neurons, we think that B-RAF-induced phospho-ERK is at least partially responsible for the normal migration.

In cortical neurons, Brn-2 controls in a cell autonomous manner the expression of p35, a regulatory subunit of Cdk5 (McEvelly et al., 2002) or mDab1, one target of both p35/Cdk5 and Reelin signalling (Sugitani et al., 2002) and is therefore involved in regulating the migration of cortical neurons. B-RAF activation of Brn-2 as observed in melanoma cells (Goodall et al., 2004) reminded us whether B-RAF takes advantage of the p35/Cdk5 pathway via Brn-2 to regulate the migration of cortical neurons. Indeed, p35/Cdk5 has proved to take the central stage on regulation of neuronal migration in cortex development (Bielas et al., 2004). To test if B-RAF plays around with p35/Cdk5 to function in the proper migration and positioning of neocortical neurons, we analyzed the expression of p35 in B-RAF null forebrains from E12.5 to E16.5. No difference in the total amount of p35 proteins between KIN and WT was displayed (Fig. 2.11). The next step will be Cdk5 kinase assay to check if there was abnormal kinase activity of Cdk5 in the mutant mice.

3.6. Role of B-RAF in FGF2 and TrkB signalling during cortex development

FGFs are among the regulatory signaling molecules in neocortex development (Dono, 2003). The expression of *Fgfs* and *FgfRs* in the developing rodent neocortices is spatially and temporally regulated. In particular, the cells of the VZ express high levels of *FgfR1*, *FgfR2*, and *FgfR3* during the expansion of the neocortical progenitor pool and throughout neurogenesis. In agreement with receptor distribution, FGF ligands are also found in the VZ. Especially, FGF2 proteins are abundant at early developmental stages and nearly absent by the end of neurogenesis (Nurcombe et al., 1993; Dono et al., 1998; Raballo et al., 2000).

As one of the most characterized members, FGF2 has proved to be the important regulator of cortex development. FGF2 turned out to be among the most potent mitogenic and survival factors for many CNS cell types, including embryonic neocortical VZ cells. Other studies have shown that FGF2 acts either alone or in combination with neurotrophins to promote differentiation of neocortical precursor cells.

Genetic analysis of FGF2 functions in mice has shown that FGF2 regulates neuronal density and cytoarchitecture of the developing neocortex (Dono et al., 1998; Ortega et al., 1998; Vaccarino et al., 1999). Neocortices of FGF2-deficient mice contain fewer neurons at maturity because of possible defects in proliferation of progenitors. In addition, a fraction of postmitotic neurons fail to reach their target layer in the developing neocortex of FGF2-deficient mice. These cells either remain in deeper layers or accumulate in the corpus callosum (Dono et al., 1998). These genetic studies show that lack of FGF2 affects cell positioning in the developing neocortex. Thus it is likely that FGF2 is part of the signaling network that acts on the progenitor cells and defines the cell fate and migratory path of postmitotic neurons. The neuronal defects observed in FGF2-deficient cortices predominantly affect the frontal motor sensory areas (Dono et al., 1998; Ortega et al., 1998; Vaccarino et al., 1999). This observation raises the possibility that FGFs are part of the signaling network regulating differential growth and patterning of neocortical areas.

FGF2 binding to FGFR1 stimulates the RAS/ERK pathway and also the PI3K/Akt pathway. In addition, FGFR1 signalling activates the PLC γ /PKC pathway (Dono, 2003). The phenotype of FGF2-deficient mice is very similar to that of the rescued B-RAF-null mice, which implicate that B-RAF really stays inside the core pathway of FGF2 signalling network in cortex development, presumably with RAS-MAPK cascade.

With the subtle targeting strategy, TrkB, a high-affinity receptor tyrosine kinase of the neurotrophin BDNF has been implicated to regulate neocortex formation (Medina et al.,

2004). TrkB transduces the extracellular signal through the Shc-mediated RAS/ERK and PI3K/Akt pathways, as well as the PLC γ -mediated PKC pathway. It was shown that conditional deletion of the TrkB receptor from the embryonic CNS affected the timing of migration of newly born cortical neurons, resulting in their altered positioning in the newly forming cortical layers. In the adults, abnormal compression of the cortical layers and affected maturing differentiation was observed. The further comparison of three different knockin models with compromised Shc- or/and PLC γ -mediated signalling respectively indicated that the RAS/ERK, PI3K/Akt and PLC γ /PKC pathways are all involved in TrkB-mediated control of neuronal migration. Compared to the present observation in *B-RAF*^{KIN/KIN} mice, we speculate that B-RAF have an irreplaceable role in mediating TrkB signalling during neocortex development, probably in a similar way that B-RAF serves for FGF2 signalling.

3.7. Generation of conditional KO by gene targeting

In the conventional *B-RAF* knockout (Wojnowski et al., 1997), an embryonic lethal phenotype was provoked, precluding any further functional analysis till adulthood. Pleiotropic side effects as a compensatory reaction to the introduced germ line mutation might obscure or prevent a clear-cut analysis. Moreover, since the *B-RAF* gene has a wide expression pattern, its general inactivation may induce a highly complex accumulative phenotype involving multiple tissues. To overcome these weaknesses, we attempted to generate conditional KO models, which permit to regulate the expression of the *B-RAF* target gene in a temporally or/and spatially controlled manner.

Among all the successful strategies, exploration of Cre/loxP system and application of the reversible tetracycline-based switch are two of the most impressive for creating conditional loss-of-function mouse models (Gossen and Bujard, 2002).

For creating Cre-mediated knockout, it is essential to introduce recombinase recognition site, loxP around an essential part of the gene of interest without compromising its functionality. It often is sufficient to simply position the loxP sequences in the intronic sequence around one essential exon or a few ones. To avoid unwanted transcriptional interference with the natural transcriptional program of the targeted locus, it will be important to remove the selectable marker (for example, a neomycin resistance expression cassette) after the chosen allele has been targeted. When designing the targeting vector, this can be achieved by the use of three loxP sites in the targeting vector, two of which are flanking the marker and the third placed in a location that after removal of the marker the two remaining loxP sites are positioned around the part to be removed (Gu et al., 1993). The outcome of any recombinase-mediated conditional knockout experiment will depend very much on the individual deleter strain expected to express the recombinase at a high enough level and specificity to introduce the desired alteration.

We followed this strategy and introduced a single loxP site and one floxed neo cassette flanking exon 3 into endogeneous *B-RAF* gene (Fig.2.12, Fig.2.14). In the target clones, site-specific recombination induced by Cre transduction was achieved very well, which indicated that genetic engineering by targeting the endogenous locus accomplished the first step for this goal (Fig.2.16). Once the germline for the targeted allele is established, the neo cassette will be removed in the next generation through Cre expression from EIIa-cre in all cell types of pre-implantation embryos, leading to *floxed B-RAF* allele.

In *B-RAF^{lox/lox}* mice, the tissues expressing Cre proteins in a certain time will encounter the irreversible inactivation of B-RAF. Using the transgenes, for example NESTIN-cre, active in the early neural lineage, we can make genomic deletion of floxed exon 3 and thus functional silencing of the *B-RAF* gene in the embryonic CNS, which provides a conditional mouse model to study how B-RAF plays a real role in the CNS development.

tet-switchable gene knockout has been developed through combination of tetracycline regulatory system with knock-in approaches. In order to analyze the temporal requirements for expression of the endothelin receptor B gene (*Ednrb*) in murine development, Shin et al. (Shin et al., 1999) created two different knock-in lines, the first one by substituting *Ednrb* for either tTA or rtTA, and the second by replacing the promoter of *Ednrb* with tetracycline responsive minimal CMV promoter P_{tet-1} . Crosses between these two lines made expression of *Ednrb* conditionally dependent on Dox. In another study, Adelman and coworkers (Bond et al., 2000) analyzed a gene for one of the subunits of calcium-activated potassium channels, SK3. Here, only one knock-in targeting construct was used to bring tTA under control of the endogenous SK3 promoter and to simultaneously place P_{tet-1} in front of the endogenous gene. When the respective mice were bred to homozygosity, the functional null mutation was induced by administration of Dox. Not only did that study exemplify the tight control that the Tet system can exert over endogenous genes, it also demonstrated that expression levels for endogenous genes can be achieved well in excess of the natural situation.

According to the previous concept, the dox-on tet-switch has been knocked into the first exon of *B-RAF* gene in ES cells (Fig.2.13, Fig.2.15). Because of the use of rtTA-M2 (Urlinger et al., 2000) and neo cassette suppression of responsive promoter leakage, our tet-switch system performed very well as expected: minimal basal expression, sufficient induction in cell culture (Fig.2.17), and *in vivo* effective inducibility shown in the highly chimeric animal (Fig. 2.18 C). As soon as *tet B-RAF* mouse line is founded, *tet B-RAF* homozygotes will be dox-fed for rescuing the null phenotype or free of Dox to recapitulate the null phenotype. The appropriate administration programs will help us to identify the critical period when B-RAF specific signalling is required and together the critical role that B-RAF plays in vascular and neuronal development. Notably, this modified strategy, integration of the dox-on combined tet-switch into the untranslated transcript start region, enables the diploid rescue of the null

phenotype comparable to WT, and offers additional advantage when the target gene like *B-RAF* encodes multiple protein isoforms with tissue-specific expression.

3.8. Preparation of tet-regulated B-RAF transgene line as an alternative way

Exploration of a tet-regulated transgene to restore expression of a target gene which has been disrupted in the endogenous locus, has been shown to be a very useful method for creation of conditional KO in cells or animals (Tanahashi-Hori et al., 2003; Holland et al., 2002). In the situation that conventional targeted line is founded, there is one great advantage from this avenue: a single transgene line crossed into the null genetic background can generate tet-regulated knockout line. Notably, because the *B-RAF* gene encodes a few isoforms in mouse embryo and adult, a common isoform expressed from the transgene may be insufficient for the full recapitulation of the WT phenotype. Though, there is worthy of taking this alternative strategy for investigation of B-RAF function.

In 1996, Schultze et al. first reported efficient control of gene expression by a single step integration of tet system in transgenic mice. Apart from its relative simplicity, this approach ensures the balanced integration of both transactivator and responder units at the same chromosomal locus, and complete prevention of genetic segregation of the regulation and expression units. Based on this strategy, we constructed a vector of tet-regulated human B-RAF transgene with EGFP tag (Fig.2.19). In this vector, the *B-RAF* promoter drives rtTA expression, and then human B-RAF with in-frame fusion to EGFP is expressed depending on the presence of Dox. There are some successful studies using C-RAF with GFP tag in its C terminus, which proved that the labelled fluorescence protein does not interfere with cellular function of RAF protein (Rizzo et al., 1999; Rizzo et al., 2000; Bondeva et al., 2002). In the transiently transfected NIH3T3 cells, B-Raf-EGFP fusion proteins were, as expected, distributed in cytosolic compartment, differing from the pure EGFPs were.

Hopefully, this transgenic mouse line will be established quickly, as the germline transmission is not the bottleneck here. After that, the *B-RAF*^{-/-}:tet-BrafEGFP mice will be available for the further subtle analysis of B-RAF function.

4. MATERIALS AND METHODS

The methods described in this section are all based upon today's standard molecular and cellular biology techniques.

4.1. Materials

4.1.1. Instruments

Hardware

Bacterial incubator
 Bacterial shaker
 Cell culture hood
 Cell culture incubator
 Cell culture microscope
 Glass coverslip
 Deparaffinization machine
 Developing machine
 Dissection microscope
 DNA Sequencer
 Electrophoresis power supply
 Electrophoresis unit, small
 Fine scale
 Fluorescence Microscope (CCD)
 Gene pulser
 Heat block
 Homogenizer
 Horizontal electrophoresis gel
 Injection microscope
 Inverted microscope
 Mega centrifuge

 Microlumat
 Microscope Slides, Super Frost[®] Plus
 Mikrotome (rotating/sliding)
 Mini centrifuge
 pH meter
 Phosphoimager

 Scale

Manufacturer

Heraeus B 6200
 New Brunswick Scientific innova 4330
 Heraeus Instrument
 Heraeus Instrument
 Leica
 Marienfeld
 Leica ASP200
 Agfa
 Leica
 ABI PRISM 373, ABI
 Bio-Rad
 Bio-Rad Mini-Protean II
 Scaltec SBC 21
 Leica (Hamamatsu Orca)
 Bio-Rad
 Liebisch, Type 2099-DA
 Ultra-Turrax[®]
 PEQLAB
 Leica
 Olympus
 J-6B, Beckman; Megafuge 1.0 R, Heraeus;
 RC 5B plus, Sorval
 EG&G, Berthold
 Menzel-Gläzer
 Leitz Wetzlar
 5417R, Eppendorf; Biofuge 15, Heraeus
 Microprocessor, WTW
 Fujix BAS-2000 III, Fuji,
 with plates BAS-MP 2040P, Fuji
 BP2100S, BP310S, Sartorius

Shakers	Heidolph, Unimax 2010, Edmund Bühler WS5
Spectrophotometer	Ultraspec 3000, Pharmacia Biotech
Thermocycler	PE9600, Perkin Elmer; T3, Biometra®
Ultraviolet Crosslinker	UVC500 Hoefer Scientific Instruments
Vortex	Scientific Industries Genie-2
Water bath	GFL 1083, Amersham-Buchler

4.1.2. Chemical reagents and general materials

<i>Reagent</i>	<i>Purchased from</i>
[α - ³² P]dCTP (370MBq/ml)	Amersham
1 kb DNA ladder	Invitrogen, MBI
Acrylamide (30%)/Bisacrylamide (0.8%)	Roth
Adenosin-5'Triphosphate (ATP)	Sigma
Agarose, ultra pure	Invitrogen
Ammonium Acetate	Sigma
Ammonium peroxydisulfate (APS)	Sigma
Ampicillin	Sigma
AntifoamA	Sigma
Aprotinin	Roth
Bacto-Agar	Roth
Bovine serum albumin (BSA)	Sigma
Bradford-reagent	Bio-Rad
Bromodeoxyuridine (BrdU)	Sigma
Bromphenolblue	Sigma
β -Mercaptoethanol	Roth
Calciumchloride (CaCl ₂)	Sigma
Chloroform	Roth
Chloralhydrate	Roth
DAPI	Sigma
Deoxycholate (DOC)	Sigma
Diethyl pyrocarbonate (DEPC)	Merck
Dimethylsulfoxide (DMSO)	Sigma
Dithiothreitol (DTT)	Sigma
dNTPs	MBI
Ethylenediaminetetraacetic acid-disodium salt (EDTA)	Sigma
EGTA	Sigma
Ethanol	Roth
Ethidiumbromide	Invitrogen
Formaldehyde	Roth
Formamide	Roth
Glutathion-sepharose	Pharmacia
Glycerol	Sigma
Guanidine thiocyanate	Roth
Hydrochloride (HCl)	Roth
Hybond-N membrane	Amersham
IGEPAL (NP-40)	Sigma
Isoropyl-1-thio- β -D-thiogalactopyranoside (IPTG)	Roth
Isopropanol	Merck
Leupeptin	Sigma
Magnesiumchloride	Sigma
Mowiol	Calbiochem
Natrium Chloride	Roth
3-(N-morpholino)propanesulfonic acid (MOPS)	Sigma
Paraffin wax (Histosec Pastillen)	Merck

Paraformaldehyde (PFA)	Sigma
Pefablock	Roth
Phenol	Roth
Phenol:Chloroform:Isoamylalcohol	Roth
Phenol/Chloroform (TE saturated)	Roth
Ponceau S	Sigma
Potassium acetate (KAc)	Sigma
Potassiumchloride (KCl)	Sigma
Potassiumdihydrophosphate (KH ₂ PO ₄)	Merck
Protein ladder, BenchMark™	Invitrogen, MBI
PROTRAN membrane	Schleicher & Schüll
SDS ultra pure	Roth
Sodium citrate	Merck
Sodiumdihydrophosphate (NaH ₂ PO ₄)	Merck
Sodiumhydrophosphate (NaHPO ₄)	Merck
Sodiumhydroxide (NaOH)	Sigma
sodium morpholineethanesulfonate (Na-MES)	Sigma
Sodium orthovanadate	Sigma
Sonicated fish sperm DNA	Roche
TEMED	Roth
Tris-(hydroxymethyl)-aminomethane (Tris)	Roth
Triton-X100	Sigma
Uracil	Sigma
Whatman 3MM Paper	Schleicher & Schüll
X-gal	Sigma
X-ray film	Amersham
Xylencyanol	Roth
Yeast extract	Invitrogen

4.1.3. Cell culture and embryo manipulation materials

<i>Reagent</i>	<i>Source</i>
B27	Invitrogen
bFGF	Tebu-bio
β-mercaptoethanol	Invitrogen
CMF-HBSS	Invitrogen
Dispase	Invitrogen
DMEM	Invitrogen
DNase I	Roche
Doxycycline (Dox)	Sigma
EGF	Tebu-bio
Fetal calf serum (FCS)	Invitrogen
FCS tested for ES cell	Invitrogen
G418 sulfate	Calbiochem
Gancyclovir (Cymeven i.v.)	Roche
Horse serum	Invitrogen
HTNC	Gift from F. Edenhofer
laminin	Sigma
LIF	Supernatant from LIF-transfected CHO cells (from L.Nitschke)
Lipofectamine2000	Invitrogen
L-Glutamine	Invitrogen
M2 embryo flashing medium	Sigma
M16 embryo incubation medium	Sigma
Mineral oil (embryo tested)	Sigma
Mitomycin C	Sigma
Neurobasal	Invitrogen
Non-essential amino acids	Invitrogen

Poly-DL-ornithine	Sigma
Phosphate buffered saline (PBS)	Invitrogen
Penicillin/Streptomycin	Invitrogen
Poly-D-Lysine	Sigma
Trypsin-EDTA	Invitrogen
Trypanblue	Sigma

4.1.4. Antibodies used for Western blot and immunochemistry

<i>Antibodies for WB</i>	<i>Antigens</i>	<i>Source</i>
anti-A-RAF (rabbit polyclonal)	C terminus	Santa Cruz
anti-B-RAF (rabbit polyclonal)	C terminus	Santa Cruz
anti-Cdk5 (rabbit polyclonal)	C terminus	Santa Cruz
anti-C-RAF (rabbit polyclonal)	C terminus	Santa Cruz
anti-ERK2 (rabbit polyclonal)	C terminus	Santa Cruz
anti-GAPDH (mouse monoclonal)		Chemicon
anti-p35 (rabbit polyclonal)	C terminus	Santa Cruz
anti-p(Thr202/Tyr204) ERK1/2 (rabbit polyclonal)	p(Thr202/Tyr204) peptide	Cell signalling
anti-Mouse IgG conjugated peroxidase		Amersham
anti-Rabbit IgG conjugated peroxidase		Amersham

<i>Antibodies for IC</i>	<i>Antigens</i>	<i>Source</i>
anti-BrdU (rat monoclonal)		abcam
anti-Brn-2 (rabbit polyclonal)		gift from Dr. M. Wegner
anti-GFAP (rabbit polyclonal)		Dako
anti-MAP2 (mouse monoclonal)		abcam
anti-Nestin (mouse monoclonal)		DSHB
anti-O4 (mouse IgM)		R&D systems
anti-p(Thr202/Tyr204) ERK1/2 (rabbit monoclonal)	p(Thr202/Tyr204) peptide	Cell signalling
anti-Reelin (mouse monoclonal)	Peptide 164-496	abcam
anti-Tuj1 (mouse monoclonal)		Chemicon
Alexa488 goat anti-rat		Molecular Probes
FITC donkey anti-rabbit		Jackson ImmunoResearch
FITC goat anti-mouse IgM		Jackson ImmunoResearch
Rhodamine donkey anti-mouse		Jackson ImmunoResearch

4.1.5. Enzymes

<i>Items</i>	<i>Source</i>
BioTherm DNA polymerase	Gene Craft
Calf Intestinal Phosphatase (CIP)	New England Biolabs (NEB)

DNase I, PCR grade	MBI
Klenow Fragment	MBI
M-MuLV-RT (reverse transcriptase)	MBI
Pfu polymerase	Stratagene
Proteinase K	Roth
Restriction Endonucleases	MBI, NEB, Amersham
RNaseA	Roche
T4 Ligase	NEB

4.1.6. Kit

<i>Items</i>	<i>Source</i>
ECL Western blotting detection reagents	Amersham
Luciferase Assay kit	Promega
Nucltrap [®] column purification kit	Stratagene
QIAEX II Gel Extraction Kit	Qiagen
QIAGEN Plasmid Kit (Maxi)	Qiagen
QIAquick PCR purification Kit	Qiagen
Quikhyb solution	Stratagene
rediprime [™] II random prime labelling system	Amersham Pharmacia Biotech
TRIzol [®] LS reagent	Invitrogen
Vectastain [®] ABC-peroxidase kit	Vector

4.1.7. Plasmid DNA

<i>Plasmids</i>	<i>Source</i>
<u>Basic Vectors</u>	
pBluescript II KS+/-	Stratagene
pUC18	MBI
pUhr6.2	H. Bujard
pbi5	H. Bujard
pKSTK ^{neo} LoxP	I. Girkontaite, K.D. Fischer
pEGFP-N3	BD Biosciences
<u>B-RAF genomic clones</u>	
pBSK-BamHI(8kb)Ex3-BRaf (p7)	L. Wojnowski
pUC18-EcoRI(9kb)Ex1-BRaf (L34-37)	R. Gotz
<u>Human B-RAF cDNA clone</u>	
pFastBacHThubrafWT	U. Rennefarht

B-RAF targeting vectors

pfloxedB-Raf

C. Xiang

ptetB-Raf

C. Xiang

B-RAF transgene vectors

pbi-BRafEGFP

C. Xiang

ptet-BRafEGFP

C. Xiang

4.1.8. Oligonucleotides

Primer name

Sequence

Genotyping primers for KO and KIN

mB3-1

5'-gcctatgaagagtacaccagcaagctagatgcc-3'

mBdel

5'-taggtttctgtggtgacttggggttctccgtga-3'

NeoL

5'-agtgccagcgggctgctaaa -3'

A-Raf (SacI) long

5'-ggacctcgacaatgagctcctcgcc-3'

RT-PCR primers

Brafex8a

5'-aatcagtttggcaacgagacc-3'

Brafex11re

5'-gtggcggacaagcctgtggt-3'

ex10E3

5'-ttgaattctgaacctgggcccaggtc-3'

pCMV01

5'-accgggaccgatccagcctc-3'

brafel1s1

5'-gacccggccattcctgaagag-3'

brafe3as3

5'-ggttgttccgtgatgcatctgt -3'

actins1

5'-gtcgtaccacaggcattgtgatgg-3'

actinas1

5'-gcaatgcctgggtacatggtgg-3'

Cloning primer for constructs

rtTA5

5'-cccatcgattgacgcaaatgggcggtg g-3'

rtTA3

5'-cccctcgagttaccgggggagcatg-3'

hubrafseq1

5'-atccacagagacctcaagag-3'

EX19stop

5'-ttg gat ccg tgg act gga aac cca cca tat-3'

Sequencing primers

5XhoI

5'-cctgaaagctgctagtagaagac-3'

neo5a

5'-acggagccggttggcgctca-3'

neo3a

5'-agaacgagatcagcagcctctg-3'

rtTA5

5'-cccatcgattgacgcaaatgggcggtg g-3'

puhs2

5'-agttgagcagcctaccctgtac-3'

puhs3

5'-gcaaaagaggaaagagagacacc-3'

rttas1

5'-gctctgcttatatagacctccac-3'

pCMV01

5'-accgggaccgatccagcctc-3'

egfpas1	5'-cggacacgctgaactgtgg-3'
<u>3' probe primers (floxed B-RAF targeting)</u>	
brafgs14	5'-agcagagttgccaactaccac-3'
brafgas19	5'-gcagccagtacttctaaccacc-3'
<u>Screening primers for targeted clones</u>	
Neo3a	5'-agaacgagatcagcagcctctg-3'
Int3R+	5'-tgg gta gtt ggc aac tct gct-3'
5Xho1	5'-cctgaaagctgctagtagaac-3'
BaXh	5'-acattgttgatgctgctgatcc-3'
pCMV01	5'-accgggaccgatccagcctc-3'
HRP1	5'-gccagatcacttaaacccacta-3'

4.1.9. Cell lines, mouse lines and bacterial strains

<i>Cell lines</i>	<i>Source</i>
R1	Mouse embryonic stem cells, from H. Westphal
E14	Mouse embryonic stem cells, from M. Sendtner
MEF	Primary mouse embryonic fibroblasts (MSZ)
NIH3T3-CMVtTA	NIH3T3 constitutively expressing tTA transactivators (R. Houben)
<i>Mouse lines</i>	<i>Source</i>
B6D2F1	All were obtained from Harlan Winkelmann GmbH
C57Bl6	
CD-1	
NMRI	
<i>Bacterial strains</i>	<i>Source</i>
DH5 α	Bethesda Research Laboratories. Optimised for DNA transformation and replication

4.2. Solutions and buffers

4.2.1. Bacterial medium and plasmid isolation buffers

LB (Luria-Bertani) medium

10g/L Bacto-tryptone

10g/L NaCl

5g/L yeast extract

Adjust pH to 7.5 with NaOH

For plates, add 15 g Bacto-agar per liter

SOB medium (1 L)

20g Bacto-tryptone

0.5g NaCl, 5g yeast extract

10ml 250mM KCl

Adjust pH to 7.5 with NaOH

(Before use add 5ml 2M MgCl₂)

X-Gal stock solution

20mg/ml X-gal (5-Bromo-4-Chloro-3-Indolyl-β-D-Galactopyranosid) dissolved in DMF and aliquoted at -20°C in darkness.

Buffer P1 (resuspension buffer)

50mM Tris-HCl

10mM EDTA

10μg/ml RNaseA; pH 8.0

Buffer P2 (Lysis buffer)

10% SDS

200 mM NaOH

Buffer P3 (Neutralization buffer)

3 M potassium acetate, pH5.5

Buffer QBT (Equilibration buffer)

15% ethanol

0.15% Triton X-100

Buffer QC (Wash buffer)

2.0 M NaCl

50 mM MOPS, pH7.0

15% ethanol

Buffer QF (Elution buffer)

1.25 mM NaCl

50 mM Tris-HCl, pH 8.5

15% ethanol

4.2.2. DNA buffers

Tail Lysis Buffer

50 mM EDTA

50 mM Tris-HCl

0.5% SDS; pH8.0

10x TE

0.1 M Tris-HCl

10 mM EDTA; pH 7.5

10x DNA Gel Loading Buffer

40% (w/v) saccharose

0.25% bromphenolblue

0.25% xylencyanol; use as 1x solution

1x Tris-Acetate-EDTA (TAE)

40 mM Tris-HCl

40 mM acetic acid
2 mM EDTA; pH7.8

20x SSC

175.3g/L NaCl

88.2g/L sodium citrate; pH 7.0

Washing buffer 1

2x SSC

0.1% SDS

Washing buffer 2

0.1x SSC

0.1% SDS

4.2.3. Protein analysis buffers

NP40 lysis buffer

10 mM Hepes, pH 7.4

145 mM KCl

5 mM MgCl₂

1 mM EGTA

0.2% IGEPAL

1 mM pefablock

1 mM sodium vanadate

5 mM benzamidine

5 µg/ml aprotinin

5 µg/ml leupeptin

5x SDS-loading Buffer (for SDS-PAGE)

31 mM Tris-HCl, pH6.8

1% SDS

5 % Glycerin

2.5 % β-Mercaptoethanol

0.05 % Bromphenolblue; use as 1x solution

Running Buffer (for SDS-PAGE)

25 mM Tris

250 mM Glycine

0.1 % SDS

Blotting Buffer

25 mM Tris

192 mM Glycine

10% Methanol

10x Tris-Buffered Saline (TBS)

500 mM Tris-HCl, pH7.4

1.5 M NaCl

TBST

1x TBS + 0.05% Tween 20

Blocking Buffer

5% (w/v) of non-fat dry milk in TBST

4.2.4. Histological buffers

Eosin solution

1% Eosin in H₂O

Hematoxylin solution (per 100 ml)

1 g Hematoxylin

0.2 g NaIO₃

50 g KAl(SO₄)₂·12H₂O

1 g sodium citrate

25 g chloral hydrate

4.3. Methods

4.3.1. Bacterial manipulation

Plasmid transformed bacteria are selected on LB plates with the appropriate antibiotic for 16 hr. For overnight mini cultures, single colonies are picked and inoculated in LB medium with antibiotic and shaken overnight at 37°C. This preculture is then used for preparing frozen glycerine cultures or plasmid DNA. For storage of bacteria, a glycerol stock culture is prepared by growing bacteria to an OD of 0.8 at a wavelength of 600nm in culture medium. 500µl bacterial culture is taken and added to 500 µl 80% glycerine and then mix thoroughly in a small 1.5ml tube. This stock solution is subsequently frozen at -80°C. To inoculate an overnight culture again, take out bacteria and hold at room temperature (RT) until surface is thawed. Pick a small amount of cells and mix into 2-5 ml culture medium and leave to grow for several hours at 37°C in a bacterial culture shaker. The frozen stock is immediately returned to the -80°C.

4.3.1.1. Preparation of competent cells (CaCl₂ method)

On the first day, inoculate an overnight preculture from a single colony on a prestreaked plate (from glycerol stock) in 2ml LB media by incubation at 37°C and shaking to aerate. The second day, inoculate 1 ml of the preculture in 100ml fresh media and grow the culture at 37°C until OD at wavelength 600nm of the culture reaches between 0.2 and 0.3. Cool down the culture on ice for at least 15 min. (The following procedures should be carried out at 4°C in pre-cooled sterile tubes). Harvest the cells in a centrifuge at 5000 g for 5 min, and discard the supernatant. Resuspend the bacterial pellets thoroughly in a small volume of ice-cold 100mM CaCl₂. Dilute the suspension with the CaCl₂ solution to a final volume of 30-40 ml, and leave on ice for 25 min with occasional shaking. Spin down the cells as before, discard the supernatant carefully and resuspend the pellets in 5 ml glycerol/CaCl₂. The suspension can be aliquoted in 100 to 400 µl aliquots and stored at -70°C. The transformation efficiency of the bacteria prepared by this method should reach at least 10⁶.

4.3.1.2. Transformation of competent bacteria

Thaw the competent bacteria from a desired origin on ice. Add a maximum of 20ng ligated DNA or purified plasmid-DNA to 100 µl competent cells in a cold 1.5 ml microfuge tube. Mix carefully and keep on ice for 30 min or longer. Heat-shock the bacteria then at 42°C for 90 sec, add 1 ml antibiotic-free LB medium, and aerate at 37°C for 45 min. Selection of transformed bacteria is done by plating 100 µl of the bacterial suspension on antibiotic containing agar plates. Only bacteria that have taken up the desired plasmids, which contain ampicillin or kanamycin resistance cassette, can grow on the agar plates. A single colony can then be expanded in LB medium and used for DNA preparation.

4.3.2. DNA methods

4.3.2.1. Electrophoresis of DNA on agarose gel

Double stranded DNA fragments with lengths between 0.5 kb and 10 kb can be separated according to their lengths on agarose gels. Agarose is added to 1x TAE to obtain a final concentration between 0.7-2%. Boil the suspension in the microwave until the agarose is completely solubilised. Allow the agarose to cool down to around 50°C before adding ethidium bromide up to 0.5 µg/ml and pour into the gel apparatus. Add DNA gel loading buffer to the DNA sample and apply on the gel. Electrophorese in 1x TAE buffer at 100 volts. The DNA can be visualised under UV-light.

4.3.2.2. Isolation of plasmid DNA from agarose (QIAEX II agarose gel extraction protocol)

This protocol is designed for the extraction of 40-bp to 50-kbp DNA fragments from 0.3-2% standard agarose gels in TAE or TBE buffer. DNA molecules are adsorbed to QIAEX II silica particles in the presence of high salt. All non-nucleic acid impurities such as agarose, proteins, salts, and ethidium bromide are removed during washing steps.

Excise the desired DNA band from the agarose gel under the UV light. Weigh the gel slice and add 3 volumes of Buffer QG to 1 volume of gel for DNA fragments 100-bp to 4 kbp; for DNA fragments more than 4 kbp, add 2 volume of QG plus 2 volumes of H₂O. Resuspend QIAEA II by vortexing for 30 sec; add 10 µl (or 30 µl) of QIAEX II to the sample containing not more than 10 µg of DNA (between 2-10 µg). Incubate at 50°C for 10 min to solubilise the agarose and bind the DNA. Mix by vortexing every 2 min to keep QIAEX II in suspension. Centrifuge the sample for 30 sec and carefully remove supernatant with a pipette. Wash the pellet with 500 µl of Buffer QG and then twice with Buffer PE. Air-dry the pellet and elute the DNA in 10 mM Tris-HCl (pH 7.8) or H₂O and resuspend the pellet by vortexing. Incubate at RT for 5 min (or at 50°C for 5 min) for DNA fragments not more than 4 kbp (for DNA fragments between 4-10 kbp). Centrifuge for 30 sec and carefully pipette supernatant into a clean tube.

4.3.2.3. Purification of plasmid DNA (QIAquick PCR purification kit)

This protocol is designed to purify single- or double-stranded PCR products or DNA plasmids ranging from 100 bp to 10 kbp. DNA adsorbs to the silica-membrane in the presence of high salt while contaminants pass through the column. The impurities are washed away and pure DNA is eluted with Tris buffer or H₂O.

Add 5 volume of buffer PB to 1 volume of the contaminants and mix. Place a QIAquick spin column in a 2 ml collection tube. Apply the mixed sample to the QIAquick column and centrifuge 30-60 sec. Discard flow-through and place QIAquick column back into the same collection tube. Add 0.75 ml Washing Buffer PE to column and centrifuge 30-60 sec. Discard flow-through and place QIAquick column back into the same collection tube. Centrifuge column for an additional 1 min at maximum speed. Place QIAquick column in a clean 1.5 ml microfuge tube. Add 50 µl Elution Buffer EB or H₂O to the centre of the QIAquick column and centrifuge for 1 min. Store the purified DNA at - 20°C.

4.3.2.4. Ligation of DNA fragments

Alkaline phosphatase catalyses the removal of 5' phosphate groups from DNA, RNA and ribo- and deoxyribonucleoside triphosphates. For blunt end ligation, the 5' phosphate group of the vector must be removed by Calf-intestinal-phosphatase (CIP) reaction. This reaction is also used to prevent the re-ligation of the vectors. 2.5 µg of DNA fragments is phosphorylated at 37°C for 30 min in 100 µl of reaction volumes consisting of 1x CIP buffer and 1 µl of phosphatase. 5 mM EDTA is then added to the reaction and incubated with the reaction at 65°C for 15 min to inactivate the enzyme. The DNA fragments are purified by phenol and ethanol precipitation before ligation reaction.

4.3.2.5. Cohesive-end ligation

Prepare the plasmid DNA or DNA fragment by cutting it with suitable restriction enzymes, which is followed by purification. 1:3 molar ratio of vector: insert DNA fragments together with 1 µl of T4 ligase are incubated in 1x Ligation Buffer in a total volume of 20 µl for 4 hr at RT or overnight at 16°C. Heat the mixture at 65°C for 10 min to inactivate the enzyme.

4.3.2.6. Mini-preparation of plasmid DNA

Grow 3 ml overnight culture in LB with 100 µg/ml ampicillin at 37°C overnight. Pellet the cells at 14,000 rpm for 1 min. Remove the supernatant and resuspend the pellets in 100 µl Buffer. Add 200 µl Buffer P2 (Lysis Buffer) and incubate at RT for 5 min. Add 150 µl ice-cold 3 M acidic KAc (Neutralisation Buffer), mix by inverting the tubes for 6-7 times and incubate on ice for 5 min. Centrifuge at 15,000 rpm for 3 min. Transfer the supernatant to a fresh Eppendorf tube and add 900 µl of pre-cooled 100% ethanol, precipitate at -70°C for 10 min. Centrifuge the pellet at 15,000 rpm for 10 min. Wash the pellet with 200 µl 70% ethanol. Air-dry the pellet and resuspend it in 30-50µl 10 mM Tris-HCl, pH 7.8.

4.3.2.7. Maxi-preparation of plasmid DNA

Grow culture in 50 ml LB media containing plasmids or recombinant plasmids overnight in a 37°C incubator with shaking at 200 rpm. Collect the bacteria and isolate DNA plasmids by using a Qiagen Plasmid Maxi Kit. This extraction method is based on Birnboim's alkali lysis principle. Resuspend the bacterial pellet in 10 ml of Buffer P1. Add 10 ml of Buffer P2, mix gently, and incubate at RT for 5 min. Add 10 ml of chilled Buffer P3, mix immediately, and incubate on ice for 20 min. Centrifuge at 4,000 rpm for 30 min at 4°C. Filter the supernatant over a prewetted, folded filter. Apply the supernatant to an

equilibrated QIAGEN-tip 500 and allow it to enter the resin by gravity flow. Wash the QIAGEN-tip twice with Buffer QC. Elute DNA with 15 ml Buffer QF. These processes result in the isolation of a DNA-salt pellet, which is precipitated by 0.7 volumes (10.5 ml) of isopropanol and centrifuged further at 4000 rpm for 30 min. Washed the resulting pellet twice with 70% ethanol and air-dry at RT. The pellet is then carefully resuspended in TE buffer and used for transfection of cultured mammalian cells.

4.3.2.8. Measurement of DNA concentration

The DNA concentration is determined by using a UV spectrophotometer at wavelength of 260 nm. The absorption of 1 at 260 nm corresponds to a concentration of 50 µg/ml double stranded DNA. Identity, integrity and possible purity of the DNA can be subsequently analysed on an agarose gel.

4.3.2.9. DNA Sequencing (Sanger Dideoxy Method)

DNA can be sequenced by generating fragments through the controlled interruption of enzymatic replication. DNA polymerase I is used to copy a particular sequence of a single-stranded DNA. The synthesis is primed by complementary fragment, which may be obtained from a restriction enzyme digest or synthesised chemically. In addition to the four deoxyribonucleoside triphosphates (dNTP), the incubation mixture contains a 2', 3'-dideoxy analogue of one of them. The incorporation of this analogue blocks further growth of the new chain because it lacks the 3'-hydroxyl terminus needed to form the next phosphodiester bond. A fluorescent tag is attached to the oligonucleotide primer, a differently coloured one in each of the four chain-terminating reaction mixtures. The reaction mixtures are combined and electrophoresed together. The separated bands of DNA are then detected by their fluorescence as they pass out the bottom of the tube, and the sequence of their colours directly yields the base sequence.

1. Sequencing Reaction:

The "Taq Cycle Sequencing" is performed by using "PRISM™ Ready Reaction DyeDeoxy™ Terminator Cycle Sequencing Kit". Mix the following reagents in a 0.6 ml double-snap-cap microfuge tube:

Terminator premix*	9.5 µl
DNA template	100ng-1.0 µg
Primer	10 pmol
dH ₂ O	Adjust the final reaction volume to 20 µl

*A-Dye Terminator labelled with dichloro[R6G]

C-Dye Terminator labelled with dichloro[TAMRA]

G-Dye Terminator labelled with dichloro[R110]

T-Dye Terminator labelled with dichloro[ROX]

Place the tubes in a thermal cycler preheated to 96°C which is followed by 25 cycles of thermal cycling steps: 96°C for 15 sec; 48°C for 15 sec; 60°C for 4 min; and keep at 4°C after the reaction.

2. Removal of the excess dye terminators by using CENTRI-SEP Columns:

CENTRI-SEP Columns are designed for the fast and efficient purification of large molecules from small molecules.

Prepare the CENTRI-SEP columns according to the standard procedures (PRINCETON SEPARATIONS, INC.). Transfer the DyeDeoxy™ terminator reaction mixture to the top of the gel. Carefully dispense the sample gently onto the centre of the gel bed at the top of the column without disturbing the gel surface. Place the column into the sample collection tube and place both into the rotor. Maintain proper column orientation. Spin the column and collection tube at 750 g for 2 min. The purified sample will be collected in the bottom of the sample collection tube. Dry the sample in a vacuum centrifuge.

3. Preparation and Loading of the samples:

Resuspend the pellet in 4 µl of the following reagent mixture containing 5 µl deionised formamide and 1 µl 25 mM EDTA with blue dextran (50 mg/ml). Centrifuge the solution to collect all the liquid at the bottom of the tube. Denature the samples at 95°C for 2 min and transfer them immediately on ice. The samples are then separated on polyacrylamide gel on the ABI PRISM 373 DNA Sequencer with the appropriate run module, DT {dR Set Any-Primer} mobility file, and matrix file.

DNA sequencing is done by R. Krug (MSZ, Würzburg).

4.3.2.10. Isolation of genomic DNA from cells and tissues

Digest a small piece of mouse tail (0.5-1 cm), 50-100 mg of other tissues or 5×10^6 cells in 500 µl of the Tail Lysis Buffer with 0.4 mg/ml Proteinase K overnight at 55°C. Vortex and spin down the lysate, then transfer the supernant to the new tube. Add 160 µl ~6M NaCl and vortex, followed by incubation for 5 min at RT. Therefore, centrifuge at 10,000 rpm for 15 min and transfer the supernant (~600 µl) to the new tube. After adding 400 µl Isopropanol, mix carefully and pellet the DNA by the same centrifuge. Wash the pellet with 75% Ethanol, air dry and then dissolve in 150-200 µl TE. Measure DNA concentration, and store at 4°C for PCR genotyping or Southern blot analysis.

4.3.2.11. Southern blot

After sufficient digestion of genomic DNA by specific restriction enzymes, separate the fragments on 0.7-0.9% agarose gel with ethidium bromide in TAE at 3V/cm overnight. Photograph the gel and then capillary transfer DNA onto Hybond-N membrane in 20x SSC Buffer according to manufacturer instruction (Hybond-N, Amersham). Cross-link DNA to membrane using UV-light, 120 mJ/cm². The membrane is first incubated in QuikHyb solution with 100µg/ml single-stranded fish sperm DNA, for 30 min at 68°C. During the prehybridization, 5' and 3' probes are ³²P-labelled according to the Rediprime™ kit protocol as a standard Klenow based technique, and purified through a column purification kit. The solution is mixed with one radiolabelled probe before hybridisation is done for 1-2 hour at 68°C. Following hybridisation, the membrane is then subjected to washing at 68°C. The membrane is washed once with washing buffer 1, followed by three times with washing buffer 2, each for 15 min. The membrane is then rinsed to remove excess SDS and exposed with X-ray film overnight or longer at -80°C.

4.3.3. RNA methods

4.3.3.1. Isolation of RNA from cells and tissues

RNA is extremely sensitive to degradation by RNases, and should therefore be handled where possible with RNase-free materials. Cells can be directly lysed in TRIzol LS reagent, 5×10^6 cells/ml. Frozen or fresh embryonic forebrains should be put in TRIzol LS reagent solution, 50-100mg/ml, and homogenized by pipeting up and down. Add 0.2 ml Chloroform per 1ml TRIzol LS reagent, mix on a Vortex for 25 sec then place on ice for 15 min. Next, centrifuge at 10,000 rpm for 15 min at 4°C and transfer the upper aqueous phase to the new tube. Add 0.5 ml Isopropanol, incubate 30 min at RT and centrifuge at 10,000 rpm for 15 min. Wash RNA pellet with 75% Ethanol, air dry and dissolve in 100µl DEPC-H₂O. Measure concentration, based on that one unit of A_{260nm} corresponds to a concentration of 40 µg/ml RNA, and store at -20°C for use.

4.3.3.2. RT-PCR

Total RNA prepared from cells or tissues are treated with amplification grade DNase I. For RT-PCR, cDNA is prepared by reverse transcription (RT) of 1µg of each RNA sample using Moloney-murine leukaemia virus reverse transcriptase (M-MuLV-RT) and random hexamer primers according manufacturer instructions. The PCR amplifications are performed in a 30 µl reaction volume containing 1/20 volume of each cDNA and 10% DMSO. In detection of exon10-specific *B-RAF* expression in forebrains, primers for amplification between exon 8a and exon 11 are ex8a/ex11re, while exon8a/ex10E3 used for selective amplification of exon 10-containing isoforms. To monitor regulation of *B-RAF* transcription by tet-switch from *tet B-RAF* allele, we take two primers, pCMV01 and brafe3as3, to amplify the transcripts from *tet B-RAF* allele, whereas brafe1s1/brafe3as3 pairs used to detect total expression from WT and *tet B-RAF* loci, and additionally primers actin1 and actin1 detect β-actin mRNA as a internal control,. The conditions for amplification are as follows: 94°C for 30 sec, 60°C (exon 10 detection) or 56°C (tet-switch regulation) for 30 sec, 72°C for 1 min for 35 cycles after the initiating denaturation, with the last extension for 5 min at 72°C. PCR control reaction without RT yields no detectable fragments with either primer pair.

4.3.4. Protein methodologies

4.3.4.1. Measurement of Protein concentration (Bio-Rad protein assay)

The Bio-Rad Protein Assay is based on the observation that when Coomassie Brilliant Blue G-250 binds to the protein, the absorbency maximum shifts from 450 nm to 595 nm. Equal volume of precleared cell or tissue lysate, in either NP40 lysis buffer or CCLR buffer, containing 1-20 µg of protein is added to diluted Dye Reagent and mixed well (1:5 dilution of Dye Reagent Concentrate in ddH₂O). After a period of 5-10 min, the absorption at wavelength 595 is measured versus reagent blank (which contains only the lysis buffer). By the way, BSA is used as a standard.

4.3.4.2. Sodium dodecyl sulfate polyacrylamide gel electrophoresis (SDS PAGE)

Proteins can be easily separated on the basis of mass by electrophoresis in a polyacrylamide gel under denaturing conditions. 5x SDS-loading Buffer is used to denature 20-50 µg protein in precleared lysates,

and then heated at 95°C for 5 min. SDS is an anionic detergent that disrupts nearly all noncovalent interactions in native proteins. β -Mercaptoethanol is also included in the sample buffer to reduce disulfide bonds. The SDS complexes with the denatured proteins are then electrophoresed on a polyacrylamide gel in the form of a thin vertical slab. Vertical gels are set in between 2 glass plates with an internal thickness of 1.5 mm between the two plates. In this chamber, the acrylamide mix is poured and left to polymerise for at least 30 min at RT. The gels are composed of two layers: a 6-15% separating gel (pH 8.8) that separates the proteins according to size; and a lower percentage (5%) stacking gel (pH 6.8) that insures the proteins simultaneous entry into the separating gel at the same height.

	Separating gel	Stacking gel
Tris pH 8.8	2.5 ml.	1.25 ml
Acrylamide/bisacrylamide 29:1 (30%)	2.0-5.0 ml	1.7 ml
10% SDS	0.1 ml	0.1 ml
ddH ₂ O	5.4-2.4 ml	6.8 ml
10% APS	0.1 ml	0.1 ml

The separating gel is poured in between two glass plates, leaving a space of about 1cm plus the length of the teeth of the comb. Isopropanol is added to the surface of the gel to exclude air. After the separating gel is polymerised, the isopropanol is removed. The stacking gel poured on top of the separating gel, the comb inserted, and allowed to polymerise. The samples are loaded into the wells of the gel and running buffer is added to the chamber. A cover is then placed over the gel chamber and 45 mA are applied. The negatively charged SDS-protein complexes migrate in the direction of the anode at the bottom of the gel. Small proteins move rapidly through the gel, whereas large ones migrate slower. Proteins that differ in mass by about 2% can be distinguished with this method. The electrophoretic mobility of many proteins in SDS-polyacrylamide gels is proportional to the logarithm of their mass.

4.3.4.3. Immunoblotting

After the lysates are subjected to SDS-PAGE, the proteins are transferred by electroblotting to TranspranTM membrane. SDS-PAGE gels are electroblotted at 400 mA in blotting buffer for 60 min. Ponceau S fixative dye solution (containing Ponceau S, trichloroacetic acid, and sulfosalicylic acid) is used to check if the transfer has occurred. Stain for 5 min and wash with deionised water. For Western blot analysis, incubate the membranes in blocking buffer for 1 hr at RT or overnight at 4°C on a shaker. Dilute the first antibody in TBST/2% milk (unless otherwise indicated), add to the membrane, and incubate for 2 hr at RT or overnight at 4°C. Wash the membrane three times with TBST, each time for 10 min. Dilute the appropriate peroxidase-conjugated secondary antibody in TBST/2% milk (or according to manufacturer's instructions), add to the membrane, incubate at RT for 45 min, and wash. This step is followed by the standard enhanced chemiluminescence reaction (ECL-system): incubate the membrane in a 1:1 mixture of ECL solutions 1 and 2. This reaction is based on a peroxidase catalysed oxidation of Luminol, which leads to the emission

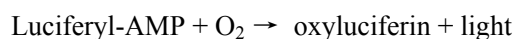
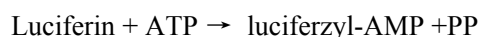
of light photons that can be detected on X-ray film. Thus the peroxidase conjugated secondary antibodies bound to the primary antibody detect the protein of interest.

4.3.4.4. Immunoblot stripping

The removal of primary and secondary antibodies from a membrane is possible, so that it may be probed with alternative antibodies. To make 50 ml stripping buffer, mix 3.125 ml of 1M Tris-HCl solution (pH 6.7), 5 ml of 20% SDS solution and 0.35 ml of 4.3 M β -Mercaptoethanol with 42ml distilled H₂O. Incubate the membrane in stripping buffer for 30 min at 50°C. The membrane should be washed at least 5 times with TBST. The membrane can then be re-probed as described above.

4.3.4.5. Luciferase reporter gene assay

Bioluminescence is characterized by light emission catalyzed by an enzyme. Firefly luciferase catalyses the release of light upon addition of luciferin and ATP. The luciferase activity is assayed and quantified by measurement of light production. The photon production by catalytic oxidation of beetle luciferin occurs from an enzyme intermediate, luciferyl-AMP.



Luciferin is first activated by addition of ATP. The activated luciferin reacts with oxygen to form dioxetane. Dioxetane decomposes and excites the molecule, which transfers to its ground state by emission of fluorescence light.

The targeted cells by *tet B-RAF* vector are directly lysed in 100 μ l of CCLR lysis buffer, mixed well, and incubated on ice for 30 min. The tissues from adult chimera of target ES cells are put in 1ml CCLR buffer and homogenized in Ultra-Turrax for 30 sec at speed "5" (speed "6" for bone) on ice. The crude lysates are precleared by centrifugation at maximum speed for 1 min. 20 μ l of precleared lysates is added per well in 96-well plate, which is then placed into a Berthold luminometer. Automatically, 100 μ l of Luciferase Assay Reagent is injected into each well, and the activity is immediately measured for 5 sec. Results are presented as relative luciferase units normalized to protein concentration.

4.3.5. Cell culture techniques

4.3.5.1. *in vitro* neurosphere assay for neural stem cells

For suspension culture of neural stem cells (NSC), forebrain vesicles were dissected from E10.5 embryos and transferred into ice-cold CMF-HBSS with 1U/ml Dispase. Incubate for 5 min at 37°C water bath, and then spin down at 1500rpm in the microfuge. Resuspend the pellet in Neurobasal medium, containing 2% B27 Supplement, 20 ng/ml each of bFGF and EGF, 1% L-Glutamine, and 1% Penicillin/Streptomycin, and triturate into single cells by plastic pipette. 20,000 living cells were seeded into 24-well suspension culture plates (Sarstedt) per well with 0.5 ml medium in duplicate. 4 DIC later neurosphere cultures were moved to 6-well suspension culture plates (Sarstedt). The cells were cultivated with medium change every second day at 37°C in a 5% CO₂ and humidified atmosphere all the time. At 11 DIC the numbers of neurospheres (>50 μ m) were determined and their relative size in terms of cell number was measured. Cultures of

secondary neurospheres were obtained by dissociation of primary neurospheres and culturing in a density of 10,000 cells per well for 9 days as described above.

Differentiation of primary neurospheres was performed by seeding and culturing single neurospheres on poly-DL-ornithine coated glass coverslips in Neurobasal/B27 medium containing 1% horse serum instead of bFGF and EGF for 14 days. The flat neurospheres attached to coverslips were fixed with 4% paraformaldehyde for 20 minutes, washed with PBS and incubated in blocking solution (10% goat or donkey serum, 0.1% triton in PBS). Cells were immunostained overnight at 4°C with α -GFAP (1:200) and α -TuJ-1 (1:100) antibodies, and with α -O4 (1:50). After washing with PBS neurospheres were incubated with secondary antibodies labelled with either Rhodamine or FITC dye (1:100). The nuclei were stained by DAPI (200 μ l in 10ml Methanol). All immunochemical reactions were carried out in parallel with reactions lacking primary antibodies to ensure the specificity of the observed staining.

4.3.5.2. Primary cortical cell culture

Cortical tissue, obtained from *B-RAF^{KIN/KIN}* and control mice at embryonic day 12.5, was dissected in ice-cold HBSS and then transferred into ice-cold Neurobasal medium containing 2% B27 supplement, 500 μ M glutamine, and 1% penicillin-streptomycin. The tissue was mechanically dissociated with a plastic pipette into single cells.

For acutely stimulation of progenitors, 400,000 cells were plated per well in 24-well adherent culture plate (Sarstedt), precoated with laminin and poly-D-Lysine. Four hours after seeding at 37°C in 5% CO₂, these cells were stimulated with 150ng/ml bFGF for 15, 30 and 60 min, and then harvested in NP40 lysis buffer for Western blot analysis.

For proliferation of progenitors, 400,000 cells were plated on coverslips precoated with laminin and poly-D-Lysine in 24-well plate, and cultivated in Neurobasal/B27 medium supplemented with 40 ng/ml bFGF for 2 days. Then the cells were fixed with 4% paraformaldehyde for 20 minutes, washed with PBS and incubated in blocking solution (10% donkey serum, 0.1% triton in PBS). After incubation overnight at 4°C with α -pERK antibodies (1:100), the cells were immunostained with FITC-labelled secondary antibodies. In parallel, the PFA-fixed cells were stained with 0.6 μ M FITC-phalloidin in PBS for 10 min at room temperature.

4.3.5.3. ES Cell maintenance

The primary mouse embryonic fibroblasts (MEFs) were cultured in Dulbecco's modified Eagle's medium (DMEM) supplemented with 10% heat inactivated (30 min, 56°C) fetal calf serum (FCS), 1% penicillin and streptomycin, and 2 mM L-glutamine, at 37°C in humidified air with 5% CO₂. The embryonic stem cells (ES, R1 and E14) were grown on the Mitomycin C treated feeder (MEF) layer in DMEM supplemented with 15% heat inactivated ES cell tested FCS, 1x nonessential amino acids, 1% penicillin and streptomycin, 2 mM L-glutamine, 0.1 mM β -mercaptoethanol, 1/200 volume of recombinant LIF (Supernant from LIF-transfected CHO cells) at 37°C in humidified air with 5% CO₂. The cells were

passed every two days and the medium was changed every day. The number of cells should never exceed 1.5×10^7 /10 cm plate.

4.3.5.4. Targeting of ES cell by vectors

Upon one electroporation, 25 μ g of linearized targeting vector was used to transfect 10×10^6 ES cells. Suspend cells in 800 μ l Electroporation buffer (for R1) or PBS (for E14), mix them with DNA in electroporation cuvette (Bio-Rad), and then apply 400V/250 μ F (for R1) or 230V/500 μ F plus 240V/500 μ F (for E14). Plate the cells into several 10 cm dishes by a suitable density. 24 h later, change the medium and start G418 selection (350 μ g/ml for R1, 180 μ g/ml for E14), while Gancyclovir selection was done from 48h after electroporation. Continue double selection for about 5 days, until single colonies are big enough to pick.

4.3.5.5. Identification of positive clones

All procedures have to be done in sterile conditions. After selection by higher concentration of G418, totally more than 100 single R1 colonies with good morphology can be isolated for screening homologous recombinants. However, more than 400 single good colonies were available to obtain for test after weaker selection of electroporated E14 cells. Add 25 μ l Trypsin/EDTA per well in 96-well U-bottom plates, before ES cell colonies in dishes were covered by 10 ml PBS instead of ES medium. Pick single colonies under binocular microscope using yellow tips, and place one each well in the U-bottom plates. Incubate for 5 min at 37°C, triturate until cell clumps dispersed, and transfer to 96-well flat plates with feeder cells. After 3 days, the clones should be ready for splitting and freezing. Half of the cell suspension was used for DNA isolation and PCR screening. All PCR positive clones were expanded for one more PCR test, Southern blot analysis and stock preparation.

4.3.5.6. Transduction and induction of targeted ES cells

The targeted cells by *floxed B-RAF* targeting vector were transduced by a recombinant Cre recombinase, HTNC, to test Cre-mediated site-specific recombination:

1. Plate the mutant cells on inactivated feeder cells as usual
2. After 5-6 hours, remove the medium and wash two times carefully with PBS
3. Incubate the cells for 16-20 h with 1.5 μ M sterile HTNC in 1:1 PBS/DMEM (w/o FCS)
4. Wash with PBS and change to normal ES medium
5. 3 days later harvest the cells for PCR test

For check of tet-switch, the targeted cells with *tet B-RAF* allele were induced by Dox with the following protocol:

1. Plate the targeted cells on inactivated feeder cells as usual
2. One day later, feed the cells with ES medium containing no or 1 μ g/ml Dox for 2 days
3. Harvest the cells for RT-PCR of *B-RAF* mRNA, Western blot of B-RAF and Luciferase assay of reporter gene to test expression control by tet-switch

4. In parallel, in presence or absence of 1 µg/ml Dox, starve the cells with serum/LIF-free medium for 24 h prior to stimulation by LIF (1:200) for 15 min
5. Collect the cells for Western blot of B-RAF and phosphorylated ERK

4.3.5.7. Blastocyst injection of targeted ES cells

The (C57B16xDBA2) F1 (abbreviated as B6D2F1) hybrid mice were used for blastocyst production. Their host embryos are well suited for germline transmission (g.l.t.) of the 129/Sv-derived ES cells such as R1 and E14 lines. At day 3.5 post coitum (dpc), blastocysts were flushed from the uteri with prewarmed M2 medium and kept in M16 droplet cultures under mineral oil at 38.5°C, 5% CO₂ until injection. ES cells were prepared for injection as follows: 2–3 days before injection the cells were plated on the low-density feeder layer and passaged at least one time. 2–4 hours before injection they were fed with fresh ES medium. Then the cells were trypsinized and resuspended in M2 medium containing DNase I on ice. Approximately 10–15 ES cells were injected per blastocyst. After reexpansion of the blastocoels (1–2 h), every 8–20 blastocysts was transferred into one 2.5 dpc pseudopregnant NMRI foster. The chimerism of the delivered mice was identified on the basis of agouti pigmentation in the coat eight to nine days after birth. All male and some female with high chimerism (>50%) were tested for g.l.t. by mating with C57B16 (B6) mice. The transmission of mutated locus from target ES cells into the germline can be first featured with agouti coat colour of progeny, and then confirmed by standard PCR test and Southern blot analysis.

Blastocyst injection is done by H. Troll (MSZ, Würzburg).

4.3.5.8. Transient transfection of NIH3T3 CMV-tTA

NIH3T3 cells constitutively expressing tTA were cultured as MEFs. One day before transfection, 1.5x 10⁵ cells per well were seeded on glass coverslips in 24-well plates, and maintained in 0.5ml of normal medium only without antibiotics. On the day of transfection, dilute 0.8 µg DNA and 2µl Lipofectamine 2000 (LF2000), respectively, into 50µl OPTI-MEM per well. 5 min later, combine the diluted DNA with the diluted LF2000 and incubate for 20 min at RT. Feed the cells 0.5 ml fresh medium without serum and antibiotics each well, and add the DNA-LF2000 complexes (100 µl) directly. After gently rocking the plate back and forth, incubate at 37°C in 5% CO₂ incubator for 4–5 h., and then change the medium with normal growth medium. One more day later, the cells were fixed with 4% paraformaldehyde for 20 minutes, washed with PBS and mounted by Mowiol.

4.3.6. Histological methods

4.3.6.1. Embedding in paraffin

Whole embryos at E10.5 to E16.5 and brains of E17.5 or postnatal mice were dissected into cold phosphate-buffered saline (PBS), fixed overnight in fresh 4% paraformaldehyde at RT. Incubate as follow: 40 min in 50% Ethanol, 40 min in 70% Ethanol, 40 min in 80% Ethanol, 40 min in 90% Ethanol, 40 min in 95% Ethanol, 3x 40 min in 100% Ethanol, 2x 30 min in 1:1 (Chloroform:Ethanol), 30 min in Chloroform:Ethanol. All procedures perform at RT. Transfer embryos or organs into melted Paraffin, and incubate for 1h at 65°C. Change Paraffin and incubate for 2h or overnight at 65°C. Prepare the Paraffin

blocks. Embryos and organs are sectioned into 6-10 μm microsections and can be used for the further histological analysis.

4.3.6.2. Hematoxylin/eosin staining

All procedures are performed at RT. After deparaffinization in machine wash the glasses in water, incubate 3 min in Hematoxylin solution. Transfer the glasses into water with ammonium (1 drop of liquid ammonium/100 ml H_2O) for 1 min. Transfer into 1% Eosin solution for 30 sec. Incubate the slides 3x 1 min in Ethanol, and then 3x 2 min in Ethanol. Transfer in Xylol, incubate 2x 1 min and 1x 5 min in Xylol. Mount in Depex.

4.3.6.3. Immunohistochemistry

Paraffin-embedded 6 μm thick sections were deparaffinized in machine, rehydrated and microwaved 6 min in 10 mM sodium citrate buffer, pH 5.5 and washed 3x5 min in PBS. Subsequently the slides were incubated for 6 min in peroxidase blocking solution (1.5% H_2O_2 in PBS) and washed 3x5 min in PBS. After antigen retrieval, slides were rinsed in distilled water, placed in 20% sucrose/PBS at 4°C for 30 min, washed in PBS and preincubated in blocking serum (10% donkey or goat serum, 0.1% Triton in PBS) for 40 min. Subsequently the slides were incubated in the presence of the primary antibodies diluted in blocking serum overnight at 4°C. The primary antibodies used were: α -TuJ-1 monoclonal (1:100), α -MAP2 monoclonal (1:500), α -NeuN monoclonal (1:100), Brn-2 rabbit polyclonal (1:800), α -Nestin monoclonal (1:5), and α -Reelin (1:1000).

Immunolabelling was revealed by the indirect immunofluorescence procedure using Rhodamine-conjugated secondary antibodies (Vector, 1:200) or by the avidin-biotin-HRP method. When biotinylated secondary antibodies in blocking serum were applied, the slides were incubated for 1h at RT. The Antigen-antibody complexes were detected using immunoperoxidase system (Vectastain[®] ABC Kit, Vector) and DAB staining according to manufacturer instructions. The sections were then counterstained with hematoxylin to stain the nuclei. All immunohistochemical reactions were carried out in parallel with reactions lacking primary antibodies to ensure the specificity of the observed staining.

4.3.6.4. BrdU labelling

For BrdU labelling in embryos, pregnant females were injected intraperitoneally with BrdU (70 $\mu\text{g/g}$ body weight). 2 (for cell proliferation assay) or 72 hours (for neuron birthdating) after BrdU incorporation, embryos were removed, processed and serially sectioned as previously described. The brain sections were incubated in 2 N HCl for 1 hour at 37°C, neutralized in borate buffer (pH 8.5) for 1 hour at room temperature, rinsed twice in PBS and blocked with 3% non-fat milk for 3 hours at room temperature. The sections were then incubated with an anti-BrdU antibody (1:100) overnight at 4°C, rinsed twice in PBS, followed by incubation with an Alexa-488 conjugated secondary antibody (1:100). In cell proliferation assay, three embryos were analyzed for each genotype at the indicated stages and three or four nonadjacent sections at the level of the olfactory bulb were selected to determine the BrdU labelling index. This index was calculated by dividing the number of BrdU-positive nuclei by the total number of the nuclei identified

in units of 200- μ m-wide VZ in 40X optical view of the KIN and control cortical regions. In neuron birthdating analysis, parasagittal sections at the level of the olfactory bulb were used to determine the distributions of the postmitotic cells labelled with BrdU about 72 hours before. At this level, the entire cortical region was divided in three equal parts: upper at the level of CP, middle at the level of IZ, and deep at the level of VZ. The number of BrdU-labelled cells was counted and normalized to account for the relative distribution in different parts.

4.3.7. Statistical analysis

For both sectioned material and cell culture experiments, data sets from independent experiments were pooled, and the results were expressed as mean and standard deviation (SD). Statistical significance between data sets was assessed by Students t-test and assigned when $P < 0.05$.

REFERENCES

- Alavi, A., Hood, J.D., Frausto, R., Stupack, D.G., and Cheresch, D.A. (2003). Role of Raf in vascular protection from distinct apoptotic stimuli. *Science* *301*, 94-96.
- Allen, L.F., Sebolt-Leopold, J., and Meyer, M.B. (2003). CI-1040 (PD184352), a targeted signal transduction inhibitor of MEK (MAPKK). *Semin. Oncol.* *30*, 105–116.
- Angevine, J.Jr., and Sidman, R.L. (1961). Autoradiographic study of cell migration during histogenesis of cerebral cortex in the mouse. *Nature* *192*, 766-768.
- Anselmo, A.N., Bumeister, R., Thomas, J.M., and White, M.A. (2002). Critical contribution of linker proteins to Raf kinase activation. *J. Biol. Chem.* *277*, 5940–5943.
- Barnabe-Heider, F., and Miller, F.D. (2003). Endogenously produced neurotrophins regulate survival and differentiation of cortical progenitors via distinct signaling pathways. *J. Neurosci.* *23*, 5149-5160.
- Barnier, J.V., Papin, C., Eychène, A., Lecoq, O., and Calothy, G. (1995). The mouse B-raf gene encodes multiple protein isoforms with tissue-specific expression. *J. Biol. Chem.* *270*, 23381-23389.
- Baumann, B., Weber, C.K., Troppmair, J., Whiteside, S., Israel, A., Rapp, U.R., and Wirth, T. (2000). Raf induces NF-kappaB by membrane shuttle kinase MEKK1, a signaling pathway critical for transformation. *Proc. Natl. Acad. Sci. USA* *97*, 4615-4620.
- Bielas, S., Higginbotham, H., Koizumi, H., Tanaka, T., and Gleeson, J.G. (2004). Cortical neuronal migration mutants suggest separate but intersecting pathways. *Annu. Rev. Cell Dev. Biol.* *20*, 593-618.
- Bogoyevitch, M.A., Marshall, C.J., and Sugden, P.H. (1995). Hypertrophic agonists stimulate the activities of the protein kinases c-Raf and A-Raf in cultured ventricular myocytes. *J. Biol. Chem.* *270*, 26303–26310.
- Bond, C.T., Sprengel, R., Bissonnette, J.M., Kaufmann, W.A., Pribnow, D., Neelands, T., Storck, T., Baetscher, M., Jerecic, J., Maylie, J., Knaus, H.G., Seeburg, P.H., and Adelman, J.P. (2000). Respiration and parturition affected by conditional overexpression of the Ca²⁺-activated K⁺ channel subunit, SK3. *Science* *289*, 1942–1946.
- Bondeva, T., Balla, A., Varnai, P., and Balla, T. (2002). Structural determinants of Ras-Raf interaction analyzed in live cells. *Mol. Biol. Cell* *13*, 2323-2333.
- Bos, J.L. (1998). All in the family? New insights and questions regarding interconnectivity of Ras, Rap1 and Ral. *EMBO J.* *17*, 6776-6782.
- Breier, G., and Risau, W. (1996). The role of vascular endothelial growth factor in blood vessel formation. *Trends Cell. Biol.* *6*, 454-456.
- Brummer, T., Shaw, P.E., Reth, M., and Misawa, Y. (2002). Inducible gene deletion reveals different roles for B-Raf and Raf-1 in B-cell antigen receptor signalling. *EMBO J.* *21*, 5611-5622.

- Campos, L.S., Leone, D.P., Relvas, J.B., Brakebusch, C., Fassler, R., Suter, U., and French-Constant, C. (2004). Beta1 integrins activate a MAPK signalling pathway in neural stem cells that contributes to their maintenance. *Development* *131*, 3433-3444.
- Catling, A.D., Reuter, C.W., Cox, M.E., Parsons, S.J., and Weber, M.J. (1994). Partial purification of a mitogen-activated protein kinase kinase activator from bovine brain. Identification as B-Raf or a B-Raf-associated activity. *J. Biol. Chem.* *269*, 30014–30021.
- Chadee, D.N., and Kyriakis, J.M. (2004). MLK3 is required for mitogen activation of B-Raf, ERK and cell proliferation. *Nat. Cell Biol.* *6*, 770-776.
- Chaudhary, A., King, W.G., Mattaliano, M.D., Frost, J.A., Diaz, B., Morrison, D.K., Cobb, M.H., Marshall, M.S., and Brugge, J.S. (2000). Phosphatidylinositol 3-kinase regulates Raf1 through Pak phosphorylation of serine 338. *Curr. Biol.* *10*, 551–554.
- Chen, J., Fujii, K., Zhang, L., Roberts, T., and Fu, H. (2001). Raf-1 promotes cell survival by antagonizing apoptosis signal-regulating kinase 1 through a MEK–ERK independent mechanism. *Proc. Natl Acad. Sci. USA* *98*, 7783–7788.
- Chiloeches, A., Mason, C.S., and Marais, R. (2001). S338 phosphorylation of Raf-1 is independent of phosphatidylinositol 3-kinase and Pak3. *Mol. Cell. Biol.* *21*, 2423–2434.
- Chong, H., Lee, J., and Guan, K.L. (2001). Positive and negative regulation of Raf kinase activity and function by phosphorylation. *EMBO J.* *20*, 3716–3727.
- Chong, H., Vikis, H.G., and Guan, K.L. (2003). Mechanisms of regulating the Raf kinase family. *Cell Signal.* *15*, 463-469.
- Chow, Y.H., Pumiglia, K., Jun, T.H., Dent, P., Sturgill, T.W., and Jove, R. (1995). Functional mapping of the N-terminal regulatory domain in the human Raf-1 protein kinase. *J. Biol. Chem.* *270*, 14100–14106.
- Cook, S.J., Rubinfeld, B., Albert, I., and McCormick, F. (1993). RapV12 antagonizes Ras-dependent activation of ERK1 and ERK2 by LPA and EGF in Rat-1 fibroblasts. *EMBO J.* *12*, 3475-3485.
- Corbit, K.C., Soh, J.W., Yoshida, K., Eves, E.M., Weinstein, I.B., and Rosner, M.R. (2000). Different protein kinase C isoforms determine growth factor specificity in neuronal cells. *Mol. Cell. Biol.* *20*, 5392–5403.
- Corson, L.B., Yamanaka, Y., Lai, K.M., and Rossant, J. (2003). Spatial and temporal patterns of ERK signaling during mouse embryogenesis. *Development* *130*, 4527-4537.
- Davies, H., Bignell, G.R., Cox, C., Stephens, P., Edkins, S., Clegg, S., Teague, J., Woffendin, H., Garnett, M.J., Bottomley, W., Davis, N., Dicks, E., Ewing, R., Floyd, Y., Gray, K., Hall, S., Hawes, R., Hughes, J., Kosmidou, V., Menzies, A., Mould, C., Parker, A., Stevens, C., Watt, S., Hooper, S., Wilson, R., Jayatilake, H., Gusterson, B.A., Cooper, C., Shipley, J., Hargrave, D., Pritchard-Jones, K., Maitland, N., Chenevix-Trench, G., Riggins, G.J., Bigner, D.D., Palmieri, G., Cossu, A., Flanagan, A., Nicholson, A., Ho, J.W., Leung, S.Y., Yuen, S.T., Weber, B.L., Seigler, H.F., Darrow, T.L., Paterson, H., Marais, R., Marshall, C.J., Wooster, R., Stratton, M.R., and Futreal, P.A. (2002). Mutations of the *BRAF* gene in human cancer. *Nature* *417*, 949–954.

- Delehanty, L.L., Mogass, M., Gonias, S.L., Racke, F.K., Johnstone, B., and Goldfarb, A.N. (2003). Stromal inhibition of megakaryocytic differentiation is associated with blockade of sustained Rap1 activation. *Blood* 101, 1744–1751.
- Denouel-Galy, A., Douville, E.M., Warne, P.H., Papin, C., Laugier, D., Calothy, G., Downward, J., and Eychene, A. (1998). Murine Ksr interacts with MEK and inhibits Ras-induced transformation. *Curr. Biol.* 8, 46–55.
- Dhillon, A.S., Pollock, C., Steen, H., Shaw, P.E., Mischak, H., and Kolch, W. (2002). Cyclic AMP-dependent kinase regulates Raf-1 kinase mainly by phosphorylation of serine 259. *Mol. Cell. Biol.* 22, 3237–3246.
- Dono, R. (2003). Fibroblast growth factors as regulators of central nervous system development and function. *Am. J. Physiol. Regul. Integr. Comp. Physiol.* 284, 867–881.
- Dono, R., Texido, G., Dussel, R., Ehmke, H., and Zeller, R. (1998). Impaired cerebral cortex development and blood pressure regulation in FGF-2-deficient mice. *EMBO J.* 17, 4213–4225.
- Dumaz, N., Light, Y., and Marais, R. (2002). Cyclic AMP blocks cell growth through Raf-1-dependent and Raf-1-independent mechanisms. *Mol. Cell. Biol.* 22, 3717–3728.
- Dumaz, N., and Marais, R. (2003). Protein kinase A blocks Raf-1 activity by stimulating 14-3-3 binding and blocking Raf-1 interaction with Ras. *J. Biol. Chem.* 278, 29819–29823.
- Ehrenreiter, K., Piazzolla, D., Velamoor, V., Sobczak, I., Small, J.V., Takeda, J., Leung, T., and Baccarini, M. (2005). Raf-1 regulates Rho signaling and cell migration. *J. Cell Biol.* 168, 955–964.
- Eychene, A., Barnier, J.V., Apiou, F., Dutrillaux, B., and Calothy, G. (1992). Chromosomal assignment of two human B-raf(Rmil) proto-oncogene loci: B-raf-1 encoding the p94Braf/Rmil and B-raf-2, a processed pseudogene. *Oncogene* 7, 1657–1660.
- Fabian, J.R., Daar, I.O., and Morrison, D.K. (1993). Critical tyrosine residues regulate the enzymatic and biological activity of Raf-1 kinase. *Mol. Cell. Biol.* 13, 7170–7179.
- Fedorov, L.M., Haegel-Kronenberger, H., and Hirchenhain, J.A. (1997). Comparison of the germline potential of differently aged ES cell lines and their transfected descendants. *Transgenic Res.* 6, 223–231.
- Ferreira, A., and Caceres, A. (1992). Expression of the class III beta-tubulin isotype in developing neurons in culture. *J. Neurosci. Res.* 32, 516–529.
- Futter, M., Uematsu, K., Bullock, S.A., Kim, Y., Hemmings, H.C.Jr., Nishi, A., Greengard, P., and Nairn, A.C. (2005). Phosphorylation of spinophilin by ERK and cyclin-dependent PK 5 (Cdk5). *Proc. Natl. Acad. Sci. USA* 102, 3489–3494.
- Galaktionov, K., Jesus, C., and Beach, D. (1995). Raf1 interaction with Cdc25 phosphatase ties mitogenic signal transduction to cell cycle activation. *Genes Dev.* 9, 1046–1058.
- Garcia, J., de Gunzburg, J., Eychene, A., Gisselbrecht, S., and Porteu, F. (2001). Thrombopoietin-mediated sustained activation of extracellular signal-regulated kinase in

- UT7-Mpl cells requires both Ras-Raf-1- and Rap1-B-Raf-dependent pathways. *Mol. Cell Biol.* *21*, 2659–2670.
- Garnett, M.J., Rana, S., Paterson, H., Barford, D., and Marais, R. (2005). Wild-type and mutant B-RAF activate C-RAF through distinct mechanisms involving heterodimerization. *Mol. Cell* *20*, 963-969.
- Goodall, J., Wellbrock, C., Dexter, T.J., Roberts, K., Marais, R., and Goding, C.R. (2004). The Brn-2 transcription factor links activated BRAF to melanoma proliferation. *Mol. Cell Biol.* *24*, 2923-2931.
- Gossen, M., and Bujard, H. (2002). Studying gene function in eukaryotes by conditional gene inactivation. *Annu. Rev. Genet.* *36*, 153-173.
- Gotz, R., Wiese, S., Takayama, S., Camarero, G.C., Rossoll, W., Schweizer, U., Troppmair, J., Jablonka, S., Holtmann, B., Reed, J.C., Rapp, U.R., and Sendtner, M. (2005). Bag1 is essential for differentiation and survival of hematopoietic and neuronal cells. *Nat. Neurosci.* *8*, 1169-1178.
- Gu, H., Zou, Y.R., and Rajewsky, K. (1993). Independent control of immunoglobulin switch recombination at individual switch regions evidenced through Cre-loxP-mediated gene targeting. *Cell* *73*, 1155–1164.
- Gupta, A., and Tsai, L.H. (2003). Cyclin-dependent kinase 5 and neuronal migration in the neocortex. *Neurosignals* *12*, 173-179.
- Hagemann, C., and Rapp, U.R. (1999). Isotype-specific functions of Raf kinases. *Exp. Cell Res.* *253*, 34-46.
- Hancock, J. F. (2003). Ras proteins: different signals from different locations. *Nat. Rev. Mol. Cell Biol.* *4*, 373–384.
- Harada, T., Morooka, T., Ogawa, S., and Nishida, E. (2001). ERK induces p35, a neuron-specific activator of Cdk5, through induction of Egr1. *Nat. Cell Biol.* *3*, 453-459.
- Hatano, N., Mori, Y., Oh-hora, M., Kosugi, A., Fujikawa, T., Nakai, N., Niwa, H., Miyazaki, J., Hamaoka, T., and Ogata, M. (2003). Essential role for ERK2 mitogen-activated protein kinase in placental development. *Genes Cells* *8*, 847-856.
- Hekman, M., Fischer, A., Wennogle, L.P., Wang, Y.K., Campbell, S.L., and Rapp, U.R. (2005). Novel C-Raf phosphorylation sites: serine 296 and 301 participate in Raf regulation. *FEBS Lett.* *579*, 464-468.
- Hekman, M., Wiese, S., Metz, R., Albert, S., Troppmair, J., Nickel, J., Sendtner, M., and Rapp, U.R. (2004). Dynamic changes in C-Raf phosphorylation and 14-3-3 protein binding in response to growth factor stimulation: differential roles of 14-3-3 protein binding sites. *J. Biol. Chem.* *279*, 14074–14086.
- Holland, A.M., Hale, M.A., Kagami, H., Hammer, R.E., and MacDonald, R.J. (2002). Experimental control of pancreatic development and maintenance. *Proc. Natl. Acad. Sci. USA* *99*, 12236-12241.

- Hu, C.D., Kariya, K., Kotani, G., Shirouzu, M., Yokoyama, S., and Kataoka, T. (1997). Coassociation of Rap1A and Ha-Ras with Raf-1 N-terminal region interferes with ras-dependent activation of Raf-1. *J. Biol. Chem.* *272*, 11702-11705.
- Humbert, S., Lanier, L.M., and Tsai, L.H. (2000). Synaptic localization of p39, a neuronal activator of cdk5. *Neuroreport* *11*, 2213-2216.
- Hüser, M., Lockett, J., Chiloeches, A., Mercer, K., Iwobi, M., Giblett, S., Sun, X.M., Brown, J., Marais, R., and Pritchard, C. (2001). MEK kinase activity is not necessary for Raf-1 function. *EMBO J.* *20*, 1940-1951.
- Jaiswal, R.K., Moodie, S.A., Wolfman, A., and Landreth, G.E. (1994). The mitogen-activated protein kinase cascade is activated by B-Raf in response to nerve growth factor through interaction with p21ras. *Mol. Cell. Biol.* *14*, 6944-6953.
- Janosch, P., Schellerer, M., Seitz, T., Reim, P., Eulitz, M., Brielmeier, M., Kolch, W., Sedivy, J.M., and Mischak, H. (1996). Characterization of I κ B kinases. I κ B- α is not phosphorylated by Raf-1 or protein kinase C isozymes, but is a casein kinase II substrate. *J. Biol. Chem.* *271*, 3868-3874.
- Jaumot, M., and Hancock, J.F. (2001). Protein phosphatases 1 and 2A promote Raf-1 activation by regulating 14-3-3 interactions. *Oncogene* *20*, 3949-3958.
- Kamata, T., Kang, J., Lee, T.H., Wojnowski, L., Pritchard, C.A., and Leavitt, A.D. (2005). A critical function for B-Raf at multiple stages of myelopoiesis. *Blood* *106*, 833-840.
- Kao, S., Jaiswal, R.K., Kolch, W., Landreth, G.E. (2001). Identification of the mechanisms regulating the differential activation of the mapk cascade by epidermal growth factor and nerve growth factor in PC12 cells. *J. Biol. Chem.* *276*, 18169-18177.
- Kerkhoff, E., and Rapp, U.R. (1998). High-intensity Raf signals convert mitotic cell cycling into cellular growth. *Cancer Res.* *58*, 1636-1640.
- King, A.J., Sun, H., Diaz, B., Barnard, D., Miao, W., Bagrodia, S., and Marshall, M.S. (1998). The protein kinase Pak3 positively regulates Raf-1 activity through phosphorylation of serine 338. *Nature* *396*, 180-183.
- King, A.J., Wireman, R.S., Hamilton, M., and Marshall, M.S. (2001). Phosphorylation site specificity of the Pak-mediated regulation of Raf-1 and cooperativity with Src. *FEBS Lett.* *497*, 6-14.
- Kirstein, M., and Farinas, I. (2002). Sensing life: regulation of sensory neuron survival by neurotrophins. *Cell. Mol. Life Sci.* *59*, 1787-1802.
- Kolbus, A., Pilat, S., Husak, Z., Deiner, E.M., Stengl, G., Beug, H., and Baccarini, M. (2002). Raf-1 antagonizes erythroid differentiation by restraining caspase activation. *J. Exp. Med.* *196*, 1347-1353.
- Lanigan, T.M., Liu, A., Huang, Y.Z., Mei, L., Margolis, B., and Guan, K.L. (2003). Human homologue of *Drosophila* CNK interacts with Ras effector proteins Raf and Rlf. *FASEB J.* *17*, 2048-2060.

- Lee, M.K., Tuttle, J.B., Rebhun, L.I., Cleveland, D.W., and Frankfurter, A. (1990). The expression and posttranslational modification of a neuron-specific beta-tubulin isotype during chick embryogenesis. *Cell Motil. Cytoskeleton* *17*, 118-132.
- Light, Y., Paterson, H., and Marais, R. (2002). 14-3-3 antagonizes Ras-mediated Raf-1 recruitment to the plasma membrane to maintain signaling fidelity. *Mol. Cell. Biol.* *22*, 4984-4996.
- Li, S., and Sedivy, J.M. (1993). Raf-1 protein kinase activates the NF- κ B transcription factor by dissociating the cytoplasmic NF- κ B-I κ B complex. *Proc. Natl. Acad. Sci. USA* *90*, 9247-9251.
- Li, W., Han, M., and Guan, K.L. (2000). The leucine-rich repeat protein SUR-8 enhances MAP kinase activation and forms a complex with Ras and Raf. *Genes Dev.* *14*, 895-900.
- Luckett, J.C., Huser, M.B., Giagtzoglou, N., Brown, J.E., and Pritchard, C.A. (2000). Expression of the *A-raf* proto-oncogene in the normal adult and embryonic mouse. *Cell Growth Differ.* *11*, 163-171.
- Majewski, M., Nieborowska-Skorska, M., Salomoni, P., Slupianek, A., Reiss, K., Trotta, R., Calabretta, B., and Skorski, T. (1999). Activation of mitochondrial Raf-1 is involved in the antiapoptotic effects of Akt. *Cancer Res.* *59*, 2815-2819.
- Marais, R., Light, Y., Paterson, H.F., and Marshall, C.J. (1995). Ras recruits Raf-1 to the plasma membrane for activation by tyrosine phosphorylation. *EMBO J.* *14*, 3136-3145.
- Marais, R., Light, Y., Paterson, H.F., Mason, C.S., and Marshall, C.J. (1997). Differential regulation of Raf-1, A-Raf, and B-Raf by oncogenic ras and tyrosine kinases. *J. Biol. Chem.* *272*, 4378-4383.
- Markus, A., Patel, T.D., and Snider, W.D. (2002). Neurotrophic factors and axonal growth. *Curr. Opin. Neurobiol.* *12*, 523-531.
- Marshall, C.J. (1995). Specificity of receptor tyrosine kinase signaling: transient versus sustained extracellular signal-regulated kinase activation. *Cell* *80*, 179-185.
- Mason, C.S., Springer, C.J., Cooper, R.G., Superti-Furga, G., Marshall, C.J., and Marais, R. (1999). Serine and tyrosine phosphorylations cooperate in Raf-1, but not B-Raf activation. *EMBO J.* *18*, 2137-2148.
- McConnell, S.K. (1995). Constructing the cerebral cortex: neurogenesis and fate determination. *Neuron* *15*, 761-768.
- McEvelly, R.J., de Diaz, M.O., Schonemann, M.D., Hooshmand, F., and Rosenfeld, M.G. (2002). Transcriptional regulation of cortical neuron migration by POU domain factors. *Science* *295*, 1528-1532.
- Medina, D.L., Sciarretta, C., Calella, A.M., Von Bohlen Und Halbach, O., Unsicker, K., and Minichiello, L. (2004). TrkB regulates neocortex formation through the Shc/PLC γ -mediated control of neuronal migration. *EMBO J.* *23*, 3803-3814.

- Menard, C., Hein, P., Paquin, A., Savelson, A., Yang, X.M., Lederfein, D., Barnabe-Heider, F., Mir, A.A., Sterneck, E., Peterson, A.C., Johnson, P.F., Vinson, C., Miller, F.D. (2002). An essential role for a MEK-C/EBP pathway during growth factor-regulated cortical neurogenesis. *Neuron* 36, 597-610.
- Mercer, K., Chiloeches, A., Huser, M., Kiernan, M., Marais, R., and Pritchard, C. (2002). ERK signalling and oncogene transformation are not impaired in cells lacking A-Raf. *Oncogene* 21, 347-355
- Mercer, K., Giblett, S., Oakden, A., Brown, J., Marais, R., and Pritchard, C. (2005). A-Raf and Raf-1 work together to influence transient ERK phosphorylation and G1/S cell cycle progression. *Oncogene* 24, 5207-5217.
- Mikula, M., Schreiber, M., Husak, Z., Kucerova, L., R uth, J., Wieser, R., Zatloukal, K., Beug, H., Wagner, E.F., and Baccarini, M. (2001). Embryonic lethality and fetal liver apoptosis in mice lacking the *c-raf-1* gene. *EMBO J.* 20, 1952-1962.
- Monuki, E.S., and Walsh, C.A. (2001). Mechanisms of cerebral cortical patterning in mice and humans. *Nat. Neurosci. Suppl.* 4, 1199-1206.
- Moodie, S.A., Paris, M.J., Kolch, W., and Wolfman, A. (1994). Association of MEK1 with p21ras-GMPPNP is dependent on B-Raf. *Mol. Cell. Biol.* 14, 7153-7162.
- Morice, C., Nothias, F., K onig, S., Vernier, P., Baccarini, M., Vincent, J.D., and Barnier, J.V. (1999). Raf-1 and B-Raf proteins have similar regional distributions but different subcellular localization in the adult rat brain. *Eur. J. Neurosci.* 11, 1995-2006.
- Morrison, D.K. (2001). KSR: a MAPK scaffold of the Ras pathway? *J. Cell Sci.* 114, 1609-1612.
- Nadarajah, B., and Parnavelas, J.G. (2002). Modes of neuronal migration in the developing cerebral cortex. *Nat. Rev. Neurosci.* 3, 423-432.
- Nantel, A., Huber, M., and Thomas, D.Y. (1999). Localization of endogenous Grb10 to the mitochondria and its interaction with the mitochondrial-associated Raf-1 pool. *J. Biol. Chem.* 274, 35719-35724.
- Noctor, S.C., Martinez-Cerdeno, V., Ivic, L., and Kriegstein, A.R. (2004). Cortical neurons arise in symmetric and asymmetric division zones and migrate through specific phases. *Nat. Neurosci.* 7, 136-144.
- Nurcombe, V., Ford, M.D., Wildchut, J.A., and Bartlett, P.F. (1993). Developmental regulation of neural response to FGF-1 and FGF-2 by heparan sulfate proteoglycan. *Science* 260, 103-106.
- Ogawa, M., Miyata, T., Nakajima, K., Yagyu, K., Seike, M., Ikenaka, K., Yamamoto, H., and Mikoshiba, K. (1995). The reeler gene-associated antigen on Cajal-Retzius neurons is a crucial molecule for laminar organization of cortical neurons. *Neuron* 14, 899-912.
- Okada, T., Hu, C.D., Jin, T.G., Kariya, K., Yamawaki-Kataoka, Y., and Kataoka, T. (1999). The strength of interaction at the Raf cysteine-rich domain is a critical determinant of response of Raf to Ras family small GTPases. *Mol. Cell. Biol.* 19, 6057-6064.

- Okano, H. (2002). Stem cell biology of the central nervous system. *J. Neurosci. Res.* *69*, 698-707.
- O'Neill, E., Rushworth, L., Baccharini, M., and Kolch, W. (2004). Role of the kinase MST2 in suppression of apoptosis by the proto-oncogene product Raf-1. *Science* *306*, 2267-2270.
- Ortega, S., Ittmann, M., Tsang, S.H., Ehrlich, M., and Basilico, C. (1998). Neuronal defects and delayed wound healing in mice lacking fibroblast growth factor 2. *Proc. Natl. Acad. Sci. USA* *95*, 5672-5677.
- Ory, S., Zhou, M., Conrads, T.P., Veenstra, T.D., and Morrison, D.K. (2003). Protein phosphatase 2A positively regulates Ras signaling by dephosphorylating KSR1 and Raf-1 on critical 14-3-3 binding sites. *Curr. Biol.* *13*, 1356-1364.
- Papin, C., Denouel, A., Calothy, G., and Eychene, A. (1996). Identification of signalling proteins interacting with B-Raf in the yeast two-hybrid system. *Oncogene* *12*, 2213-2221.
- Papin, C., Denouel-Galy, A., Laugier, D., Calothy, G., and Eychene, A. (1998). Modulation of kinase activity and oncogenic properties by alternative splicing reveals a novel regulatory mechanism for B-Raf. *J. Biol. Chem.* *273*, 24939-24947.
- Peitz, M., Pfannkuche, K., Rajewsky, K., and Edenhofer, F. (2002). Ability of the hydrophobic FGF and basic TAT peptides to promote cellular uptake of recombinant Cre recombinase: a tool for efficient genetic engineering of mammalian genomes. *Proc. Natl. Acad. Sci. USA* *99*, 4489-4494.
- Pritchard, C.A., Bolin, L., Slattery, R., Murray, R., and McMahon, M. (1996). Post-natal lethality and neurological and gastrointestinal defects in mice with targeted disruption of the A-Raf protein kinase. *Curr. Biol.* *6*, 614-617.
- Pritchard, C.A., Hayes, L., Wojnowski, L., Zimmer, A., Marais, R.M., and Norman, J.C. (2004). B-Raf acts via the ROCKII/LIMK/cofilin pathway to maintain actin stress fibers in fibroblasts. *Mol. Cell. Biol.* *24*, 5937-5952.
- Pritchard, C.A., Samuels, M.L., Bosch, E., and McMahon, M. (1995). Conditionally oncogenic forms of the A-Raf and B-Raf protein kinases display different biological and biochemical properties in NIH 3T3 cells. *Mol. Cell. Biol.* *15*, 6430-6442.
- Qiu, W., Zhuang, S., von Lintig, F.C., Boss, G.R., and Pilz, R.B. (2000). Cell type-specific regulation of B-Raf kinase by cAMP and 14-3-3 proteins. *J. Biol. Chem.* *275*, 31921-31929.
- Raballo, R., Rhee, J., Lyn-Cook, R., Leckman, J.F., Schwartz, M.L., and Vaccarino, F.M. (2000). Basic fibroblast growth factor (Fgf2) is necessary for cell proliferation and neurogenesis in the developing cerebral cortex. *J. Neurosci.* *20*, 5012-5023.
- Rajalingam, K., Wunder, C., Brinkmann, V., Churin, Y., Hekman, M., Sievers, C., Rapp, U.R., and Rudel, T. (2005). Prohibitin is required for Ras-induced Raf-MEK-ERK activation and epithelial cell migration. *Nat. Cell Biol.* *7*, 837-843.
- Rakic, P. (1972). Mode of cell migration to the superficial layers of fetal monkey neocortex. *J. Comp. Neurol.* *145*, 61-83.

- Rapp, U.R., Goldsborough, M.D., Mark, G.E., Bonner, T.I., Groffen, J., Reynolds, F.H.Jr., and Stephenson, J.R. (1983). Structure and biological activity of v-raf, a unique oncogene transduced by a retrovirus. *Proc. Natl. Acad. Sci. USA* *80*, 4218-4222.
- Reynolds, B.A., and Weiss, S. (1992). Generation of neurons and astrocytes from isolated cells of the adult mammalian central nervous system. *Science* *255*, 1707-1710.
- Rice, D.S., and Curran, T. (1999). Mutant mice with scrambled brains: understanding the signaling pathways that control cell positioning in the CNS. *Genes Dev.* *13*, 2758-2773.
- Rizzo, M.A., Shome, K., Vasudevan, C., Stolz, D.B., Sung, T.C., Frohman, M.A., Watkins, S.C., and Romero, G. (1999). Phospholipase D and its product, phosphatidic acid, mediate agonist-dependent raf-1 translocation to the plasma membrane and the activation of the mitogen-activated protein kinase pathway. *J. Biol. Chem.* *274*, 1131-1139.
- Rizzo, M.A., Shome, K., Watkins, S.C., and Romero, G. (2000). The recruitment of Raf-1 to membranes is mediated by direct interaction with phosphatidic acid and is independent of association with Ras. *J. Biol. Chem.* *275*, 23911-23918.
- Robbins, D.J., Zhen, E., Cheng, M., Xu, S., Ebert, D., and Cobb, M.H. (1994). MAP kinases ERK1 and ERK2: pleiotropic enzymes in a ubiquitous signaling network. *Adv. Cancer Res.* *63*, 93-116.
- Saba-El-Leil, M.K., Vella, F.D., Vernay, B., Voisin, L., Chen, L., Labrecque, N., Ang, S.L., and Meloche, S. (2003). An essential function of the mitogen-activated protein kinase Erk2 in mouse trophoblast development. *EMBO Rep.* *4*, 964-968.
- Schultze, N., Burki, Y., Lang, Y., Certa, U., and Bluethmann, H. (1996). Efficient control of gene expression by single step integration of the tetracycline system in transgenic mice. *Nat. Biotech.* *14*, 499-503.
- Schwartz, M. (2004). Rho signalling at a glance. *J. Cell Sci.* *117*, 5457-5458.
- Shen, Q., Goderie, S.K., Jin, L., Karanth, N., Sun, Y., Abramova, N., Vincent, P., Pumiglia, K., and Temple, S. (2004). Endothelial cells stimulate self-renewal and expand neurogenesis of neural stem cells. *Science* *304*, 1338-1340.
- Shin, MK, Levorse, J.M., Ingram, R.S., and Tilghman, S.M. (1999). The temporal requirement for endothelin receptor-B signalling during neural crest development. *Nature* *402*, 496-501.
- Sidovar, M.F., Kozlowski, P., Lee, J.W., Collins, M.A., He, Y., and Graves, L.M. (2000). Phosphorylation of serine 43 is not required for inhibition of c-Raf kinase by the cAMP-dependent protein kinase. *J. Biol. Chem.* *275*, 28688-28694.
- Storm, S.M., Cleveland, J.L., and Rapp, U.R. (1990). Expression of *raf* family proto-oncogenes in normal mouse tissues. *Oncogene* *5*, 345-351.
- Sugitani, Y., Nakai, S., Minowa, O., Nishi, M., Jishage, K., Kawano, H., Mori, K., Ogawa, M., and Noda, T. (2002). Brn-1 and Brn-2 share crucial roles in the production and positioning of mouse neocortical neurons. *Genes Dev.* *16*, 1760-1765.

- Sun, H., King, A.J., Diaz, H.B., and Marshall, M.S. (2000). Regulation of the protein kinase Raf-1 by oncogenic Ras through phosphatidylinositol 3-kinase, Cdc42/Rac and Pak. *Curr. Biol.* *10*, 281–284.
- Sutor, S.L., Vroman, B.T., Armstrong, E.A., Abraham, R.T., and Karnitz, L.M. (1999). A phosphatidylinositol 3-kinase-dependent pathway that differentially regulates c-Raf and A-Raf. *J. Biol. Chem.* *274*, 7002–7010.
- Takahashi, T., Goto, T., Miyama, S., Nowakowski, R.S., and Caviness, V.S.Jr. (1999). Sequence of neuron origin and neocortical laminar fate: relation to cell cycle of origin in the developing murine cerebral wall. *J. Neurosci.* *19*, 10357-10371.
- Tanahashi-Hori, T., Tanahashi, N., Tanaka, K., and Chiba, T. (2003). Conditional knockdown of proteasomes results in cell-cycle arrest and enhanced expression of molecular chaperones Hsp70 and Hsp40 in chicken DT-40 cells. *J. Biol. Chem.* *278*, 16237-16243.
- Temple, S. (2001). The development of neural stem cells. *Nature* *414*, 112-117.
- Tilbrook, P.A., Colley, S.M., McCarthy, D.J., Marais, R., and Klinken, S.P. (2001). Erythropoietin-stimulated Raf-1 tyrosine phosphorylation is associated with the tyrosine kinase Lyn in J2E erythroleukemic cells. *Arch. Biochem. Biophys.* *396*, 128–132.
- Troppmair, J., and Rapp, U.R. (2003). Raf and the road to cell survival: a tale of bad spells, ring bearers and detours. *Biochem. Pharmacol.* *66*, 1341–1345.
- Tsai, L.H., Delalle, I., Caviness, V.S.Jr., Chae, T., and Harlow, E. (1994). p35 is a neural-specific regulatory subunit of cyclin-dependent kinase 5. *Nature* *371*, 419-423.
- Tyrsin, O. (2003). Role of Raf family members in mouse development. Ph.D. thesis.
- Tzivion, G., Luo, Z., and Avruch, J. (1998). A dimeric 14-3-3 protein is an essential cofactor for Raf kinase activity. *Nature* *394*, 88–92.
- Urlinger, S., Baron, U., Thellmann, M., Hasan, M.T., Bujard, H., and Hillen, W. (2000). Exploring the sequence space for tetracycline-dependent transcriptional activators: novel mutations yield expanded range and sensitivity. *Proc. Natl. Acad. Sci. USA* *97*, 7963-7968.
- Vaccarino, F.M., Schwartz, M.L., Raballo, R., Nilsen, J., Rhee, J., Zhou, M., Doetschman, T., Coffin, J.D., Wyland, J.J., and Hung, Y.T. (1999). Changes in cerebral cortex size are governed by fibroblast growth factor during embryogenesis. *Nat. Neurosci.* *2*, 246-253.
- Wachs, F.P., Couillard-Despres, S., Engelhardt, M., Wilhelm, D., Ploetz, S., Vroemen, M., Kaesbauer, J., Uyanik, G., Klucken, J., Karl, C., Tebbing, J., Svendsen, C., Weidner, N., Kuhn, H.G., Winkler, J., and Aigner, L. (2003). High efficacy of clonal growth and expansion of adult neural stem cells. *Lab. Invest.* *83*, 949-962.
- Wakioka, T., Sasaki, A., Kato, R., Shouda, T., Matsumoto, A., Miyoshi, K., Tsuneoka, M., Komiya, S., Baron, R., and Yoshimura, A. (2001). Spred is a Sprouty-related suppressor of Ras signalling. *Nature* *412*, 647-651.

- Wang, H.G., Rapp, U.R., and Reed, J.C. (1996a). Bcl-2 targets the protein kinase Raf-1 to mitochondria. *Cell* 87, 629-638.
- Wang, H.G., Takayama, S., Rapp, U.R., and Reed, J.C. (1996b). Bcl-2 interacting protein, BAG-1, binds to and activates the kinase Raf-1. *Proc. Natl. Acad. Sci. USA* 93, 7063-7068.
- Wang, S., Ghosh, R.N., and Chellappan, S.P. (1998). Raf-1 physically interacts with Rb and regulates its function: a link between mitogenic signaling and cell cycle regulation. *Mol. Cell. Biol.* 18, 7487-98.
- Wan, P.T., Garnett, M.J., Roe, S.M., Lee, S., Niculescu-Duvaz, D., Good, V.M., Jones, C.M., Marshall, C.J., Springer, C.J., Barford, D., and Marais, R. (2004). Mechanism of activation of the RAF-ERK signaling pathway by oncogenic mutations of B-RAF. *Cell* 116, 855-867.
- Watanabe, H., Yokozeki, T., Yamazaki, M., Miyazaki, H., Sasaki, T., Maehama, T., Itoh, K., Frohman, M.A., and Kanaho, Y. (2004). Essential role for phospholipase D2 activation downstream of ERK MAP kinase in nerve growth factor-stimulated neurite outgrowth from PC12 cells. *J. Biol. Chem.* 279, 37870-37877.
- Weber, C.K., Slupsky, J.R., Herrmann, C., Schuler, M., Rapp, U.R., and Block, C. (2000). Mitogenic signaling of Ras is regulated by differential interaction with Raf isozymes. *Oncogene* 19, 169-176.
- Weber, C.K., Slupsky, J.R., Kalmes, H.A., and Rapp, U.R. (2001). Active Ras induces heterodimerization of cRaf and BRaf. *Cancer Res.* 61, 3595-3598.
- Weber, J.D., Raben, D.M., Phillips, P.J., and Baldassare, J.J. (1997). Sustained activation of extracellular-signal-regulated kinase 1 (ERK1) is required for the continued expression of cyclin D1 in G1 phase. *Biochem. J.* 326, 61-68.
- Wellbrock, C., Karasarides, M., and Marais, R. (2004). The RAF proteins take centre stage. *Nat. Rev. Mol. Cell Biol.* 5, 875-885.
- Wiese, S., Digby, M.R., Gunnensen, J.M., Gotz, R., Pei, G., Holtmann, B., Lowenthal, J., and Sendtner, M. (1999). The anti-apoptotic protein ITA is essential for NGF-mediated survival of embryonic chick neurons. *Nat. Neurosci.* 2, 978-983.
- Wiese, S., Pei, G., Karch, C., Troppmair, J., Holtmann, B., Rapp, U.R., and Sendtner, M. (2001). Specific function of B-Raf in mediating survival of embryonic motoneurons and sensory neurons. *Nat. Neurosci.* 4, 137-142.
- Wittinghofer, A., and Nassar, N. (1996). How Ras-related proteins talk to their effectors. *Trends Biochem. Sci.* 21, 488-491.
- Wojnowski, L., Stancato, L.F., Larner, A.C., Rapp, U.R., and Zimmer, A. (2000). Overlapping and specific functions of B-Raf and C-Raf-1 proto-oncogenes during mouse embryogenesis. *Mech. Dev.* 91, 97-104.
- Wojnowski, L., Stancato, L.F., Zimmer, A.M., Hahn, H., Beck, T.W., Larner, A.C., Rapp, U.R., and Zimmer, A. (1998). Craf-1 protein kinase is essential for mouse development. *Mech. Dev.* 76, 141-149.

- Wojnowski, L., Zimmer, A.M., Beck, T.W., Hahn, H., Bernal, R., Rapp, U.R., and Zimmer, A. (1997). Endothelial apoptosis in B-Raf deficient mice. *Nat. Genet.* *16*, 293-297.
- Woods, D., Parry, D., Cherwinski, H., Bosch, E., Lees, E., and McMahon, M. (1997). Raf-induced proliferation or cell cycle arrest is determined by the level of Raf activity with arrest mediated by p21Cip1. *Mol. Cell. Biol.* *17*, 5598-5611.
- Wu, C., Lai, C.F., Mobley, W.C. (2001). Nerve growth factor activates persistent Rap1 signaling in endosomes. *J. Neurosci.* *21*, 5406-5416.
- Wu, J., Dent, P., Jelinek, T., Wolfman, A., Weber, M.J., Sturgill, T.W. (1993). Inhibition of the EGF-activated MAP kinase signaling pathway by adenosine 3',5'-monophosphate. *Science* *262*, 1065-1069.
- Yao, Y., Li, W., Wu, J., Germann, U.A., Su, M.S., Kuida, K., and Boucher, D.M. (2003). Extracellular signal-regulated kinase 2 is necessary for mesoderm differentiation. *Proc. Natl. Acad. Sci. USA* *100*, 12759-12764.
- Yeung, K., Janosch, P., McFerran, B., Rose, D.W., Mischak, H., Sedivy, J.M., and Kolch, W. (2000). Mechanism of suppression of the Raf/MEK/extracellular signal-regulated kinase pathway by the raf kinase inhibitor protein. *Mol. Cell. Biol.* *20*, 3079-3085.
- Yeung, K., Seitz, T., Li, S., Janosch, P., McFerran, B., Kaiser, C., Fee, F., Katsanakis, K.D., Rose, D.W., Mischak, H., Sedivy, J.M., and Kolch, W. (1999). Suppression of Raf-1 kinase activity and MAP kinase signalling by RKIP. *Nature* *401*, 173-177.
- Yip-Schneider, M.T., Miao, W., Lin, A., Barnard, D.S., Tzivion, G., and Marshall, M.S. (2000). Regulation of the Raf-1 kinase domain by phosphorylation and 14-3-3 association. *Biochem. J.* *351*, 151-159.
- York, R.D., Molliver, D.C., Grewal, S.S., Stenberg, P.E., McCleskey, E.W., Stork, P.J. (2000). Role of phosphoinositide 3-kinase and endocytosis in nerve growth factor-induced extracellular signal-regulated kinase activation via ras and rap1. *Mol. Cell. Biol.* *20*, 8069-8083.
- York, R.D., Yao, H., Dillon, T., Ellig, C.L., Eckert, S.P., McCleskey, E.W., and Stork, P.J. (1998). Rap1 mediates sustained MAP kinase activation induced by nerve growth factor. *Nature* *392*, 622-626.
- Yuryev, A., Ono, M., Goff, S.A., Macaluso, F., and Wennogle, L.P. (2000). Isoform-specific localization of A-RAF in mitochondria. *Mol. Cell. Biol.* *20*, 4870-4878.
- Zang, M., Hayne, C., and Luo, Z. (2002). Interaction between active Pak1 and Raf-1 is necessary for phosphorylation and activation of Raf-1. *J. Biol. Chem.* *277*, 4395-4405.
- Zhang, B.H., and Guan, K.L. (2000). Activation of B-Raf kinase requires phosphorylation of the conserved residues Thr598 and Ser601. *EMBO J.* *19*, 5429-5439.
- Zimmermann, S., and Moelling, K. (1999). Phosphorylation and regulation of Raf by Akt (protein kinase B). *Science* *286*, 1741-1744.

APPENDIX

Abbreviations

A/P	Anterior/posterior
APS	Ammoniumpersulphate
ASK1	Apoptosis signal-regulated kinase
Asp (D)	Aspartic acid
ATP	Adenosine 5'-triphosphate
BCR	B-cell receptor
BDNF	Brain-derived neurotrophin
bFGF	Basic fibroblast growth factor
bp	Basepair
BrdU	bromodeoxyuridine
cAMP	cyclic Adenosine monophosphate
CCLR	Luciferase cell culture lysis reagent
Cdk5	Cyclin-dependent kinase 5
Chol	Cholesterol
CIP	Calf Intestinal Phosphatase
CK2 β	β subunit of casein kinase 2
CMF	Calcium- and magnesium-free
CNK	Connector-enhancer of KSR
CNS	Central nervous system
CP	Cortical plate
CR1, 2, 3	Conserved region 1, 2, 3
CRD	Cysteine-rich domain
CTL	Control
DAG	Diacylglycerin
(d)dNTP	(Di)Desoxynucleotide triphosphate
DIC	Day in culture
DMEM	Dulbecco's Modified Eagle Medium
DMF	Dimethylformamide
DMSO	Dimethylsulphoxide
Dox	Doxycycline
DTT	Dithiothreitol
E10.5	Embryonic day 10.5
ECL	Enhanced Chemoluminescence
E. coli	Escherichia coli
EDTA	Ethylendiamintetra acetic acid
e.g.	exempli gratia
EGF	Epidermal growth factor
EGFR	Epidermal growth factor receptor
ERK	Extracellular signal regulated kinase
ES cell	Embryonic stem cell
et al.	et alii
Ex	Exon
FCS	Fetal calf serum
FGF	fibroblast growth factor
FGFR	fibroblast growth factor receptor

floxed	flanked by loxP
g	gram
GAP	GTPase-activating protein
GDP	Guanosine 5'-diphosphate
GEF	Guanine nucleotide exchange factor
GFAP	Glial fibrillary acidic protein
GPCR	G protein coupled receptor
Grb	Growth factor receptor bound protein
GTP	Guanosine 5'-triphosphate
HA	Haemagglutinin
HBSS	Hanks' Balanced Salt Solution
H&E	Hematoxylin/eosin staining
HT	Heterozygote
HTNC	His-TAT-NLS-Cre
hu	Human
IAP	Inhibitor of apoptosis protein
IC	Immunochemistry
I κ B	Inhibitor of κ B
IKK	I κ B kinase
IZ	Intermediate zone
kb, kbp	Kilo basepairs
kDa	kilo Dalton
KIN	Knockin
KO	Knockout
KSR	Kinase suppressor of Ras
L	Liter
LIF	Leukemia inhibitory factor
Luc	Luciferase reporter gene
M2-PK	Type M2 pyruvate kinase
MAPK	Mitogen activated protein kinase
MAP2K	MAPK kinase
MAP3K	MAP2K kinase
MEF	Mouse embryonic fibroblast
MEK	MAPK/ERK activating kinase
MEKK	MAPK/ERK activating kinase kinase
MKK	MAP kinase kinase
ML	Molecular layer
MST2	Mammalian sterile 20-like kinase
MSZ	Institut für Medizinische Strahlenkunde und Zellforschung
MZ	Marginal zone
NEO	Neomycin resistance cassette
NF- κ B	Nuclear factor κ B
NGF	Nerve growth factor
NP40	Nonidet 40
NSC	Neural stem cell
NT-3	Neurotrophin-3
OD	Optical density
ORF	Open reading frame
pA, polyA	Polyadenylation signal
PAK	P21 activated kinase
PAGE	Polyacrylamide-Gel electrophoresis

PBS	Phosphate buffered saline
PC12	Pheochromocytoma cell 12
PCD	Programmed cell death
PCR	polymerase chain reaction
PDGF	Platelet derived growth factor
pERK	phosphoERK
Phe (F)	Phenylalanine
PI3K	Phosphatidyl inositide 3-kinase
PIP3	Phosphatidylinositol (3,4,5) trisphosphate
PKA	Protein kinase A
PKB (AKT)	Protein kinase B
PKC	Protein kinase C
PP	Preplate
PP1, 2A	Protein phosphatase1, 2A
pThr	Phosphothreonine
PTK	Protein tyrosine kinase
pTyr	Phosphotyrosine
RBD	Ras binding domain
RKIP	Raf kinase inhibitor protein
RLU	relative luciferase unit
rpm	revolutions per minute
Rsk	Ribosomal S6 kinase
RTK	Receptor protein tyrosine kinase
RT	Room temperature
Ser (S)	Serine
SH	Src Homology
Shc	Src Homology domain containing
SP	subplate
SUR8	Suppressor of Ras mutations-8
SVZ	Subventricular zone
tet	tetracycline-regulated
tetO	tetracycline operator
Thr (T)	Threonine
TK	Tymidine kinase
TrkA, B	Tyrosine receptor kinase A, B
TuJ-1	β III tubulin
Tyr (Y)	Tyrosine
v	Volume
V	Volt
VZ	Voltage-dependent anion channel
w	Weight
WB	Western blot
WT	Wild type

CURRICULUM VITAE

PERSONAL DETAILS

Name: Chaomei Xiang
Email: xiangcm@hotmail.com
Date of birth: April 12, 1970
Place of birth: Hubei, China
Nationality: Chinese
Sex: Male
Marital Status: Married

EDUCATION

04/02- : *Doctor of Philosophy*
Institute of Medical Radiation and Cell Research
Wuerzburg University, Germany
- The role of B-RAF in embryonic development of mouse forebrain:
Analysis of B-RAF null mice and generation of conditional KO
09/91-07/94: *Master of Science in Genetics*
Department of Fish Genetics and Breeding
Institute of Hydrobiology, Chinese Academy of Sciences, China
09/87-07/91: *Bachelor of Science in Biochemistry*
Department of Biology, Wuhan University, China

PROFESSIONAL EXPERIENCE

02/00-03/02: *Co-worker*
Physiological Chemistry I, Biocenter
Wuerzburg University
Germany
02/99-01/00: *Exchange Researcher for collaboration*
National Center for Mariculture
Israeli Oceanographic and Limnological Research
Israel
08/94-01/99: *Research Assistant/Associate*
Department of Fish Genetics and Breeding
Institute of Hydrobiology, Chinese Academy of Sciences
China

TECHNIQUES

- Stem cell culture and primary neuronal culture
- Molecular cloning, gene targeting, gene transfer
- Immunocytochemistry, fluorescence microscopy
- Molecular hybridization: Southern blot, Western blot
- PCR, RT-PCR, DNA sequencing
- RAPD, AFLP, microsatellite analysis
- Electrophoresis and chromatography
- Chromosome set manipulation, reproduction and breeding for fish and shellfish

SELECTED PUBLICATIONS

- Camarero G.*, **Xiang C.***, Tyrsin O. Y.*, Pfeiffer V., Wiese S., Gotz R. and Rapp U. R. (2006). Cortical migration defects in mice expressing A-RAF from the *B-RAF* locus. Submitted.
* equal contribution
- Hong Y., Winkler C., **Xiang C.** and Scharl M. Current status of embryonic stem cells and gene knockout technology in fishes. *Perspectives in Comparative Endocrinology: Unity and Diversity*, 23-43, Goos et al., Sorrento (Napoli), Italy, 2001.
- Lu R., Qiu T., **Xiang C.**, Xie H. and Zhang J. (2000). RAPD and AFLP techniques for the analysis of genetic relationships in two genera of decapod. *Crustaceana* 73, 1027-1036.
- Xie H., Lu R., **Xiang C.**, Zhang J. and Qiu T. (1999). Genetic analysis of three kinds of mitten crabs using RAPD technique. *Acta Hydrobiologica Sinica* 23,120-125 (in Chinese).
- Xiang C.**, Lu R., Xie H., Liu X. and Zhang J. (1998). Random amplified polymorphic DNA (RAPD) analysis of four species in decapod. *Acta Hydrobiologica Sinica* 22, 251-256 (in Chinese).
- Qiu T., Lu R., **Xiang C.**, Zhang J. and Xie H. (1998). Studies on sex-specific markers of *Eriocheir sinensis* using RAPD technique. *Journal of Fisheries of China* 22, 175-177 (in Chinese).

CONTRIBUTION TO CONFERENCES

- Camarero G., **Xiang C.**, Tyrsin O. Y., Fedorov L. W., Goetz R. and Rapp U. R. Essential function of B-Raf in neuronal migration. The 6th EMBL mouse molecular genetics meeting (Sep.28-Oct.2, 2005, EMBL Heidelberg). Poster.
- Hong Y., **Xiang C.**, Chen S. and Scharl M. Embryonic stem cells and gene targeting in the fish medaka. The 3rd IUBS Symposium on Molecular Aspects of Fish Genomes and Development (Feb. 19-21, 2001, Singapore). Keynote lecture.

Declaration:

I hereby declare that the submitted dissertation was completed by myself and no other. I have not used any sources or materials other than those enclosed.

Moreover I declare that the following dissertation has not been submitted further in this form or any other form, and has not been used for obtaining any other equivalent qualifications at any other organization/institution.

Additionally, I have not applied for, nor will I attempt to apply for any other degree of qualification in relation to this work.

Würzburg, den

Chaomei Xiang